Ollscoil na Gaillimhe
University of Galway

Provided by the author(s) and University of Galway in accordance with publisher policies. Please cite the published version when available.

Title	The molecular characterization of ER stress-induced autophagy and cell death
Author(s)	Deegan, Shane
Publication Date	2012-12-21
Item record	http://hdl.handle.net/10379/3695

Downloaded 2024-04-23T07:07:58Z

Some rights reserved. For more information, please see the item record link above.

The molecular characterization of ER stress-induced autophagy and cell death

A thesis submitted to the National University of Ireland Galway in fulfillment of the requirement for the degree of

Doctor of Philosophy

By

Shane Deegan

Discipline of Biochemistry, School of Natural Sciences,

National University of Ireland, Galway

Thesis Supervisors: Professor Afshin Samali

Head of School: Dr Heinz-Peter Nasheuer

November 2012

Table of Contents

Declaration

This thesis is a presentation of my original research work. The Electron Microscopy images presented in this work was carried out by Dr. David MacDonald. Wherever contributions of others are involved, every effort is made to indicate this clearly, with due reference to the literature, and acknowledgement of collaborative research and discussions.

The work was done under the guidance of Professor Afshin Samali, at the National University of Ireland Galway.

Acknowledgements

There are many people I would like to thank who have helped me over the last 4 years of my Ph.D, without their help and support this thesis would not have been possible.

I would first of all like to express my deepest gratitude to my supervisor, Prof. Afshin Samali, for his guidance, support and encouragement over the last 4 years. You have helped open the door to many opportunities for me in my career and you have always looked out for my best interests, I sincerely thank you for everything you have done.

I would like to thank Dr. Sanjeev Gupta for his support and knowledge which helped guide my project.

I would like to express many thanks to everyone in my lab; Karen Cawley, Donna Kennedy, Svetlana Saveljeva, Patricia Cleary and Susan Logue. Thank you guys for all your help and support both scientifically and personally.

Thank you Susan for your help with experiments over the last few months it really helped me out.

A special thanks to Svetlana Saveljeva who has worked so hard over the last few months to help me finish my Ph.D, it would not have been possible with out your help, thank you.

I would like to thank Dr. Adrienne Gorman and Dr. Eva Szegezdi their time help and expertise.

I would like to thank Dr. David MacDonald for carrying out the Electron Microscopy presented in this thesis.

I want to thank Tak Mak for providing me with Caspase-$9^{+/+}$ and Caspase-$9^{-/-}$ mouse embryonic fibroblasts (MEFs), Craig Thompson for providing Bax/$Bak^{+/+}$ and Bax/$Bak^{-/-}$ MEFs, Bert Volgestein for providing $Bax^{-/-}$ HCT116 cells and Alan Diehl for providing MDA-MB-468 PERK shRNA and PLKO stable cell lines.

Thank you to Genetech for providing the BV-6 Smac-mimetic.

I would like to thank Professor Peter Vandenabeele for his collaboration in this project and for welcoming me to his lab for 3 months. I would also like to thank him for providing me with caspase-8 shRNA, TRADD shRNA, FADD shRNA, TNFR1 shRNA, RIP1 miRNA and RIP3 miRNA expression plasmids.

Not forgetting my boys who have helped me keep my manhood over the years of working in a lab full of girls, especially Chris who has kept me on track when things didn't work, a few drinks solves everything. Not forgetting my non-science friends, Liam, thanks for all the IT support over the years, you saved me a bomb.

Also, thank you to everyone in the apoptosis reseach group, I have made many friends which has made the last 4 years a lot of fun.

None of this would be possible without the love and support of my amazing family; Mam, Dad, Nana, Grandad, Louise, Dave and Laura. Thank you sooooo much Mam (Caroline) and Dad (Aiden) for everything you have done to help me get to where I am today, you are amazing parents and you have instilled your best attributes into who I am today, I will never be able to thank you enough for everthing you have done for me. Thank you Nana (Mary) and Grandad (Tim), for all your love and support, you are the best grandparents anyone could ask for, you have always looked after us like your own children and I will be forever gratefull.

Most of all I would like to thank my amazing and beautiful girlfriend and best friend, Catriona. Thank you so much for all your love and support throughout this Ph.D, you have had to put up with all my bad moods over the last 4 years, of which their has been a few, but you were always able to get me out of them very quickly. Without you to come home to at the end of the day would have made the last 4 years very difficult, thank you sooo much for everything.

Publications

Published

Gupta, S., Z. Giricz, Natoni, A., Donnelly, N., **Deegan, S**., Samali, A. (2012). "NOXA contributes to the sensitivity of PERK-deficient cells to ER stress." FEBS Lett.

Deegan, S., S. Saveljeva, et al. (2012). "Stress-induced self-cannibalism: on the regulation of autophagy by endoplasmic reticulum stress." Cell Mol Life Sci.

Cawley, K., **S. Deegan**, et al. (2011). Assays for Detecting the Unfolded Protein Response. Methods in Enzymology. P. M. Conn, Academic Press. Volume 490**:** 31-51.

Gupta, S., A. Deepti, **S. Deegan**, F. Lisbona, C. Hetz, A. Samali. (2010). "HSP72 protects cells from ER stress-induced apoptosis via enhancement of IRE1alpha-XBP1 signaling through a physical interaction." PLoS Biol **8**(7): e1000410.

Samali, A., U. Fitzgerald, **S. Deegan**, S. Gupta. (2010). "Methods for monitoring endoplasmic reticulum stress and the unfolded protein response." Int J Cell Biol 2010: 830307.

In preparation

Deegan, S. et al. (2012). "Unmasking of a novel death pathway." Mol Cell.

Abstract

Autophagy is tightly regulated by the unfolded protein response (UPR). It plays an important role in the removal of unfolded proteins, damaged mitochondria and expanded endoplasmic reticulum (ER), to help relieve ER stress and reinstate homeostasis. However, when persistent, ER stress responses can switch the cytoprotective functions of UPR and autophagy into cell death promoting mechanisms. Depending on the cellular context, autophagy can either serve as a cell survival pathway, suppressing apoptosis, or it can lead to death itself. Although most cells primarily use apoptosis as a mode of cell death it is often not an option in many types of cancers and thus it is important to explore how the cell regulates other forms of cell death. The objective of this project was to determine the mode of ER stress-induced cell death in cells where the mitochondrial apoptotic pathway is compromised, and investigate how autophagy influences cell death in these conditions. For this we used caspase-$9^{-/-}$ mouse embryonic fibroblasts (MEFs), Bax/$Bak^{-/-}$ MEFs and $Bax^{-/-}$ HCT116 colon carcinoma cell line. Here we show that ER stress induces two phases of cell death, the first of which is rapid, caspase-9-dependent apoptosis and the second is a slow caspase-9-independent cell death. Further we show that the caspase-9-independent cell death is executed through a caspase-8 mediated activation of the executioner caspases. Inhibition of caspase-8 further delayed cell death however did not completely rescue the cells. Combination of caspase-8 knockdown and addition of the RIP1 kinase inhibitor, necrostatin-1, showed almost a complete rescue from cell death, further these cells were able to proliferate following removal of the drug. Interestingly knockdown of ATG5 in caspase-$9^{-/-}$ MEFs inhibited the activation of the executioner caspases and reduced the levels of cell death, implicating ATG5 as an essential component for caspase-8 activation in this model. To this end we carried out immunoprecipitation of endogenous ATG5 and showed its interaction with caspase-8, RIP1 kinase and FADD. For the first time we have identified a RIP1-containing death inducing protein complex assembled in response ER stress which executes cell death in conditions where the intrinsic pathway is compromised; furthermore we show that the formation of this complex is dependent on the autophagy protein, ATG5.

In addition to this, we studied the interplay between the UPR and autophagy during ER stress. We carried out a microarray analysis in HCT116 cells and identified the transcriptional upregulation of an array of autophagy related genes. These genes included the autophagy receptors NIX, NBR1 and p62 and were confirmed by real-

time RT-PCR. We further demonstrated that these genes were transcriptionaly upregulated by the PERK arm of the UPR, instigating ER stress-induced autophagy as a selective process.

The data presented in this thesis show that in conditions where the intrinsic mitochondrial-mediated apoptotic pathway is compromised, exposure of cells to multiple stress stimuli will execute death via alternative means. We show that this caspase-9 independent cell death requires RIP1 kinase, FADD, ATG5 and caspase-8. Further we show that depending on the cellular context, cell death can be executed through apoptosis or necroptosis. Inhibiting components of the apoptotic pathway or the necroptotic pathway independently does not completely inhibit cell death; however, coperativly inhibiting these two processes results in a significant resistance from cell death. In addition to these findings, a microarray analysis showed that the autophagy process in reponse to ER stress is highly regulated by the UPR. We focused our study on the autophagy receptor proteins and showed that these proteins are transcriptionally upregulated in response to ER stress. Further we show the PERK arm of the UPR is responsible for their transcriptional upregulation.

Abbreviations

3MA	3-Methyladenine
ACD	Autophagic cell death
ADP	Adenosine diphosphate
Alfy	Autophagy-linked FYVE-domain protein
AMPK	AMP-activated protein kinase
APAF1	Apoptotic protease activating factor 1
ARE	AU-rich element
ASK1	Apoptosis signal-regulating kinase 1
ATF4	Activating transcription factor 4
ATF6	Activating transcription factor 6
ATG	Autophagy-related Genes
ATP	Adenosine triphosphate
Bak	Bcl-2 homologous antagonist/killer
Bax	Bcl-2–associated X protein
Bcl-2	B-cell lymphoma 2
Bfa	Brefeldin A
BH3	Bcl-2 homology domain 3
BIF1	Bax interacting factor 1
BIR	Baculovirus IAP repeat
BNIP3	BCL2/adenovirus E1B 19kD-interacting protein 3
BNIP3L	BCL2/adenovirus E1B 19kD-interacting protein 3-like
Brtz	Bortezomib
Ca^{2+}	Calcium
CaMK	Ca^{2+} /calmodulin-dependent protein kinases
CARD	Caspase recruitment domains
cDNA	Complementary DNA
cFLIP	Cellular FLICE-like inhibitory protein
cFLIPL	Cellular FLICE-like inhibitory protein long isoform
cFLIPs	Cellular FLICE-like inhibitory protein short isoform

Chop	C/EBP-homologous protein
COPII	Coat protein 2
CQ	Chloroquine
DAPK	Death-Associated Protein kinase
DD	Death domain
DED	Death effector domain
DEPTOR	DEP domain containing mTOR-interacting protein
DFCP1	Double FYVE domain-containing protein
DIABLO	Direct IAP-Binding protein with Low PI
DISC	Death inducing signalling complex
DMEM	Dulbecco's Modified Eagle Medium
DMSO	Dimethyl sulfoxide
DNA	Deoxyribonucleic acid
dNTPs	Deoxyribonucleotide triphosphate
DR	Death receptor
DRAM	Damage-regulated autophagy modulator
DTT	Dithiothreitol
EDEM1	ER degradation enhancer, mannosidase alpha-like 1
eIF2α	Eukaryotic initiation factor 2 alpha
ER	Endoplasmic Reticulum
ERAD	ER-associated degradation
ERO1α	ER oxidoreductin 1 alpha
ERP72	Endoplasmic reticulum resident protein 72
ERSE	ER stress response element
Etop	Etoposide
FADD	Fas-associated protein with death domain
FIP200	FAK family kinase-interacting protein of 200 kDa
FoxO1	Forkhead box protein O1
FYCO	FYVE and coiled-coil domain containing

GABARAPS	Gamma-aminobutyric acid receptor-associated protein
GADD153	Growth arrest and DNA damage-inducible gene 153
GCL	Glutamate cysteine ligase
GRP78	Glucose regulated protein 78kDa
GST	Glutathione S-transferase
HERP	Homocysteine-inducible endoplasmic reticulum (ER) stress prote
HSPA5	Heat shock 70kDa protein 5
IAP	Inhibitor of apoptosis
IB	Immunoblotting
IBM	IAP-binding motif
iDISC	Intracellular death inducing signalling complex
IFNγ	Interferon-gamma
IKK-γ	Inhibitor of nuclear factor kappa-B kinase subunit gamma
IP	Immunoprecipitation
IP3R	Inositol trisphosphate receptor
IRE1	Inositol-requiring enzyme 1
JNK	c-JUN NH2-terminal kinases
KEAP1	Kelch-like ECH-associated protein 1
LAMP	Lysosomal-associated membrane protein
LC3	Microtubule-associated protein light chain 3
LIR	LC3 interacting region
LUBAC	Linear Ubiquitin Chain Assembly Complex
MAPK	Mitogen-activated protein (MAP) kinases
MAPs	Microtubule-associated proteins
MEFs	Mouse embryonic fibroblasts
MMA	Mitochondrial-mediated apoptosis
MOMP	Mitochondrial outer-membrane permeabilization
mRNA	Messenger Ribonucleic acid
mTOR	mammalian target of rapamycin

NBR1	Neighbor of BRCA1 gene 1 protein
Nec-1	Necrostatin-1
NEMO	NF-kappa-B essential modulator
NFkB	Nuclear factor kappa-light-chain-enhancer of activated B cells
NLS	Nuclear localization signal
NRF2	Nuclear factor erythroid 2-related factor 2
P58IPK	58-kilodalton inhibitor of protein kinase
PARP	Poly (ADP-ribose) polymerase
PAS	Pre-autophagosomal structure
PCR	Polymerase chain reaction
PDI	Protein disulphide isomerase
PE	Phosphatidylethanolamine
PERK	Pancreatic ER kinase (PKR)-like ER kinase
PI	Propidium Iodide
PI3K	Phosphatidylinositol 3-kinases
PI3P	Phosphatidylinositol 3-phosphate
PIDD	p53-induced protein with a death domain
PINK1	PTEN-induced putative kinase 1
PP2A	Protein phosphatase 2A
PRAS40	Proline-rich Akt substrate, 40 kDa
RAIDD	RIP-associated ICH-1/CED-3-homologous protein with a death domain
Raptor	Regulatory associated protein of mTOR
REDD1	Regulated in development and DNA damage responses 1
RING	Really Interesting New Gene
RIP	Receptor-Interacting Protein
RNA	Ribonucleic acid
ROS	Reactive oxygen species
S1P	Site-1 protease
S2P	Site-2 protease

SERCA	Sarcoendoplasmic reticulum (SR) calcium transport ATPase
SIRT1	Sirtuin 1
SMAC	Second Mitochondria-derived Activator of Caspases
SQSTM1	Sequestosome 1
Tg	Thapsigargin
Tm	Tunicamycin
TNF	Tumor necrosis factor
TNFR1	TNF receptor 1
TRADD	Tumor necrosis factor receptor (TNFR)1–associated death domain protein
TRAF2	TNF receptor-associated factor 2
TRAIL	The tumour necrosis factor (TNF) related apoptosis-inducing ligand
TRAILR	The tumour necrosis factor (TNF) related apoptosis-inducing ligand receptor
TRB3	Tribbles homolog 3
UBL	Ubiquitin-like proteins
ULK	Unc-51-like kinase
UPR	Unfolded Protein Response
UPRE	UPR element
UVRAG	UV radiation resistance-associated gene protein
Vps34	Vacuolar protein sorting-associated protein 34
WIPI	WD repeat domain phosphoinositide-interacting protein
XBP1	X-box binding protein 1
XBP1s	X-box binding protein 1 spliced
XIAP	X-linked inhibitor of apoptosis

Chapter 1: Introduction

1.1 Endoplasmic Reticulum

The endoplasmic reticulum (ER) is a very complex and elaborate cellular organelle. It is composed of a single continuous phospholipid membrane that is comprised of the outer nuclear envelope, flattened peripheral sheets with ribosomes (rough ER) and a complex network of smooth tubules (smooth ER) that extend throughout the cell. The ER has many different cellular functions which are accommodated by its heterogeneous structures. While detoxification of drugs, fatty acid and steroid biosynthesis and Ca^{2+} storage occurs in the smooth ER, most of the folding and post-translational processing of membrane bound and secreted proteins takes place in the rough ER. It contains an array of chaperone systems such as glycosidases, Ca^{2+}-dependent chaperones and members of the protein disulphide isomerase (PDI) family. These chaperones are responsible for the correct folding of proteins under normal physiological conditions[1]. This process is highly sensitive and is dependent on ER luminal factors such as Ca^{2+} concentration, redox homeostasis and oxygen supply[2]. The processing of nascent proteins in the ER lumen requires an array of chaperones and folding enzymes that depend on the ER's rich oxidizing environment and Ca^{2+} pools to function optimally. Physiological or pathological conditions that disrupt this fine balanced, unique environment cripples the ER's protein folding machinery and results in a condition referred to as ER stress.

1.2 Endoplasmic Reticulum Stress

The cellular responses to ER stress are multifaceted and include the activation of a set of signaling pathways termed the unfolded protein response (UPR), a catabolic process termed autophagy, and cell death[3]. These processes are not mutually exclusive, and there is significant cross-talk between these cellular stress responses.

The UPR's primary aim is to sustain cell survival by attenuating protein synthesis and restoring cellular homeostasis via the activation of a cascade of transcription factors which regulate expression of genes encoding for chaperones, components of the ER-associated degradation (ERAD) system and components of the autophagy machinery[4].

1.3 Unfolded Protein Response Signaling

Disturbances in the ER's homeostatic environment disrupts the protein folding machinery and results in an accumulation of unfolded proteins in the ER lumen, thus activating the UPR.

The UPR is orchestrated by three ER transmembrane receptors - pancreatic ER kinase (PKR)-like ER kinase (PERK), activating transcription factor 6 (ATF6) and inositol-requiring enzyme 1 (IRE1) (Fig. 1.1). In resting cells all three UPR receptors are kept inactivate through their association with the ER chaperone, glucose regulated protein 78 kDa (Grp78; also known as BiP or HSPA5). Upon ER stress, unfolded proteins accumulate in the ER lumen resulting in the dissociation of Grp78 from PERK, IRE1 and ATF6, subsequently activating the UPR[5,6].

1.3.1 PERK

PERK (EIF2AK3) is a type I ER transmembrane protein with serine/threonine kinase activity. Its N-terminus is in the ER lumen, involved in the regulation of its dimerization, and is kept inactive through interaction with Grp78, while the C-terminus is cytosolic and harbors its autophosphorylation sites and the kinase domain. Upon release of Grp78, in response to accumulated proteins in ER lumen, PERK homodimerizes and subsequently trans-autophosphorylates for activation.

PERK mediates the phosphorylation of the α sub-unit of eukaryotic initiation factor 2 (eIF2α) resulting in translation attenuation of mRNAs with a 5' cap. The proteins encoded by these mRNAs are generally destined to be involved in cell growth and proliferation[7], thus eIF2α phosphorylation reduces the protein load in the ER and attenuates cell growth and proliferation[7]. eIF2α phosphorylation results in non-canonical translation of ATF4 mRNA via an open reading frame in its 5'-untranslated region that is bypassed only when eIF2α is inactivated[8]. ATF4 mRNA encodes for a cAMP response element binding transcription factor which activates a number of genes which play roles in amino acid metabolism, redox balance, protein folding, autophagy and apoptosis[5,9,10]. Although ATF4 is an essential player in the pro-survival response of the UPR, it also plays a key role in the pro-death response via the transcriptional upregulation of C/EBP-homologous protein (CHOP) which is also called growth arrest and DNA damage-inducible gene 153 (GADD153)[11].

CHOP is reported to downregulate Bcl-2[12] and upregulate transcription of certain BH3-only proteins[13,14]. This event favors Bax/Bak activation which leads to mitochondrial outer-membrane permeabilization (MOMP) and initiation of the intrinsic apoptotic cascade[15]. Furthermore, CHOP knockout mice show lower rates of apoptosis in response to ER stress[16] Although CHOP is thought to be a major factor in determining cell fate in response to ER stress it is clear that other factors are also involved (for review see 17).

Another PERK substrate is the transcription factor, nuclear factor erythroid 2-related factor 2 (NRF2), required for free radical scavenging, detoxication of xenobiotics and maintenance of redox potential[17]. PERK phosphorylates NRF2 and causes its nuclear translocation upon dissociation from KEAP1[18]. Known targets of NRF2 are closely associated with redox homeostasis, and include glutamate cysteine ligase (GCL), both catalytic and modulatory subunits, hemeoxygenase-1, and glutathione S-transferase (GST) isoforms[19]. These genes contain AU-rich elements (AREs) in their promoter region which is recognized by NRF2, and are also believed to be activated by ATF4 in response to ER stress, suggesting that these two transcription factors can act in synergy[20].

1.3.2 ATF6

ATF6 is a type II transmembrane receptor and a member of the leucine zipper protein family, that is synthetized as an ER membrane-tethered precursor, with its C terminal domain located in the ER lumen and its N-terminal DNA-binding domain facing the cytosol [21]. There are two isoforms of ATF6, ATF6α and β. Upon ER stress Grp78 dissociates from ATF6, unmasking its two Golgi localization signals, allowing ATF6 to interact with the protein trafficking complex COPII, which causes translocation of ATF6 to the Golgi for processing[22]. At the Golgi the 90 kDa ATF6 protein is cleaved by Site-1 protease (S1P) and Site-2 protease (S2P) into its active 50 kDa fragment which translocates to the nucleus where it acts as a transcription factor[23,24].

Activated ATF6 is responsible for the transcriptional upregulation of XBP1 mRNA which subsequently undergoes processing by IRE1 (see below) to produce a spliced XBP1s mRNA which encodes an active transcription factor[25]. ATF6, together with XBP1, are capable of binding to the cis acting response elements, ER stress response

element (ERSE) and UPR element (UPRE), activating the expression of ER-localized chaperones[26]. Although, the expression of ATF6 alone is enough to fully activate transcription from ERSE, in contrast to the ability of XBP1s to fully activate the UPRE[27]. Moreover, activation of ATF6 has also been described to regulate an array of miRNAs to alleviate ER stress[28].

1.3.3 IRE1

IRE1 (ERN1) is a type I ER transmembrane protein containing a serine/threonine kinase domain and an endoribonuclease. There are two IRE1 isomers in humans, IRE1α and IRE1β. IRE1α is ubiquitously expressed, whereas IRE1β expression is restricted to the epithelial cells of the intestine and the lungs. Most of our understanding of IRE function is based on studies of IRE1α.

IRE1 is the most conserved branch of the UPR, and has been suggested to play a role in processes such as development, metabolism, immunity, inflammation and neurodegeneration[29]. Upon activation, IRE1 is known to be oligomerize through self-assembly of the cytosolic region, leading to RNase activation. It has been shown that IRE1 oligomers consist of more than four molecules and upon attenuation of its signaling during unmitigated ER stress IRE1 clusters dissociate, the kinase is dephosphorylated and its endoribonuclease activity is decreased[30]. Auto-phosphorylation at serine724 and ADP binding are other events that can be observed upon initiation of the signaling cascade[31]. Activation of IRE1 is closely associated with pro-survival pathway, providing cells an opportunity to readjust to unfavorable conditions, that cause increase in the amount of unfolded proteins[32,33]. IRE1 transmits the UPR signal through excision of a 26 base nucleotide intron from X-box-binding protein 1 (XBP1) mRNA, which is then ligated by an uncharacterized RNA ligase and translated to produce XBP1s[31]. XBP1s is widely recognized as an important pro-survival gene in the UPR artillery. XBP1s transcriptional activity leads to the translation of stable transcription factors involved in the activation of ER regulatory proteins[34]. XBP1s has been shown to be crucially important for the activation of unfolded protein response element (UPRE), controlling the expression of the ER-associated degradation system, helping to degrade unfolded proteins in the ER[27]. Interestingly, acetylation of XBP1 by p300 and deacetylation by sirtuin 1

(SIRT1) have recently been shown to provide posttranslational modifications that can enhance or inhibit XBP1 transcriptional activity[35].

In addition to its ribonuclease activity, the cytoplasmic part of IRE1 is known to bind tumor necrosis factor-α (TNF-α) receptor-associated factor 2 (TRAF2), resulting in activation of c-JUN NH_2-terminal kinases (JNK)[36]. This is one of the mechanisms necessary for the activation of nuclear factor-κB (NF-κB) upon ER stress[37].

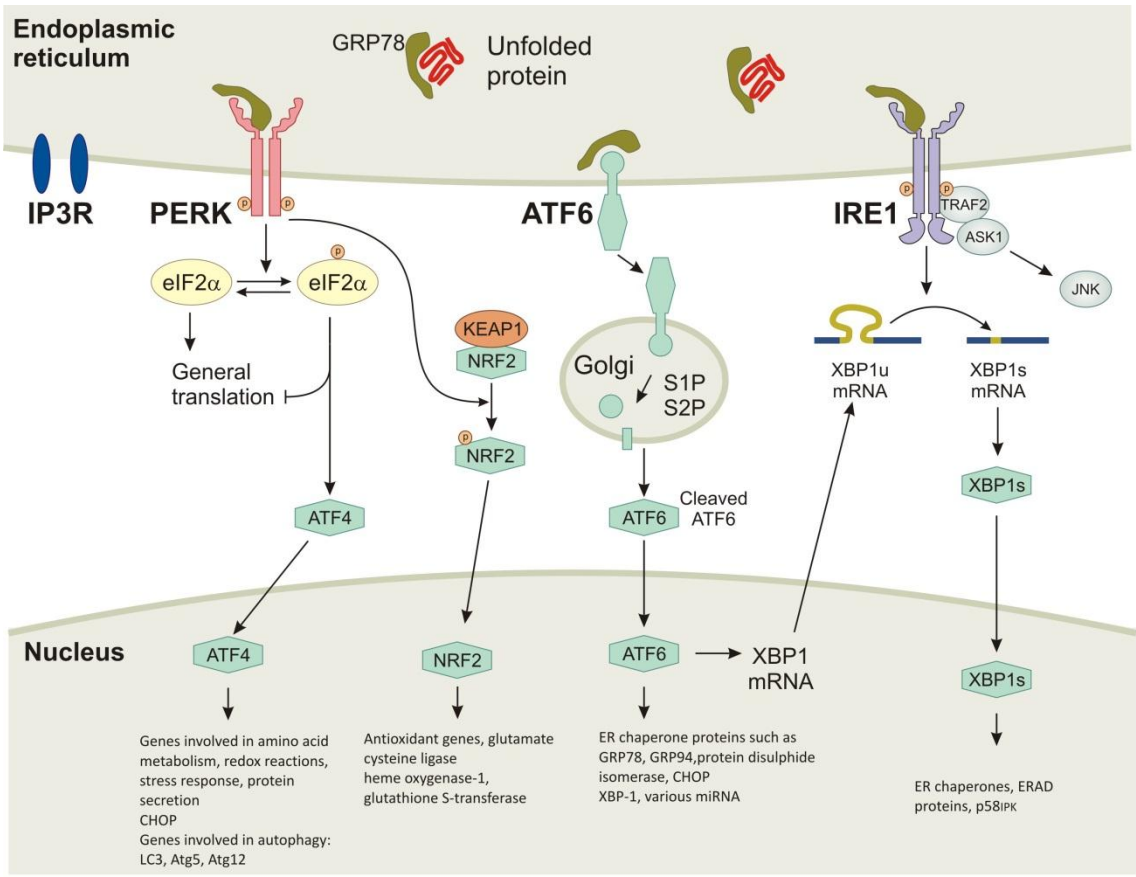

Figure 1.1: The accumulation of unfolded protein in the ER lumen results in the dissociation of Grp78 from the three UPR sensors PERK, ATF6 and IRE1. Following Grp78 dissociation PERK dimerizes and autophosphorylates, activating its cytosolic kinase domain. PERK phosphorylates EIF2α inhibiting general protein synthesis and facilitating/permitting non canonical translation of ATF4 mRNA. Active PERK also phosphorylates NRF2 resulting in its dissociation from KEAP1, allowing NRF2 to translocate to the nucleus. Activation of ATF6 leads to its translocation to the Golgi where it is processed by site 1 and site 2 proteases (S1P and S2P) into an active transcription factor which results in the transcription of XBP1 mRNA. Activation of IRE1 results from its dimerization and autophosphorylation in a manner similar to PERK. IRE1 contains an endoribonuclease domain which processes unspliced XBP1 mRNA. Spliced XBP1 (XBP1s) mRNA is translated into an active transcription factor. IRE1 also possesses a kinase domain that recruits TRAF2 and ASK1 leading to the activation of JNK (from Deegan *et al.*[38]).

1.4 Autophagy

Macroautophagy (hereafter referred to as autophagy), is an evolutionarily-conserved, lysosomal-mediated system for bulk degradation of proteins, organelles and cellular components. Autophagy was first coined in 1966 by Christian de Deuve, who identified double membraned structures during his studies of mammalian cells using electron microscopy[39]. However, the molecular machinery of autophagy was extensively characterized for the first time in yeast by Yoshinori Ohsumi[40], and later was found to be evolutionarily conserved following the identification of the mammalian orthologues of yeast autophagy genes[41].

Autophagy is characterized by the induction of a small isolation membrane which elongates into a vacuole with a double membrane, capable of engulfing large amounts of cytosolic components such as unfolded protein aggregates, damaged organelles and invading pathogens such as bacteria[42]. Autophagy is ongoing at basal levels in eukaryotic cells allowing the cell to function optimally by removing unwanted substrates which may otherwise lead to cellular toxicity[43-45]. Eukaryotic cells are continuously exposed to environmental changes which inflict minor stresses on the cell, disrupting its homeostatic environment. These constant fluctuations in the cell's environment can result in the accumulation of misfolded protein aggregates, reactive oxygen species (ROS) and damaged organelles.

While basal autophagy activity is important for general maintenance of cellular homeostasis defective autophagy may lead to cellular transformation and subsequent tumorigenesis. The exact mechanism of how defective autophagy results in tumorigenesis is still unclear; however, mounting evidence implicates autophagy as a tumor suppressor mechanism required for such events as cell death, senescence and maintenance of metabolic stress, all of which are overcome for tumorigenesis to progress (for review see [46]). Autophagy is also very important during various, more acute, cellular stress responses[41]. Autophagy is dramatically increased in response to cellular stress such as starvation, hypoxia, heat shock, microbial infection and ER stress[44]. During cellular stress large quantities of proteins are damaged resulting in their unfolding/misfolding and aggregation that accumulate and if they are not rapidly dealt with they can ultimately induce apoptosis. Autophagy's robust and

efficient removal of these toxic factors can help relieve the cell of the stress and reinstate homeostasis[45].

The autophagic process requires the induction of a double membrane which is subsequently elongated by two specialized ubiquitin-like conjugation systems. The expanding double membrane is capable of engulfing large amounts of cytoplasmic components such as unfolded proteins, protein aggregates and organelles. This elongated double membrane encloses to form a cytosolic dense, double-membraned vacuole termed an autophagosome. The mature autophagosome binds to a lysosome forming an autolysosome, where the autophagosome's contents are released into the lysosomal lumen and degraded by resident cathepsins (Fig. 1.2)[43,44]. The autophagic pathway is a very complex process, involving over 34 known proteins to assemble the machinery[47]. Here we will discuss the different stages of the autophagy pathway (autophagy induction, vesicle nucleation, origin of the phagophore, autophagosome elongation and maturation of the autophagosome), and bring to light the complexity of this unique process.

1.4.1 Autophagy Induction

1.4.1.1 ATG1/ULK Induction complex:

The induction of autophagy requires the activation of the ATG1/ULK Induction complex, a complex which consists of four known proteins, ULK1/2, mATG13, FIP200 and ATG101[47]. This complex is essential for the induction of a small double membrane known as a phagophore or an isolation membrane. The phagophore eventually matures into a double-membraned vacuole termed an autophagosome via an elongation step involving two conjugation systems[48-50]. The induction complex is regulated by two kinases, mammalian target of rapamycin (mTOR) complex (mTORC) 1 and adenosine monophosphate-activated protein kinase (AMPK), via a series of phosphorylation events[51,52]. It has long been established that mTOR is a key kinase in the regulation of autophagy[48]. It exists in two different complex forms, mTORC1 and mTORC2. mTORC1 is involved in autophagy regulation and the complex is made up of mTOR, Regulatory Associated Protein of mTOR (Raptor), mammalian LST8/G-protein β-subunit like protein (mLST8/GβL) and the recently identified partners PRAS40 and DEPTOR[53]. mTORC1 is incorporated into the ATG1/ULK induction complex and phosphorylates mATG13 and ULK1/2,

maintaining the complex in an inactive state during normal resting conditions[54]. The phosphorylation of ULK1 by mTORC1 on serine757 has been shown to destabilize AMPK binding. AMPK is the main sensor of intracellular energy under conditions of starvation or environmental stresses[52]. AMPK has been recently shown to play a crucial role in the positive regulation of the induction complex. Six AMPK phosphorylation sites have been identified on ULK1 (S467, S555, T574, S637, S777, S317) which all result in the activation of ULK1. AMPK can also negatively regulate mTORC1 via the tuberous sclerosis complex (TSC) to relieve mTORC1 inhibitory effects on ULK1[51,52]. Taken together, it is believed that ULK1 activation occurs in a stepwise series of phosphorylation events. First mTORC1 is inactivated, resulting in the dephosphorylation at serine757 which facilitates AMPK binding. AMPK then activates ULK1 via a series of phosphorylation events. To add further complexity to this process, active ULK1 is capable of relaying feedback messages to both mTORC 1 and AMPK. It phosphorylates mTORC 1 resulting in its inactivation and thus amplifying the positive regulation of ULK1[55]. In contrast, ULK1 has also been shown to phosphorylate AMPK's three subunits resulting in its inactivation and thus resulting in a negative feedback loop to ULK1[56]. It is clear that there is great complexity in the regulation of the induction complex, and different stress responses may result in different phosphorylation events to activate ULK1 (for review see[57])

1.4.2 Vesicle Nucleation

1.4.2.1 PI3K complex:

The induction of the isolation membrane via the ATG1/ULK induction complex requires the activation of the PI3K complex (also known as the beclin1 complex) for vesicle nucleation, expansion and curvature of the membrane. Mammalian cells have two forms of the PI3K complex, PI3K complex I and II. The PI3K complex I consists of the class III PI 3-kinase Vps34, p150, Beclin 1 and ATG14L. ATG14L has been shown to increase stability of Beclin 1 and Vps34 and functions as the mediator which recruits the PI3K complex I to the isolation membrane. PI3K complex II consists of Vps34, p150, Beclin 1 and UVRAG (UV radiation resistance-associated genes), ATG14L does not associate with this complex. UVRAG interacts with BIF1 and localizes to the isolation membrane. BIF1 has an N-BAR domain which has been shown to bind membranes and cause them to undergo curvature.

PI3K complex I regulates nucleation and PI3K complex II is involved in the expansion and curvature of the membrane[58].

Inhibitors of PI3K complex such as 3-methyladenine (3MA), wortmannin and LY294002 result in complete inhibition of autophagosome formation, thus emphasising the importance of the PI3K complex in the autophagy process. A lot is still unknown about how this complex regulates autophagy; however it is clear that phosphatidylinositol 3-phosphates (PI3Ps) play an important role in the signalling process. WD repeat proteins interacting with phosphoinositides (WIPI1 and WIPI2), autophagy-linked FYVE protein (Alfy) and double FYVE domain-containing protein (DFCP1) have all been reported to play important roles in the autophagy process and all require phosphatidylinositol 3-phosphate signalling for their recruitment to the phagophore. The exact function of these proteins is still to be fully elucidated. However, it is likely that they play a role in scaffolding and signalling for other autophagy machinery proteins[59-62].

1.4.3 Origin of the phagophore

The origin of the autophagic membrane has been a subject of debate for many years. Many hypotheses have been formed to explain the origin of the phagophore (also known as the isolation membrane), including suggestions that it originates from already formed membrane structures, such as the ER, the Golgi and the mitochondria, or that it is formed through *de novo* synthesis.

Early publications investigated the origin of the phagophore by fractionating the autophagosomes from rat hepatocytes and carrying out biochemical assays such as immunoblotting for protein markers of various membrane structures in the cell. These studies did not identify any positive markers and thus hypothesized that the autophagosome was in itself a unique organelle and thus was generated via *de novo* synthesis[63,64]. However, major advances in microscopy techniques and identification of new autophagy markers led to new insights into the origin of the phagophore which refuted earlier studies. Recent publications have convincingly described the phagophore originating from structures in the ER membrane termed ‘omegasomes’[61], as well as from the mitochondria[65] and the plasma membrane[66] (reviewed in 66). It is likely that the phagophore’s origin is not from a unique location in the cell, and that, depending on the stress, cell type, or the extent of

autophagy required all of these structures may contribute to the formation of the phagophore.

1.4.4 Autophagosome Elongation

The elongation of the phagophore requires two ubiquitin-like conjugation systems, the ATG12-ATG5 conjugation system and the ATG8 conjugation system.

1.4.4.1 Atg12-Atg5 conjugation system

The UBL proteins, ATG12 and ATG5, are essential players in the elongation of the pre-autophagosomal structure (PAS). The covalent conjugation of ATG12 to ATG5 is mediated by the E1 enzyme ATG7 and the E2 enzyme ATG10[47]. This complex further interacts with ATG16L through ATG5. ATG16L function is not entirely known, however because its C-terminal contains seven WD repeats it is believed to serve as a platform for protein-protein interaction at the autophagosomal membrane[67].

Recruitment of ATG12-ATG5-ATG16L complex to the autophagsomal membrane requires the formation of phosphatidylinositol 3-phosphate by the PI3K complex, however the exact mechanism for its recruitment is unknown.

1.4.4.2 ATG8 conjugation system

The UBL protein ATG8 is another major player in the elongation of the PAS. In contrast to yeast which contains only one ATG8 protein, mammals express a family of mATG8 proteins which is subdivided into LC3s and γ-aminobutyric acid receptor-associated proteins (GABARAPS). The mATG8 family proteins are translated as pro-forms which are subsequently cleaved at the C-terminal region by the protease ATG4, exposing a glycine residue. The E1 enzyme, ATG7, and the E2 enzyme, ATG3, facilitate the binding of a phosphatidylethanolamine (PE) to mATG8s exposed glycine residue via the PE amino group.

The lipidated form of ATG8 is recruited to the autophagosomal membrane, and is thought to require the ATG12-ATG5-ATG16 complex as a platform.

1.4.5 Maturation of the Autophagosome

The final stage in the autophagy pathway is the transport and fusion of the mature autophagosome to the lysosome. The trafficking of the autophagosome to the lysosome is facilitated by the cytoskeleton, specifically the microtubule network.

The FYVE protein, FYCO, functions as an adaptor protein between autophagosomes and the microtubule network to promote the trafficking of autophagosomes on the lysosome. Multiple binding partners of FYCO have been identified at the autophagosomal membrane. A complex between FYCO, phosphatidylinositol 3-phosphate, Rab7 and LC3 is believed to be formed on the autophagosomal membrane at the maturation stage. This adaptor complex is believed to bind to kinesins through FYCO and facilitate microtubule plus end–directed transport of autophagic vesicles[47,68].

It has been shown that fully formed autophagosomes can bind to early endosomes forming structures known as amphisomes, before binding to lysosomes. However, this stage of the autophagic pathway is not clearly understood and it remains unclear whether the endocytic pathway is required for autophagsomal degradation[47].

The binding of the autophagosome to the lysosome is facilitated by Rab7, which binds to LAMP1/2 on the lysosomal membrane. ATG9 is believed to be involved in the transport of the SNARE machinery, VAM9, VAM7 and Vti1b to the autophagosome to facilitate the fusion of the autophagosomal and lysosomal membranes[47].

1.4.6 Selective Autophagy

Until recently autophagy of organelles and protein aggregates was considered a non-selective process. However, identification of the autophagy receptor proteins provides compelling evidence for the selective targeting of cargo for autophagy[69]. Publications reporting selective autophagy include evidence for selective degradation of mitochondria (mitophagy), ER (ER-phagy/reticulophagy), ribosomes (ribophagy), peroxisomes (pexophagy), Golgi (crinophagy), endosomes (heterophagy), pathogens (xenophagy), aggresomes (aggrephagy) and lipids (lipophagy)[70-78]. It is becoming clear that autophagy is not as random as first perceived and can in fact be a relatively selective and regulated process. Despite this rising evidence, autophagy is still often described as a non-selective process, primarily in response to starvation. However, a study recently showed that autophagy due to starvation led to the degradation of proteins and organelles in a systematic, selective way and not in a non-selective bulk degradation manner[79].

There are several proteins which have been identified to be required for the selective removal of specific substrates, including the autophagy receptors p62, NBR1, NIX, NDP52, Smurf1/optineurin and c-Cbl. What differentiates these from other proteins involved in the selective removal of substrates is the presence of the LC3-interacting region (LIR) which mediates the interaction with the autophagosome membrane bound LC3 family members LC3/GABARAP/GATE-16, as well as a domain which recognises the specific substrate to be targeted to the autophagosome[69,80,81].

The selective autophagosomal degradation of most substrates has been shown to require p62 and NBR1[82]. However for the selective removal of invasive pathogens, NDP52 and Smurf1/optineurin have been shown to be the important mediators for their targeting to the autophagosome[81,83]. Nix has only been shown to be involved in the selective removal of mitochondria, most prominently shown during reticulocyte differentiation[84,85]. Damaged or depolarized mitochondria have also been shown to be selectively removed by autophagy (mitophagy). This process also relies on Nix for their removal; however, it also requires the kinase PINK1 and the E3 ligase Parkin for the 'priming' of the mitochondria for their selective removal[86,87]. More recently c-Cbl has been described as an autophagy receptor protein following the identification of an LIR. C-Cbl has been shown to selectively target Src to the autophagosome in conditions where FAK is compromised, in turn preventing Src toxicity and promote cancer cell survival[80].

Autophagy receptor proteins are quite well characterized both structurally and functionally; however, very little is known about their regulation and the functional consequence of their absence during different stress responses. Further discovery of autophagy receptor proteins and new insights into the regulation of these proteins in response to cellular stress responses will advance the field of selective autophagy.

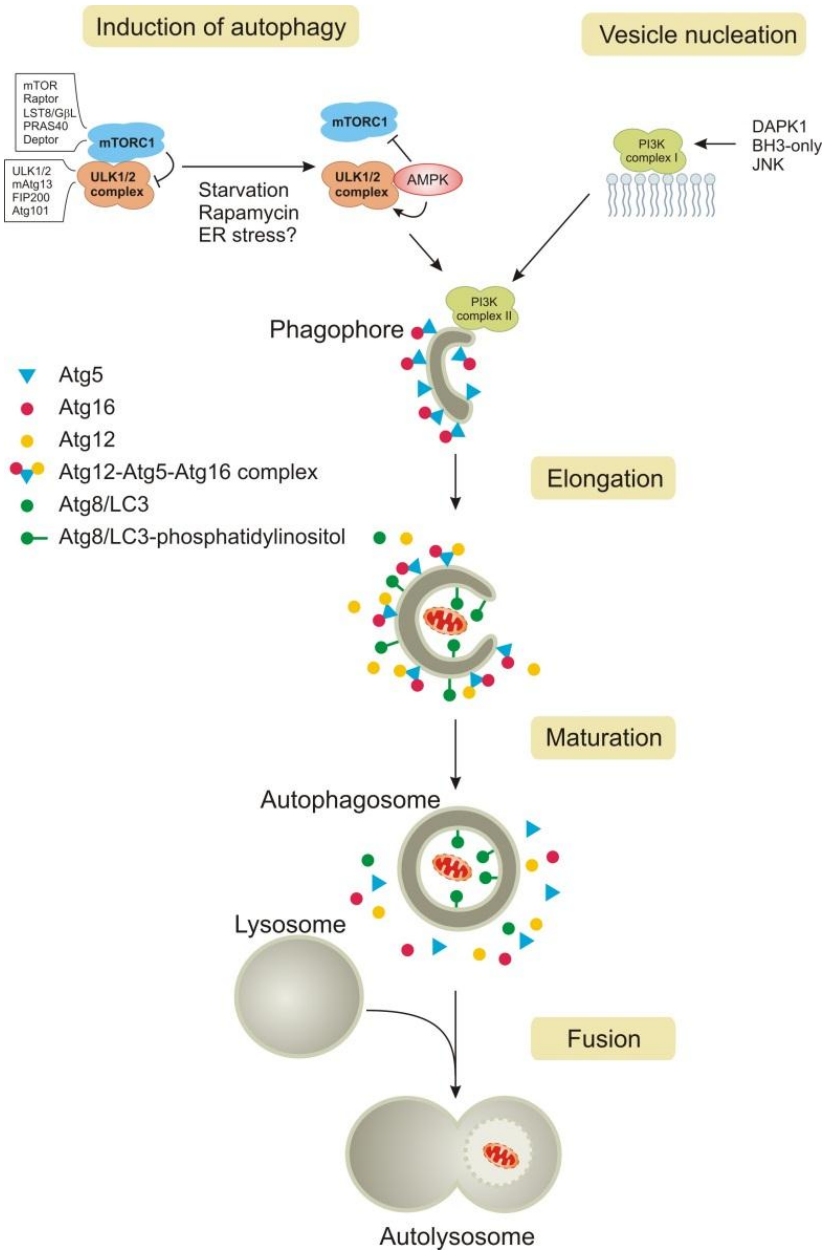

Figure 1.2: The autophagy pathway is divided into different phases; induction, vesicle nucleation, elongation, maturation, lysosomal fusion and degradation. Activation of the ULK1/2 complex requires mTORC1 inhibition and AMPK mediated phosphorylation of ULK1. This complex is essential for the initial induction of the phagophore. The PI3K complex (see text and Fig. 1.3) is activated upon Bcl-2/Bcl-xL dissociation from beclin's BH3 domain. PI3K complex I is required for the induction and nucleation of the phagophore whereas PI3K complex II is involved in the expansion and curvature of the autophagosomal membrane (see text for details). The elongation phase of the autophagsome requires the conversion of LC3I to LC3II and the formation of the ATG12-ATG5-ATG16 complex. LC3II and ATG12-5-16 complex are required for substrate specificity and scaffolding roles on the autophagosome. Upon maturation of the autophagosome, ATG12-5-16 and the outer membrane bound LC3II are recycled back in the cytosol. The mature autophagosome fuses with a lysosome where it is degraded by resident cathepsins (from Deegan *et al.*[38]).

1.5 Autophagy regulation by ER stress

ER stress and autophagy are individualy very elaborate and complex systems. It is well established that autophagy is upregulated in response to ER stress; however, very little emphasis is put on its importance as a mediator in relieving ER stress. Here we will describe what is known about how ER stress can affect various stages of autophagy including autophagy induction, vesicle nucleation and elongation of the phagophore and we will discuss/describe known autophagy machinery genes which are transcriptionaly upregulated by UPR signaling (Fig. 1.3).

1.5.1 Autophagy Induction

1.5.1.1 Calcium release:

As discussed earlier, the ER is the site of the cells Ca^{2+} stores and is required for the folding of nascent proteins by Ca^{2+}-requiring molecular chaperones in the ER lumen. The release of Ca^{2+} from the ER lumen to the cytosol can be both an inducer of ER stress or/and a result of ER stress. A commonly used pharmacological inducer of ER stress is thapsigargin, an inhibitor of the sarco/endoplasmic reticulum Ca^{2+} ATPase (SERCA) pump . Thapsigargin inhibits the reuptake of Ca^{2+} into the ER lumen and thus results in depletion of ER Ca^{2+}, resulting in malfunctioning ER chaperones and accumulation of unfolded proteins in the ER lumen.

An increase in cytosolic Ca^{2+} has been shown to lead to initiation of autophagy. Studies have also demonstrated that even $Ca_2(PO_4)_3$ precipitates, that are introduced to cells during transfections, are capable of specifically inducing autophagy in cells[88]. This process is mediated by Ca^{2+}/calmodulin-dependent kinase kinase-β which is activated in response to increased cytosolic Ca^{2+} and subsequent activation of AMPK[89]. AMPK in turn is involved in autophagy activation through inhibition of mTORC1 and direct phosphorylation of ULK1[8,90].

ER stress has been shown to be important in the modulation of this particular Ca^{2+} flux through inhibition of ER-resident Bcl-2. Under resting conditions ER-localized Bcl-2 is important for the maintainance of ER Ca^{2+} stores[91]. JNK-mediated phosphorylation of Bcl-2 affects the latter's ability to control the ER Ca^{2+} stores[92].

Another factor which contributes to ER stress-induced Ca^{2+} release is CHOP-mediated transcriptional upregulation of ER oxidoreductin 1 alpha (ERO1α).

ERO1α plays an essential role in the ER during resting conditions to provide an oxidative environment to facilitate disulfide bond formation by enzymes such as PDI during the folding of nascent proteins. Under these conditions ERO1α plays an essential protective role at the ER; however, at high levels ERO1α stimulates activity of the inositol 1,4,5-trisphosphate receptor (IP3R) resulting in the release of Ca^{2+} into the cytosol. Tabas' group have reported that CHOP-mediated transcriptional upregulation of ERO1α is required for Ca^{2+} release in response to ER stress and that knockdown of either CHOP or ERO1α prevents Ca^{2+} release and delays ER stress induced cell death[93]. ERO1α activation of IP3R is thought to be mediated independently of its oxidative ability. It is hypothesised that ERO1α activates IP3R via the sequestration of Erp44, a negative regulator of IP3R[94]. These findings may support the evidence that autophagy induction in response to fluctation in the cytosolic Ca^{2+} is directly regulated by ER stress in those conditions[89].

It is possible that a feedback mechanism between these two processes also exists, allowing autophagy to regulate the extent of ER stress-mediated autophagy through Ca^{2+} signaling. It has been shown that in T lymphocytes, defective in autophagy, ER Ca^{2+} stores are increased due to a defect in redistribution of stromal interaction molecule-1, resulting in ER expansion upon defective Ca^{2+} flux to those cells[95].

1.5.1.2 REDD1

The expression of Regulated in development and DNA damage responses 1 (REDD1; also known as DDIT4) mRNA is upregulated in response to an array of stress stimuli, including ER stress[96]. During ER stress REDD1 expression is regulated by the PERK-ATF4 arm of UPR. Experiments with $PERK^{-/-}$ and $ATF4^{-/-}$ MEFs demonstrated that ER stress failed to induce REDD1 mRNA in these cells[96]. In support of a role for PERK signalling in this process, overexpression of ATF4 in HEK293T cells was sufficient to induce upregulation of REDD1[96]. Moreover, further studies identified that activation of REDD1 during ER stress depends on ATF4 and its downstream effector CCAAT/enhancer-binding protein-β (C/EBP-β)[97]. REDD1 transactivation leads to inhibition of mTOR in a TSC1/TSC2-dependent manner, that will consequently activate the autophagic pathway upon the release of ULK1 from inactive mTOR[8,97,98].

1.5.1.3 Akt

PI3K-Akt signaling pathway is a positive regulator of mTORC1 and has been well described in a number of cell models and organisms[99,100]. The PI3K-Akt pathway is a pro-survival pathway involved in survival, cell growth and proliferation through the positive regulation of mTORC1. As described earlier, the PI3K-Akt pathway regulates mTORC1 activation[101].

ER stress results in the inactivation of the Akt pathway, contributing to the decrease of mTOR activity and subsequent autophagy induction[102,103]. The mechanism of how ER stress and the UPR can inhibit the Akt pathway is still unclear, however a few insights have been made.

The ER chaperone, Grp78 which is transcriptionally upregulated by ATF6, has been demonstrated to prevent phosphorylation of Akt at serine 473 and thus preventing Akt regulation of downstream kinases[104]. Grp78 was shown to interact with Akt at the plasma membrane in response to ER stress, however it is still unclear whether there is a direct interaction or if other factors are required[104,105].

Tribbles homolog 3 (TRB3) is a negative regulator of the Akt signaling pathway. TRB3 is transcriptionaly upregulated in response to ER stress through CHOP and ATF4 working in concert[106]. TRB3 has been shown to direcly bind to Akt and inhibit its downstream signaling[107]. Knockdown studies demonstrated that both ATF4 and CHOP are required for the transcriptional upregulation of TRB3. However, high protein levels of TBR3 result in a negative feedback loop by binding to ATF4 and CHOP and targeting them for degradation[106,107].

1.5.2 Vesicle Nucleation

1.5.2.1 CHOP

PI3K complex is required for PAS induction and vesicle nucleation. As previously discussed, Beclin 1 is a core component of the PI3K complex and can be tightly regulated by anti-apoptotic Bcl-2 family members [108,109]. CHOP expression during ER stress is tightly correlated with the inhibition of Bcl-2 expression both at the protein and transcript level providing a direct link between ER stress and Beclin 1 activation[110,111].

1.5.2.2 JNK

In response to ER stress, IRE1 kinase domain recruits the adaptor molecule TRAF2. Apoptosis-signal-regulating kinase (ASK1) is recruited by the IRE1-TRAF2 arm where it mediates signaling by MAP kinases, JNK and p38[112]. JNK activation results in phosphorylation of pro-apoptotic proteins enhancing their activity and also phosphorylates anti-apoptotic Bcl-2 inhibiting its activity[113,114]. Under cellular resting conditions PI3K remains in an inactive state due to the association of the anti-apoptotic proteins Bcl-2 and Bcl-X_L with Beclin's BH3 domain. JNK-dependent phosphorylation of Bcl-2 and Bcl-X_L results in their dissociation from Beclin's BH3 domain and the activation of the PI3K complex[115].

Study of cells deficient in IRE1, ATF6 or PERK showed that IRE1 plays a significant role in induction of autophagy, as measured by the intensity of LC3 puncta formation and LC3-I conversion to LC3-II[116]. In this report, the importance of transient JNK activation was highlighted in the promotion of pro-survival autophagy against prolonged autophagy that leads to initiation of apoptosis[117]. Independent studies, using dihydrocapsaicin treatments, confirmed that ER stress-induced autophagy relies heavily on transient activation of JNK signaling[118].

1.5.2.3 DAPK1

Death-associated protein kinase 1 (DAPK1) is a calcium/calmodulin (CaM)-regulated serine/threonine kinase. DAPK1 is activated in response to ER stress mediated via its dephosphorylation allowing CaMK to bind and positively regulate it. It is believed that protein phosphatase 2A (PP2A) is involved in the dephosphorylation of DAPK1 in response to ER stress; however the involvement of other phosphatases also play a role in this process. DAPK1 is a positive regulator of autophagy and it exerts its effects via the phosphorylation of Beclin 1[119]. DAPK1-mediated phosphorylation of Beclin 1 reduces its affinity for Bcl-2 and thus causes dissociation of Beclin 1, relieving its inhibitory effects and allowing the formation of the Vps34 complex[120].

1.5.3 Elongation of the phagophore

1.5.3.1 PERK-ATF4-CHOP

As discussed above the elongation of the phagophore requires two events to occur, the conversion of LC3I to LC3II and the covalent binding of ATG12 to ATG5.

During prolonged stress-induced autophagy ATG5, ATG12 and LC3I are quickly engaged in autophagosome formation, and thus these genes must be transcriptionally upregulated in order to maintain flux through the pathway. PERK activation results in the transcriptional upregulation of ATG5, ATG12 and LC3[121,122]. ATG12 is transcriptionally upregulated in response to ER stress in a PERK-eIF2α-dependent manner, however the transcription factor involved in its upregulation has yet to be identified[121]. LC3 and ATG5 are also transcriptionally upregulated through the PERK-eIF2α arm; however, LC3 is upregulated by ATF4 whereas ATG5 is upregulated by CHOP[122]. Thus, during ER stress-induced autophagy PERK replenishes cellular supplies of ATG5 ATG12 and LC3I allowing for sustained autophagy flux.

1.5.4 Negative Regulation of Autophagy by the UPR

1.5.4.1 XBP1

FoxO1 has been described as a major regulator of autophagy in various cell lines, both as a cytosolic protein and a transcription factor[123,124]. For example, acting as a transcription factor FoxO1 is involved in BNip3 expression and neuronal survival[125]. On the other hand, acetylated cytosolic FoxO1 binds to ATG7, can promote autophagy in response to stress and leading to cell death[126]. Studies in Hungtington's disease mouse models have demonstrated that XBP1 deficiency leads to increased levels of macroautophagy in cells, and this was correlated with high expression of FoxO1[127]. This suggests that ER stress can also act as a negative regulator of autophagy, being unfavourable for the physiological outcome in this particular disease model.

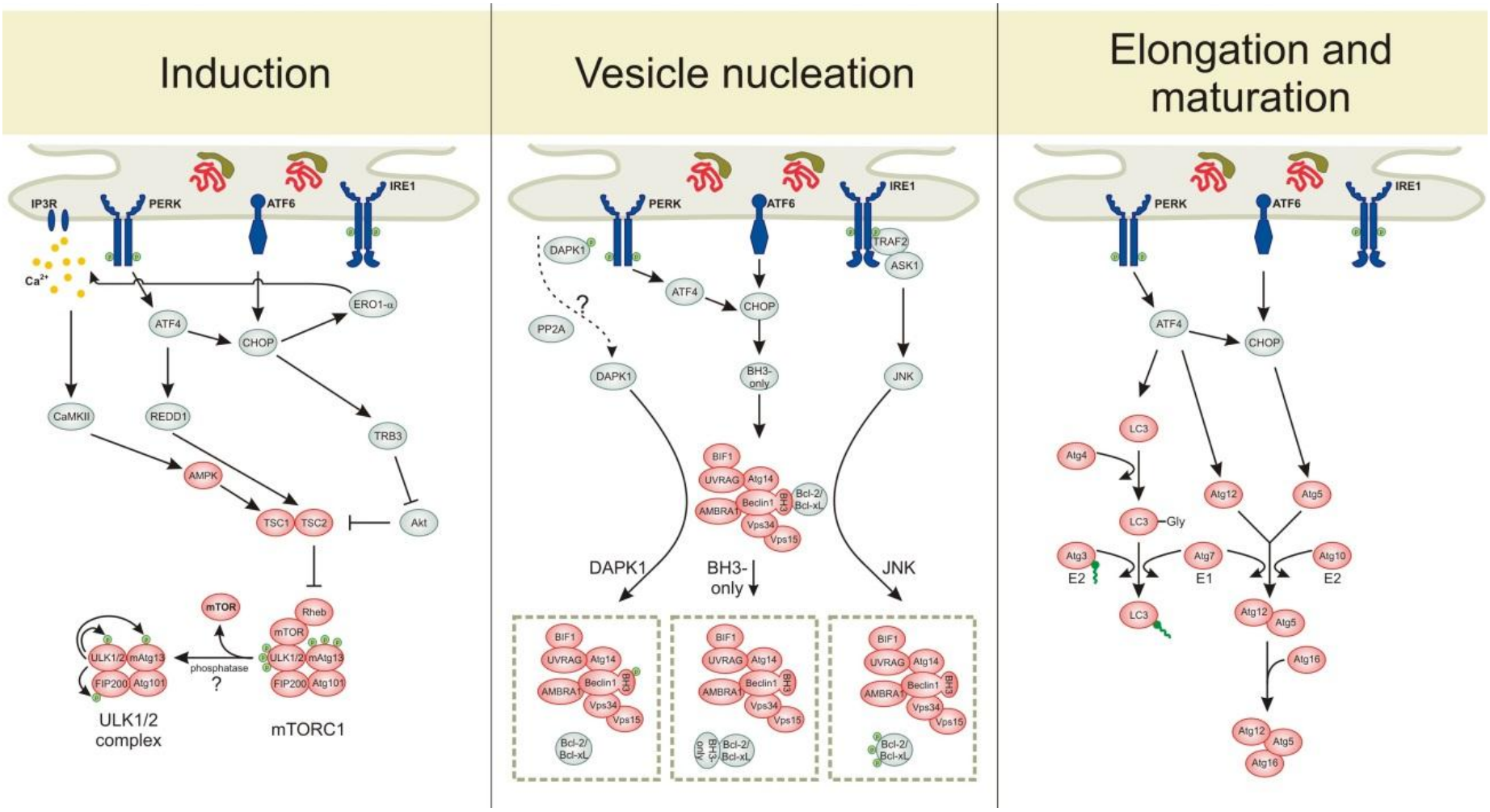
Induction
Vesicle nucleation
Elongation and maturation
IP3R
PERK
ATF6
IRE1
Ca2+
ERO1-α
ATF4
CHOP
CaMKII
REDD1
TRB3
AMPK
TSC1
TSC2
Akt
mTOR
Rheb
ULK1/2
mAtg13
FIP200
Atg101
phosphatase
?
ULK1/2 complex
mTORC1
DAPK1
PP2A
TRAF2
ASK1
JNK
BH3-only
BIF1
UVRAG
Atg14
Beclin1
BH3
AMBRA1
Vps34
Vps15
Bcl-2/Bcl-xL
LC3
Atg4
Gly
Atg3
E2
Atg7
E1
Atg10
Atg12
Atg5
Atg16

Figure 1.3: The UPR can regulate autophagy at different stages in the process, induction, vesicle nucleation, and elongation and maturation. Left hand panel: Induction of autophagy by the UPR can occur through multiple pathways. Ca^{2+} release from the ER lumen via the Inositol 1,4,5-trisphosphate receptor (IP3R) can activate calcium calmodulin kinase II (CaMKII). CaMKII can subsequently phosphorylate and activate AMP kinase (AMPK) which in turn phosphorylates and activates the tuberous sclerosis complex (TSC). TCS inhibits mTORC1 and subsequently relieves mTORC1 inhibition on the ULK1/2 complex. PERK activation results in the non-canonical translation of the transcription factor ATF4. ATF4 can transcriptionally upregulate REDD1 which results in the activation of TSC and subsequent inhibition of mTORC1. ATF4 can also transcriptionally upregulate another transcription factor known as CHOP. CHOP increases the expression of tribbles-related protein 3 (TRB3). TRB3 can directly inhibit Akt which relieves Akt's inhibitory effects on TSC, resulting in mTORC1 inhibition and subsequent activation of ULK1/2 complex. CHOP also transcriptionally upregulates ERO1-α. ERO1-α has been shown to stimulate IP3R-mediated Ca^{2+} release from the ER lumen resulting in activation of CaMKII-AMPK-TSC arm leading to mTORC1 inhibition and subsequent activation of ULK1/2 complex. Middle panel: The activation of the PI3K complex is an essential step for the induction, nucleation and curvature of the phagophore. Multiple players are involved in the activation of the PI3K complex in response to ER stress. DAPK1 remains in a phosphorylated inactive state under resting conditions. In response to ER stress DAPK1 is dephosphorylated resulting in the activation of its kinase domain. DAPK1 can phosphorylate Beclin's BH3 domain preventing the inhibitory association of Bcl-2/Bcl-xL. The PERK-ATF4-CHOP arm can also promote the activation of the PI3K complex. CHOP has been reportrd to transcriptionally upregulate BH3-only proteins. BH3-only proteins can bind to Bcl-2/Bcl-xL and displace them from Beclin's BH3 domain. IRE1-mediated activation of JNK can also result in activation of the PI3K complex. JNK has been shown to phosphorylate Bcl-2/Bcl-xL and inhibit their association with Beclin1. Right hand panel: Elongation and maturation of the phagophore requires two important processes to occur, the conversion of LC3I to LC3II and the formation of the ATG12-5-16 complex (see text for details). ATF4 can transcriptionally upregulate LC3 and ATG12, while CHOP can transcriptionally upregulate ATG5. The transcriptional upregulation of these three proteins is essential for the formation of the autophagosome (from Deegan *et al.*[38]).

1.6 ER stress and Cell Death

The UPR and Autophagy both function to relieve cellular stress and reinstate homeostatic environment. However prolonged or unresolved stress can result in these responses to convert from pro-survival to a pro-death response.

The mechanism by which ER stress-induces apoptosis is not fully delineated, but what is clear is that the intrinsic apoptosis pathway leading to mitochondrial damage and mitochondrial outer membrane permeabilization (MOMP), release of mitochondrial factors and activation of apoptosome and caspase-9 is central to the process[128]. This pathway is generally thought to be regulated by the balance between anti-apoptotic and pro-apoptotic Bcl-2 family proteins. If this balance favours the pro-apoptotic Bcl-2 family proteins mitochondrial permeabilization will occur and lead to the activation of the intrinsic pathway. It has been well established that caspase-9 is the apical caspase required to execute apoptosis in response to ER stress; however, studies have also suggested that caspase-2 may play a role in inducing MOMP in certain cell models upstream of caspase-9 activation[128].

Autophagy has also been shown to be a destructive process under certain cellular stress conditions; however, the mechanism by which autophagy executes cell death is still under investigation. Studies have shown that in conditions where the intrinsic pathway is compromised ER stress can result in a form of autophagic cell death with features of necrosis[129]. More recent studies are suggesting that the autophagosome may be acting as a platform for the formation of a death inducing signaling complex, similar to that found at the plasma membrane, resulting in a form of autophagy mediated apoptosis[130].

There are many types of cell death however they are generally subdivided under three groups, apoptosis, necroptosis and autophagic cell death[131]. Within these groups various death inducing complexes have been identified depending on the stress inflicted on the cell. With this multitude of death pathways, it is likely that in conditions where the cells primary death pathway is compromised the cell will switch to an alternative form of cell death.

1.7 Apoptosis

Apoptosis is a form of programmed cell death that occurs normally during physiological events such as embryonic development, optimal functioning of the immune system, turnover of old and damaged cells and in response to cellular stresses. Apoptosis is characterized by morphological features such as cell shrinkage, plasma membrane blebbing, formation of apoptotic bodies and chromatin condensation (karyorrhexis)[132]. The biochemical events that ultimately lead to these morphological features require the activation of a family of proteolytic enzymes known as caspases (cysteinyl aspartate specific proteases). Caspases are highly specific proteases which cleave a multitude of proteins directly after aspartate residues in short tetrapeptide motifs, these events ultimately lead to the cells demise[133]. There has been hundreds of caspase substrates identified including, pro-survival proteins that are cleaved for inactivation, pro-death proteins that are cleaved for activation and some are considered to be innocent bystanders[134]. Caspases are divided in two groups; apical caspases, which include caspase-8 caspase-10, caspase-2 and caspase-9, and executioner caspases which include caspase-3, caspase-6 and caspase-7[135]. Apical caspase activation is generally a prerequisite for executioner caspase activation. Apical caspases require the formation of a multi-protein complex as a platform to be activated. These complexes include death inducing signaling complex (DISC), Complex II, Apoptosome and PIDDosome[135] and more recently the Ripoptosome[136]. Apoptosis can be activated by both the extrinsic and intrinsic pathways.

1.7.1 Inhibitor of Apoptosis Proteins (IAPs)

Inhibitors of Apoptosis Proteins (IAPs) were first identified in insect cells infected with baculovirus. Baculovirus encodes these genes in its genetic makeup to prevent the host cell dying upon infection[137]. These proteins were later identified in a range of species including mammals. The proteins were structurally characterized by the presence of baculovirus IAP repeats (BIR) domains in the C-terminus of the protein. IAPs contain between 1 and 3 BIR domains and are capable of supporting protein-protein interactions[137]. Some of the IAP family members contain a RING (**R**eally **I**nteresting **N**ew **G**ene) finger domain in its C-terminal, capable of carrying out E3 ligase activity[138]. Functionally, IAPs are important regulators of apoptosis as they are capable of binding to and inhibiting the proteolytic activity of caspases. The

mammalian IAP family consists of eight members including, X-linked IAP (XIAP; also known as ILP-1, MIHA and BIRC4), cellular IAP 1 (cIAP1; also known as hIAP1, MIHB and BIRC2), cellular IAP 2 (cIAP2; also known as hIAP2, MIHC and BIRC3), IAP-like protein 2 (ILP2; also known as BIRC8 and TS-IAP), Melanoma IAP (ML-IAP; also known as livin, KIAP and BIRC7), neuronal apoptosis inhibitor proteins (NAIP; also known as BIRC1), survivin (also known as TIAP and BIRC5), BIR repeat-containing ubiquitin conjugate enzyme system (BRUCE; also known as BIRC6 and apollon)[139].

The most extensively characterized of these IAPs are XIAP, c-IAP1 and c-IAP2. While all IAPs are thought to have the potential to bind to caspases only XIAP has found to be a direct inhibitor, with caspase-9, -3 and -7. XIAP binds to these caspases via an IAP-binding motif (IBM), obstructing their substrate binding site[140]. c-IAP1 and c-IAP2 are more commonly known to interact with TRAF-1 and TRAF-2 , playing a crucial in receptor mediated signaling pathways, most widely known in regulating assembly and signaling of Complex I at the TNFR1 cytosolic tail. Downregulation of cIAP1 and cIAP2 in response to TNFα stimuli results in formation of Complex II and massive sensitization to apoptosis, emphasizing the importance of cIAPs in pro-survival signaling at the cell membrane receptors[141].

The downregulation of the IAP family members sensitizes cells to pro-apoptotic stimuli. Mammalian cells contain natural IAP antagonists, Smac/DIABLO and Omi/Htr2, which are released from the mitochondria following MOMP. Smac/DIABLO and Omi/Htr2 are BIR-interacting proteins which contain an IAP binding motif (IBM) capable of binding to BIR2 and BIR3 domains on IAPs, inhibiting their function. Smac/DIABLO binds to cIAP1 and cIAP2 and induces IAP ubiquitination and subsequent proteasomal degradation[142]. Smac/DIABLO inhibitory effects on XIAP seem to be more of a neutralization effect rather than promoting its degradation[143]. Omi/HtrA2 is a mitochondrial serine protease inhibitor which is released into the cytosol following MOMP. Omi/HtrA2 binds to IAPs BIR domain and subsequently cleaves the protein into inactive fragments and thus promoting caspase activation and apoptosis[144].

1.7.2 Extrinsic Apoptotic Pathway

The extrinsic apoptotic pathway is mediated through a subclass of the TNF receptor (TNFR) superfamily, collectively referred to as the death receptors. The TNFR superfamily consists of 29 receptors, characterized by an extracellular cysteine-rich domain. Eight of these receptors contain an 80 amino acid cytosolic region which is capable of transducing apoptotic signals, these receptors are known as the death receptors[145].

The death receptors include tumor necrosis factor receptor 1 (TNFR1), Fas (also known as DR2, CD95, APO-1), APO-3 (also known as TRAMP, LARD, DR3, WSL1), TNF-related apoptosis-inducing ligand receptor 1 (TRAILR1; also known as APO-2 and DR4), TRAILR2 (also known as KILLER, TRICK2 and DR5), ectodysplasin A receptor (EDAR), nerve growth factor receptor (NGFR1) and death receptor 6 (DR6). The receptors are activated by the binding of a specific member of the TNF ligand superfamily which includes TNFα, FasL (also known as CD95L), Tweak (also known as APO3L), TRAIL (also known as APO2L), EDA-A1 and NGF respectively, the ligand for DR6 is still unknown. These receptors mediate their signaling through the recruitment of an array of proteins to the cytosolic tail of the receptor[145].

It is generally accepted that two types of protein complexes can accumulate at the cytosolic tail of the death receptor; (1) The Death Inducing Signaling Complex (DISC) which comprises of the adaptor protein Fas-Associated protein with Death Domain (FADD) and caspase8/10, resulting in activation of downstream execution caspases and subsequent apoptosis. (2) Alternatively it has been shown that a pro-survival complex that activates NFκB signaling can assembly, comprising of the adaptor protein TNF Receptor type-1 Associated Death Domain protein (TRADD), TNF Receptor Associated Factor-2 (TRAF-2) and Receptor Interacting Protein 1 (RIP1)[146].

The binding of the respective ligand to Fas, TRAILR1 and TRAILR2 primarily result in the recruitment of FADD to the receptors death domain via its own C-terminal death domain. FADD N-terminal death effector domain (DED) facilitates the recruitment of other DED containing proteins, primarily caspase-8, but also caspase-10 and cFLIP proteins. In the event of caspase-8 or caspase-10 binding, the

DISC complex facilitates there activation resulting in apoptosis[147]. It was also demonstrated in multiple B and T cell lines that Fas receptor activation can also result in the formation of a secondary Complex, denoted Complex II[148]. Complex II is a cytosolic complex consisting of FADD, caspase-8 and cFLIPL, however does not contain Fas receptor. It is not yet known how Complex II is formed however it is most likely a secondary event to DISC formation and is believed to function as an amplification complex to ensure cell death following stimulus. Conversely it was shown in activated cytotoxic T Cells that Fas stimulation can activate NFκB signaling; however, it is unclear how it mediates NFκB signaling, but seems to be independent of its death domain[149]. TRAILR activation can also result in the recruitment of RIP1, TRADD, TRAF-2 and NEMO, which mediates a pro-survival and proliferative effect due to activation of NFκB; however the exact mechanism is still unclear to how NFκB signaling is activated[150].

In contrast to Fas and TRAIL receptors, TNFR1 activation initially results in the recruitment of the pro-survival Complex I. Complex I is an NFκB signaling complex which consists of TNFR1, TRADD, TRAF2, TRAF5, LUBAC, RIP1 and IAPs.TRAF2 and cIAP1/2 attach K-63 linked poly-ubiquitinated chains to RIP1, promoting NFκB signaling and the recruitment of linear ubiquitination chain assembly complex (LUBAC). LUBAC stabilizes Complex I by attaching linear ubiquitinated chains to NFκB essential modulator (NEMO). Under conditions of IAP1/2 depletion, Complex I convert to the death signaling Complex II. Complex II consists of RIP1, TRADD, FADD and caspase-8, facilitating caspase-8 activation and subsequent apoptosis[151,152].

The other members of the death receptor family are not as well characterized as Fas, TRAILR and TNFR1. APO-3 Receptor is abundant in T cells and is believed to behave in a similar way to TNFR1[153]. EDAR has been shown to bind TRAF family members and activate NFkB and JNK, however very little is known about its capabilities of transmitting death signals[154]. DR6 is not well characterized and its mode of activation is still unknown; however, a recent studied showed that DR6 induces cell death in a Type I and Type II independent manner however is dependent on Bax activation. Although DR6 is a member of the death receptor family it does not behave in a similar manner[155].

1.7.3 Intrinsic Apoptotic Pathway

Activation of the intrinsic apoptotic pathway canonically requires mitochondrial outer membrane permeabilization (MOMP) assembly of the apoptosome and caspase-9 activation. Intrinsic cellular stresses converge at the mitochondrial membrane resulting in MOMP and release of pro-apoptotic mitochondrial proteins such as cytochrome c, Smac/DIABLO and OMI/HtA2, resulting in apoptosome assembly, IAP depletion and subsequent apoptosis. MOMP requires activation and homo-oligomerization of Bax and Bak, creating pores in the mitochondrial membrane, releasing pro-apoptotic mitochondrial factors. The activation of Bax and Bak is dependent on the ratio of pro-apoptotic Bcl-2 proteins to anti-apoptotic Bcl-2 proteins. In response to prolonged or acute cellular stresses the balance between pro-apoptotic and anti-apoptotic proteins will generally determine the cells fate[156].

1.7.4 Bcl-2 Family

The B cell CLL/lymphoma-2 (Bcl-2) family are a conserved group of proteins which are characterized by the presence of at least one of four α helical motifs known as Bcl-2 homology (BH) domain[157]. The Bcl-2 family proteins are major regulators of the intrinsic apoptotic pathway by controlling the outer mitochondrial membrane (OMM) and the pro-apoptotic Bcl-2 proteins. The anti-apoptotic Bcl-2 proteins include, A1, Bcl-2, Bcl-xl, Bcl-w and Mcl-1, all of which function to maintain the integrity of the outer mitochondrial membrane by inhibiting the pro-apoptotic Bcl-2 proteins[158]. The pro-apoptotic proteins can be divided into two groups, the multi-domain effectors (Bax, Bak and Bok) which contain BH1-3 domains, and the BH3 only proteins which contain just a BH3 domain. The BH3 only proteins can be again sub-grouped into sensitizers (BAD, BIK, BMF, HRK, Noxa and Puma) and direct activators (Bid and Bim). The sensitizers can bind members of the anti-apoptotic proteins and neutralize there activity. The direct activators can bind and neutralize all the anti-apoptotic repertoire, in addition they can bind and directly activate Bax and Bak[158,159]. Upon activation, Bax and Bak homo-oligomerize to form proteolipid pores in the mitochondrial outer membrane resulting in MOMP and release of pro-apoptotic mitochondrial factors such as cytochrome c, Smac/DIABLO and OMI/HtrA2[160]. MOMP is an essential step in the intrinsic pathway. Cytochrome c results in the assembly of the apoptosome[161] while Smac/DIABLO and OMI/HtrA2impede Inhibitor of Apoptosis Proteins (IAPS)[144,162].

1.7.5 Apoptosome

Caspase-9 is considered to be the primary apical caspase activated by the intrinsic pathway in response to cellular stresses. Activation of caspase-9 requires the assembly of a heptameric, wheel-like complex referred to as the apoptosome[163], Apoptotic activating protease inhibitor-1 (APAF-1), a core component of the apoptosome, contains three domains essential for its function, N-terminal CARD domain, an expanded nucleotide-binding domain and a C-terminal domain consisting of 13 WD40 repeats[164]. During resting conditions APAF-1 takes a conformation in which its CARD domain is masked by its C-terminal WD40 repeats. An ADP nucleotide is also bound to the nucleotide-binding domain which stabilizes the complex in this conformation[165]. Following MOMP, cytochrome c is released into cytosol where it binds to the WD40 repeats in the C-terminal region of APAF-1. In addition to cytochrome c binding, ADP to ATP substitution occurs on the nucleotide-binding domain, an essential event to promote conformational change, exposing APAF-1 CARD domain and facilitating APAF1 oligomerization. The apoptosome recruits pro-caspase-9 zymogen, facilitating its dimerization and auto-processing into active caspase-9[161,165]. Active caspase-9 directly activates the executioner caspases-3,6 and 7, ensuring apoptotic cell death.

1.7.6 PIDDosome

PIDD (p53-induced protein with a death domain) is structurally similar to that of other caspase activating molecules such as APAF-1. Like APAF-1 in the apoptosome, PIDD forms the core of a hierarchy complex with a wheel-like structure known as the PIDDosome. As its name suggests PIDD is a p53 inducible protein which is upregulated in response to DNA damage to form the PIDDosome[166]. Although the PIDDosome is primarily assembled in response to DNA damage[167], studies have showed PIDDosome assembly in response to other cellular stresses such as ER stress[168] and heat shock[169,170].

There are two distinct forms which the PIDDosome complex can take, a pro-survival NFκB signaling complex (PIDD-RIP1-NEMO)[171] and a pro-apoptotic signaling complex (PIDD-RAIDD-Caspase-2)[172].

The pro-form of PIDD consists of seven leucine-rich repeats (LRR) at its N-terminal, followed by two ZU-5 domains and a C-terminal death domain (DD)[173].

PIDD must undergo auto-processing before recruitment of its interacting partners. PIDD can cleave itself at two sites, S446 and S588, producing an N-terminal fragment (48kDa, PIDD-N), and two C-terminal fragments (55kDa, PIDD-C and 37kDa PIDD-CC). The complex which the PIDDosome forms depends on the C-terminal fragment that is produced[174]. PIDD-C has been shown to translocate to the nucleus where it recruits RIP1 and NEMO. In response to DNA damage, NEMO is sumoylated to signal its translocation to the nucleus. NEMO is then phosphorylated and ubiquitinated in an ATM depending manner, resulting in its translocation to the cytosol where it activates the IKK complex, activating NFκB and exerting a pro-survival response. However if the stress persists or becomes too severe, PIDD will undergo a second cleavage event at S588, producing PIDD-CC. PIDD-CC moves to the cytosol where it recruits the adaptor protein RAIDD (RIP-associated ICH-1/CAD3 homologous protein with a death domain). RAIDD consists of an N-terminal CARD domain and a C-terminal death domain. RAIDD interacts with PIDD-CC via their individual death domains and facilitates the recruitment of caspase-2 via its CARD domain. Once recruited, pro-caspase-2 dimerizes and undergoes auto-processing to form an active caspase[174,175].

The pro-apoptotic potential of caspase-2 is highly speculated throughout the literature. It is generally considered that caspase-2 potentiates its apoptotic effect through the cleavage of the Bcl-2 family protein Bid to its active form, tBid[176]. tBid is classed as a direct activator and can directly activate Bax and Bak homo-oligomerization, inducing MOMP and activating the apoptosome[177]. Although this is the most likely route in which caspase-2 initiates apoptosis, it has been demonstrated that caspase-2 is much less efficient than caspase-8 at cleaving Bid and thus an exceptionally large amount of active caspase-2 is required to cleave enough Bid for it to activate Bax and BAK[176].

The exact function of caspase-2 in the cell is still unclear. Caspase-2 contains a nuclear localizing signal (NLS) and is basally located at the Golgi and in the nucleus[178]. It has been implicated in playing roles in DNA damage[179] and in cell cycle arrest[180]. Studies to date suggest that caspase-2 is not a dominant apical caspase in most cellular stress responses and thus it would seem likely that caspase-2 may play a more important and prominent role independent of apoptosis.

1.7.7 Ripoptosome and other RIP1-containing complexes

The recently discovered Ripoptosome is a 2MDa, intracellular death signaling complex which can induce cell death through either apoptosis or necroptosis, depending on the cellular content. The core component of this complex includes RIP1K, FADD, Caspase-8 and most likely RIP3K[136].

The form of cell death the ripoptosome executes is dependent on the levels of the caspase inhibitor cFLIP isoforms, cFLIPs and cFLIPL, which heterodimerize with caspase-8, either inhibiting Ripoptosome formation in the case of cFLIPL or promoting formation of the Necrosome, a RIP1-RIP3 complex which induces necroptosis, in the case of cFLIPs[181].

The current working model of the Ripoptosome and how the dynamics between apoptosis and necroptosis transpire were proposed as follows. Upon Ripoptosome formation, caspase-8 is recruited to RIP1-FADD platform resulting in homo-dimerization and auto-processing to generate an active caspase-8 heterotetramer. Active caspase-8 subsequently cleaves RIP1 in the complex, preventing RIP1 mediated necroptosis. Under these conditions the ripoptosome primarily executes cell death through apoptosis. Conversely, high levels of cFLIPs will result in caspase-8-cFLIPs heterodimer and thus inhibition of caspase-8 activity. Under these circumstances RIP1 does not undergo cleavage in the complex. This will result in RIP1 mediated phosphorylation of RIP3 and subsequent Necrosome formation, inducing necroptosis. Finally caspase-8-cFLIPL heterodimers will result in proximal enzymatic activity of caspase-8 allowing for RIP1 cleavage, however insufficient to initiate apoptosis resulting in cell survival[181].

The inhibitor of apoptosis protein (IAPS) cIAP1, cIAP2 and XIAP also negatively regulate the assembly of the Ripoptosome, most likely through ubiquitination of essential components of the Ripoptosome, inactivating there activity or targeting them for proteasomal degradation. It was shown that knockdown of all three, cIAP1, cIAP2 and XIAP, was necessary for Ripoptosome formation, whereas individual knockdown of them showed no effect[136,181].

The Ripoptosome has many similarities to TNF stimulated Complex IIB formation, however the use of blocking antibodies for TNFR1, CD95 and TRAIL did not inhibit the formation of this complex or its effect on cell death. Also the

overexpression of Bcl-2 to block the mitochondrial apoptotic pathway had no effect on Ripoptosome formation indicating that this is both independent of extrinsic and canonical intrinsic apoptotic signaling[136].

1.8 Necroptosis/Necrosis

Necrosis is a form of cell death which was morphologically characterized by the rounding of the cell, enhanced cell volume, swelling of organelles, lack of inter-nucleosomal fragmentation, and plasma membrane rupture[182]. Necrosis was originally defined as a caspase independent, uncontrolled form a cell death usually observed in response to severe trauma. From extensive work carried out on TNF mediated necrosis, receptor-interacting protein kinase 1 (RIP1K) was identified. It was later shown that RIP1 and RIP3 could form a complex referred to a Necrosome, which could induce cell death with all the features of necrosis. Inactivation of these kinases blocked necrosis and for the first time showed that at least not all forms of necrosis were uncontrolled processes; this form of programmed necrosis was referred to as necroptosis[183].

1.9 Autophagic cell death

As previously discussed autophagy is a "bulk" degradation system which occurs basally for the turnover of long lived protein and organelles. Autophagy is significantly upregulated in response to multiple stress stimuli for the degradation of unfolded proteins, protein aggregates and damaged organelles. Autophagy is generally referred to as a protective response initiated by the cell during adverse conditions, however under certain conditions autophagy has been shown to induce cell death denoted as autophagic cell death or type II cell death.

The term autophagic cell death has become very controversial over recent years with no defined mechanism of how it executes cell death. Characterization of autophagic cell death is simply conversion of LC3I to LC3II and knockdown of an essential autophagy component, observing a rescue in cell death.

It was initially hypothesized that autophagic cell death was simply an uncontrolled bulk degradation of the cell; however, recent findings suggest that the autophagosome may act as a molecular platform for assembly of signaling complex that can lead to caspase activation e.g., intracellular death inducing signaling

complex (iDISC)[130]. One of the first indications that the autophagosome may act as a signaling platform for a caspase activating complex was described in 2005 by Yong-Keun Jung[184]. For the first time Jung showed a direct interaction between the C-Terminal region of the autophagy gene ATG5 and the death domain of the adaptor protein FADD by immunoprecipitation (IP). He further showed that HeLa cells exposed to IFN-γ underwent cell death which could be inhibited by down-regulation of ATG5 or by using the caspase inhibitor z-VAD-FMK.

Further confirmation that DISCs can use autophagosomes as signaling platforms was shown during T cell proliferation. Previous studies have demonstrated the importance of the DISC components FADD, cFLIP and caspase-8 in mature T cell proliferation[185-187]. Furthermore, independent studies monitoring the effects of autophagy in T cell maintenance and proliferation demonstrated that autophagy was essential in these processes[188,189]. The group of Craig M. Walsh was the first to connect the DISC proteins and autophagy. They confirmed that knockdown of autophagy genes, caspase-8 or FADD during T-cell expansion resulted in necroptosis which could be blocked by necrostatin-1, an inhibitor of RIP1 kinase. There model proposed a complex containing ATG5-ATG12, RIP1, FADD and Caspase-8, forming on autophagosomes during T-cell expansion. Minimal caspase-8 activity controls RIP1 kinase activity by cleaving and inactivating its function, subsequently inhibiting necroptosis and reducing levels of autophagy during T-cell expansion. However if caspase-8 or FADD is removed from the system RIP1 kinase remains active and induces necroptosis. Moreover if autophagy is knocked down the DISC like complex has no platform to assemble and thus RIP1 kinase remains active. They further confirmed the interaction between the components of the complex by overexpressing HA-ATG5 in mouse embryonic fibroblasts (MEFs) and immunoprecipitating (IP) HA, pulling down with it RIP1 kinase, caspase-8 and FADD. Although this was an overexpression system it confirmed that these components were capable of interacting.

Recent publications by the group of Marcus Rehm[190] and the group of Hong-Gang Wang[130] further enforced the idea that DISC like complexes can signal from autophagosomes; however, it is proving difficult to show that an actual DISC complex can form on an autophagosome and that these are not two independent processes. Furthermore this only explains cases where autophagy mediates cell

death via apoptosis; however many studies show that autophagic cell death is caspase independent with morphological features of necrosis[129,191-193]. The conclusion drawn from autophagy mediated necrotic-like cell death suggests a possible over degradation of the cell by the autophagosome; however these conclusions were drawn without examining if the necrosis that occurred was uncontrolled or if it was regulated by RIP kinase.

A Recent study by Jean-Pierre Bourquin[194] showed that the upregulation of autophagy sensitized acute lymphoblastic leukemia (ALL) to glucocorticoids and a range of chemotherapeutic drugs. Autophagy upregulation was stimulated by inhibition of mTOR, using rapamycin or with obatoclax, a Bcl-2 antagonist which displaced Bcl-2 from beclin1 complex. Moreover they showed that the cell death bypassed the mitochondrial block and induced autophagy-dependent necroptosis, which could be completely blocked using necrostatin-1, an inhibitor of RIP1 kinase or 3MA an inhibitor of the beclin1 complex.

To date the mechanism of autophagic cell death still remains undefined; however with the extensive research that is been carried out on autophagy-mediated death it is slowly being unraveled.

1.10 Aims and Objectives

The aim of this thesis is to investigate the mechanism of ER stress induced cell death in conditions where the intrinsic apoptotic pathway is functional and in conditions where it is compromised. Furthermore, we aim to delineate the role of autophagy in these conditions and provide further mechanistic insights into the relationship between the UPR, autophagy and cell death.

Chapter 2: Materials and Methods

2.1 Cell culture and treatments

Caspase-$9^{+/+}$ and Caspase-$9^{-/-}$ Mouse embryonic fibroblasts (MEFs) were a kind gift from "Tak Mak", Bax/$Bak^{+/+}$ and Bax/$Bak^{-/-}$ MEFs were a kind gift from "Craig Thompson", wild-type and $Bax^{-/-}$ HCT116 cells were a kind gift from "Bert Volgestein", MDA-MB-468 PLKO and MDA-MB-468 PERK shRNA cells were a kind gift from "Alan Diehl", HEK 293T/17 cells were purchased from ATCC (CRL-11268). MEFs and human embryonic kidney (HEK) 293T cells were cultured in Dulbecco's modified Eagle's medium (DMEM) from Sigma (D6429) supplemented with 10% heat inactivated fetal bovine serum (FBS), 100 U/ml penicillin and 100 mg/ml streptomycin. HCT116 colon cancer cells were cultured in McCOYs 5A medium modified from Sigma (M9309) supplemented with 10% heat inactivated FBS, 100 U/ml penicillin and 100 mg/ml streptomycin. MDA-MB-468 breast cancer cells were cultured in DMEM from Sigma (D6429) supplemented with 10% heat inactivated FBS, 100 U/ml penicillin and 100 mg/ml streptomycin and 10 µg/ml of insulin. All cells were cultured at 37 °C, 5% CO_2 in a humidified incubator. Cells were seeded at a 60-70% density 24 h prior to treatment. To induce apoptosis, cells were treated with thapsigargin (Tg), tunicamycin (Tm), brefeldin A (Bfa), etoposide (Etop) and bortezomib (Brtz) at the indicated concentrations for the indicated time. To inhibit autophagosome degradation, cells were treated with 60 µM of chloroquine. To inhibit caspases, cells were treated with 20 µM of Boc-D-Fmk. To inhibit RIP1 kinase, cells were treated with necrostatin-1 (Nec1). All reagents were purchased from Sigma-Aldrich unless otherwise stated.

Thapsigargin is an irreversible inhibitor of the class of enzymes called sarco/endoplasmic reticulum Ca^{2+} ATPase (SERCA), which is extracted from the roots of the plant *Thapsia Garganica.* Thapsigargin inhibits SERCA mediated uptake of calcium into the endoplasmic reticulum (ER), resulting in ER calcium pool depletion[195].

Tunicamycin is a mixture of homologous nucleoside antibiotics which inhibit N-acetylglucosamine transferases, thus inhibiting the first step of N-glycosylation of newly synthesized glycoproteins in the ER. This results in extensive misfolding of proteins in the ER, activating the UPR. There are about 10 different homologues of

tunicamycins produced by the bacteria *Streptomyces Lysosuperficus*, a combination of these homolouges are used in the commercially available drugs[196].

Brefedin A is a lactone antibiotic produced by the fungus *Eupenicillium brefeldianum.* Brefeldin A inhibits transport of proteins from ER to the Golgi and promotes retrograde protein transport from the Golgi to the ER. This results in the accumulation of protein in the ER, resulting in activation of the UPR.

Etoposide was synthesised based on the chemical makeup of a toxin derived from the plant *Podophyllum peltatum.* Etoposide is a topoisomerase inhibitor which forms a complex with topoisomerase II, inhibiting its function to ligate cleaved DNA molecules resulting in the accumulation of single and double strand DNA breaks.

Bortezomib is a proteasome inhibitor which binds to the catalytic domain of the 26S proteasome with high affinity, inhibiting the degradation of incoming ubiquitinated proteins.

Boc-D-FMK is a synthetic peptide that is used a broad spectrum caspase inhibitor. Boc-D-FMK irreversibly binds to the catalytic site of caspases inhibiting there proteolytic activity.

BV-6 is a Smac-mimetic that binds to the IAP family proteins, cIAP1, cIAP2 and XIAP, inducing autoubiquitination and subsequent degradation of these protiens. BV-6 was supplied to us by Genentech through a material transfer agreement.

Chloroquine is classed as a lysosomotropic agent and thus accumulates in lysosomes increasing lysosomal pH and inactivating cathepsins catalytic properties.

Necrostatin-1 is a member of a family of synthetic drugs known as necrostatins. Necrostatin-1 is a potent inhibitor of the RIP1 kinase activity by inhibiting an essential conformational change required for RIP1 kinase activity.

All the above drugs were prepared in dimethysulfoxide (DMSO) and stored at -20 °C.

2.2 Plasmids

Plasmids (Table 1) were transformed into competent *Escherichia coli* strain DH5α cells. In an eppendorf, 1µl of plasmid was added to 25 µl of DH5α cells and

incubated on ice for 30 min. The eppendorf was placed on a heat block at 42 °C and the cells were heat-shocked for 30 sec. Cells were placed directly back onto ice and left to recover for 2 min. 250 µl of LB Broth was added to the cells and placed into a 37 °C shaker for 1 h at 200 rpm. Following incubation, 50 µl of the transformation mixture was spread onto an agar plate containing the appropriate antibiotic, 100 µg/ml of ampicillin or 30 µg/ml of kanamycin. The plate was incubated overnight at 37 °C to allow for colony formation. A single colony was inoculated in 5 ml of LB broth containing the appropriate antibiotic (starter culture) and placed into a 37 °C shaker for 6 h. Following incubation, 1 ml of starter culture was added to 100 ml of LB broth containing the appropriate antibiotic, and placed into a 37 °C shaker overnight. The following day the culture was centrifuged at 5,000 × g for 20 min to pellet the bacterial cells containing the plasmid of interest. Plasmid extraction was carried out using Qiagen maxi-prep kit (Cat. No. 12163).

Vector	Insert	Selection	Species	Obtained from
PGIPZ	Empty	GFP/Puro	M	Open biosystems
PGIPZ	ATG5 shRNA	GFP/Puro	M	Open biosystems
PLKO	FADD shRNA	Puro	M	Peter Vandenabeele
PLKO	TRADD shRNA	Puro	M	Peter Vandenabeele
PLKO	Caspase-8 shRNA	Puro	M	Peter Vandenabeele
PLKO	TNFR1 shRNA	Puro	M	Peter Vandenabeele
PEGFP-C2	GFP-LC3 cDNA	GFP-Fusion	H	Addgene (#24920)
Plenti	RIP1 shRNA	GFP	M	Peter Vandenabeele
Plenti	RIP3 shRNA	GFP	M	Peter Vandenabeele
Plenti	Empty	GFP	M	Peter Vandenabeele
PMD2.G	VSV G	None	HIV Packaging	Addgene (#12259)
PRSV	Rev	None	HIV Packaging	Addgene (#12253)

psPAX2	none	None	HIV Packaging	Addgene (#12260)

Table 1: Plasmids

2.3 Transfections

Transfection of GFP-LC3 expression plasmid into MEF cells was carried out using the transfection reagent Turbofect (Fermentas; Cat No. R0531). MEFs were seeded at 100,000 cells/well in a 6-well plate 24 h prior to transfection. Transfection of MEFs with Turbofect requires a 1:1 ratio of DNA to lipid. Next, 2 μg of DNA per well, and 2 μl of Turbofect per well, were directly added to empty DMEM medium and incubated for 25 min at RT. During the incubation period the medium from the cells was replaced with 1 ml of fresh DMEM medium containing only 10% FBS. Following incubation of DNA and lipids, the DNA-lipid complexes were added drop wise to the dish and returned to the incubator for 3 h. The transfection mixture was removed after the 3 h incubation and replaced with fresh growth medium. The next day the transfection efficiency was determined by fluorescent microscopy and the cells were treated as discussed in the results section.

Transfection of plasmids into 293T cells was carried out using the transfection reagent JET PEI (Polyplus; Cat No. 101-01N). 293T cells were primarily transfected for the production of lentiviruses. The day before transfection, 10×10^6 293T cells were seeded into a T175 flask. The following day the 293T cells were 60-70% confluent. The cells were transfected with a mixture of 4 plasmids, 3 lentiviral packaging plasmids (6 μg of pMD2.G, 14 μg of psPAX2 and 6 μg of pRSV-Rev) and 14 μg of the transfer plasmid. In total the cells were transfected with 40 μg of DNA. In an eppendorf, the DNA was pooled and diluted in 500 μl of sodium chloride solution and in a separate eppendorf 80 μl of JET PEI was added to 500 μl of sodium chloride solution, these were incubated at RT for 5 min. Following incubation the JET PEI mixture was added drop wise into the DNA mixture, pipetted up and down, and left to incubate for 25 min.

During incubation the media was removed from the 293T cells and replaced with 15 ml of DMEM containing just 10% FBS and returned to the incubator for 20 min. After the incubation period the media was again removed from the cells and

replaced with 15 ml of fresh DMEM 10% FBS. The transfection mixture was then added drop wise to the cells and returned to the 37 °C incubator.

2.4 Lentivirus Production

Lentivirus for pGIPZ-ATG5 shRNA (Open Biosystems Cat# RMM4431-99342719), pGIPZ-empty (Open Biosystems Cat# RHS4349), PLKO-empty, PLKO-caspase-8 shRNA, PLKO-TRADD shRNA, PLKO-FADD shRNA, PLKO-TNFR1 shRNA, pLENTI6-empty, pLENTI6-RIP3K miRNA, pLENTI6-RIP1K miRNA, was generated by co-transfecting the above transfer plasmids with a 2^{nd} generation lentivirus packaging system (Addgene, pMD2.G Cat#12259, psPAX2 Cat#12260, pRSV-Rev Cat#12253) using JET PEI transfection reagent (Polyplus Transfection, Cat#101-01N) into HEK 293T cells as discussed above. 24 h post transfection the supernatant (containing lentivirus) of the transfected cells was harvested and replaced with 15 ml of fresh growth medium. The second round of lentivirus harvest was carried out 24 h later. The supernatant containing the lentivirus was filtered through a 0.45 nm Nalgene filter to remove any cells. The virus can be used immediately for transduction of cells, stored at 4 °C for 1 week or aliquoted into cryotubes and stored in -80 °C freezer.

2.5 Lentivirus Transduction

Lentivirus was used to generate stable subclones of wild-type and caspase-$9^{-/-}$ MEFs (Table 2). MEFs were seeded at a low density (30-40% density) in a 6-well plate the day before transduction. On day of transduction, lentivirus was incubated with 5 μg/ml of polybrene for 5 min. Media was removed from the cells in the 6-well plate and 1.5 ml of lentiviral-polybrene mixture was added per well. The plates were then centrifuged for 90 min at 1500 rpm (400 g) at room temperature. Following centrifugation cells were placed directly into the incubator and left overnight. The next day, virus was removed and replaced with fresh complete medium.

Once the cells recovered and were proliferating normally they were selected with the addition of 5 μg/ml of puromycin or 5 μg/ml of blasticidin for 5 days. After selection cells were left recover for 2 passages before seeded for experiments.

Cell line	Stably expressing	Ctrl Vector	Resistance marker
WT MEF	ATG5 shRNA/GFP	PGIPZ-GFP	PURO
WT MEF	Caspase-8 shRNA	PLKO	PURO
C9-/- MEF	Caspase-8 shRNA	PLKO	PURO
C9-/- MEF	FADD shRNA	PLKO	PURO
C9-/- MEF	TRADD shRNA	PLKO	PURO
C9-/- MEF	TNFR1 shRNA	PLKO	PURO
C9-/- MEF	RIP1K miRNA/GFP	PLENTI-GFP	Blasticidin
C9-/- MEF	RIP3K miRNA/GFP	PLENTI-GFP	Blasticidin
C9-/- MEF	ATG5 shRNA/GFP	PGIPZ-GFP	PURO

Table 2: Generated stable cell lines

2.6 Microscopy

2.6.1 Fluorescent Confocal Microscopy:

To monitor autophagosome formation, WT and $C9^{-/-}$ MEFs were transfected using Turbofect, as discussed above, with a vector expressing a GFP-LC3 fusion protein. 24 h post-transfection MEFs were treated with Tg for 6, 12 and 24 h. Following treatment cells were fixed using 10% Formalin. Cell nucleus was stained using 0.5 μg/ml solution of 4-6-Diamidino-2-phenylindote (DAPI), a DNA Intercalating fluorophore with an emission max of 460 nm. The cells were visualized using confocal microscopy at 40X magnification.

2.6.2 Bright Field Microscopy:

WT and $C9^{-/-}$ MEFs were treated with either Tg, Tm or BFA for the indicated timepoints. The cells were fixed using 10% Formalin and stained with hematoxylin and eosin stain to visualize the cells. Images of the cells were taken in bright field using Olympus microscope at 20X magnification.

2.6.3 Transmission Electron Microscopy

WT and $C9^{-/-}$ MEFs were treated with Tg for 24 h. Cells were fixed using 2% glutaraldehyde for 1 h. Cells were washed for 3x5 min in phosphate buffered saline (PBS). Cells were then subjected to a secondary fixation buffer of 1% Osmium tetraoxide for 1 h. Cells were then dehydrated by sequential washes in 25% ethanol (10 min), 50% ethanol (10 min) 70% ethanol (10 min) 90% ethanol (10 min) 100% ethanol (10 min). Cells were then embedded in 50% resin for 1 h followed by 100% resin for 1 h. Polymerization was carried out at 70 °C for 8 h.

2.7 RNA Extraction

Cells were seeded in a 6-well plate at 70-80% density. After experimental treatment, the 6-well plate was placed on ice; cells were scraped into the media and transferred to an eppendorf. Samples were centrifuged at 1,000 g for 5 min at 4 °C to pellet the cells. Cells were resuspended and lysed in 500 µl of TRI reagent (Invitrogen; Cat No. #9738) and incubated for 5 min at room temperature (RT) to allow full dissociation of any nucleoprotein complexes. Next, 100 µl of chloroform was added to each tube and vortexed for 10 secs. Samples were incubated at RT for 3 min before centrifugation at 12,000 g for 15 min at 4 °C. Following centrifugation the sample will have separated into 3 phases, a lower red phenol-chloroform phase, a white interphase and an upper colourless aqueous phase. The lower and interphase contain a mixture of proteins and DNA, whereas the aqueous phase contains RNA. The aqueous phase was carefully pipetted out and transferred into a sterile eppendorf. Next, 250 µl of isopropanol was added to the aqueous phase and inverted 6 times followed by incubation at -70 °C for 1 h. Following incubation, samples were removed from the freezer and centrifuged at 12,000 g for 15 min at 4 °C. Supernatant was removed and the RNA pellet was washed in 500 µl of 75% ethanol. Sample was centrifuged at 7,000 g for 8 min at 4 °C. Supernatant was removed and RNA pellet was left to dry at RT for 5-10 min (important not to let dry completely or it will not dissolve in water efficiently). RNA was resuspended in 30 µl of sigma clean water and heated at 60 °C for 10 min followed by pipetting up and down to resuspend RNA. RNA concentration was determined by measuring absorbance at 260 nm (A260 nm) using spectrophotometer (Nanodrop). RNA purity was assessed using A260 nm/A280 nm ratio, ensuring the ratio of nucleic acid/protein was between 1.7 and 2.1. RNA was stored in the -80 °C freezer.

2.8 cDNA synthesis

To monitor gene expression, the isolated RNA was reverse transcribed into cDNA. For this, 2 μ*g* of RNA was transferred to a PCR tube with 1 U DNase-1, 1 μl of 10X DNase-1 buffer, made up to 8 μl with sterile ddH2O. The sample was incubated at room temperature (RT) for 15 min to allow degradation of any DNA contamination. The DNase was inactivated with 1 μl of 25 mM EDTA incubated at 65 °C for 8 min. 1 μl of Oligo dT (cDNA primer) was added to the reaction mixture and incubated at 65 °C for 2 min (denaturation) followed by 42 °C for 2 min to allow the primer to anneal to the poly(A) tail of the mRNA. To the reaction mixture, 10 μl of master mix was added which contained 2.6 μl sterile ddH2O, 4 μl of 5X 1st strand buffer, 2 μl of a 100 mM DTT (dithiothreitol), 1 μl of 10 mM dNTPs, 0.4 μl superscript II. Mixture was incubated at 42 °C for 50 min for cDNA synthesis followed by 75 °C for 10 min to inactivate superscript reverse transcriptase. (Reagents purchased from Invitrogen).

2.9 Conventional Polymerase Chain Reaction (PCR)

For conventional-PCR, a reaction mixture was made up, containing 2 μl of cDNA product, 2 μl of a 100 nM forward and reverse primer(Table 3), 4 μl ddH2O and 10 μl 2X PCR master mix (Promega #M7122). The reactions were placed in a thermocycler and cDNA was amplified under the following conditions. The reaction mixtures underwent 25- 35 cycles, depending on the product, for 1 min denaturation at 95°C, 1 min annealing at 60 °C and 1 min extension at 72 °C. (Primers were designed and purchased from Sigma).

Species	gene	Forward Primer	Reverse Primer
M	ATG5	5’-ATGAAGGCACACCCCTGAAATG-3’	5’-ATTCTGCAGTCCCATCCAGAGC-3’
M	TNFR1	5’-CAGTCTGCAGGGAGTGTGAA-3’	5’-CACGCACTGGAAGTGTGTCT-3’
M/H/R	GAPDH	5’-ACCACAGTCCATGCCATC-3’	5’-TCCACCACCTGTTGCTG-3’

Table 3: Primers

2.10 Real Time PCR

Assays for EDEM1, ERP72, ATF4, HERP, CHOP, p58IPK and GRP78 were purchased from Applied Biosystems. These probes are in Applied Biosystems inventories and are assigned an assay code for reordering; however details of the primers and probe sequences are not supplied (Table 4). The assays for PERK, p62, NBR1 and NIX were supplied from Integrated DNA technologies (IDT) (Table 4).

cDNA was diluted 1:5 ratio in ddH_2O, the assay probes (1 µl/well) were diluted in the supplied 2X master mix (10 µl/well) and ddH20 (4 µl/well). Next, 5 µl of cDNA was pipetted into each well of the 96 well reaction plate (Applied Biosystems; cat no. N8010560). To this, 15 µl of the master mix containing the probe of interest was added to each well. The plate was sealed and centrifuged 400 g for 1 min to mix the reaction. The plate was placed into the thermocycler and subjected to 40 cycles of PCR. Relative expression was evaluated with ΔΔCT method and GAPDH was used as the house keeping gene to normalize gene expression.

Gene	Accession No.	Assay code	Species
EDEM1	NM_138677.2	Mm00551797_m1	Mouse
ERP72	NM_009787.2	Mm00437958_m1	Mouse
ATF4	NM_009716.2	Mm01298604_g1	Mouse
HERP	NM_022331.1	Mm01249592_m1	Mouse
CHOP	NM_007837.2	Mm00492097_m1	Mouse
P58ipk	NM_008929	Mm00515299_m1	Mouse
GRP78	NM_005347.2	Hs00607129_gH	Human
GAPDH	NM_008084.2	Mm99999915_g1	Mouse
Applied Biosystems			

Gene	Primer1	Primer2	Probe	Species
PERK	5'-GAACCAGACGATGAG	5'-GGATGACACCAAGG	5'-/56-FAM/AGCAGTGGG/ZEN/ATTT	Human

	ACAGAG-3'	AACCG-3'	GGATGTGGGAT/3IABkFQ/-3'	
NBR1	5'-AGTAGATCCTTTCCCCTCCG-3'	5'-TGCTCAGTCACTTCACCAAG-3'	5'-/56-FAM/AGTTTCCTC/ZEN/TTGCTGGCAGGTGA/3IABkFQ/-3'	Human
p62 (SQSTM1)	5'-AAGAACTATGACATCGGAGCG-3'	5'-AGAGGTGGGCAAAAGTGG-3'	5'-/56-FAM/ACACCATCC/ZEN/AGTATTCAAAGCATCCCC/3IABkFQ/-3'	Human
NIX (BNIP3L)	5'-CTCTTCCTTTCTCATGTTTTGGC-3'	5'-ACTTCACAGGTCACACGC-3'	5'-/56-FAM/TGCTCAGTC/ZEN/GCTTTCCAATATAGATGCC/3IABkFQ/-3'	Human
GAPDH	5'-TCTTCCTCTTGTGCTCTTGC-3'	5'-CTTTGTCAAGCTCATTTCCTGG-3'	5'-/56-FAM/CACCCTGTT/ZEN/GCTGTAGCCAAATTCG/3IABkFQ/-3'	Human
Integrated DNA Technologies (IDT)				

Table 4: Real -time PCR Assays

2.11 Protein sample preparation and Sodium dodecyl sulphate-polyacrylamide gel electrophoresis (SDS-PAGE)

Cells were seeded in a 6-well plate for protein sample preparation. Following treatment, the 6-well plate was placed on ice. Media and floating cells were transferred into an eppendorf on ice. Cells on the plate were washed once with PBS, PBS was transferred from the cells to the corresponding eppendorf containing media and floating cells. Eppendorfs were centrifuged at 1000 g for 5 min at 4 °C and the supernatant was removed from cell pellet. The pellet was washed with PBS, centrifuged and PBS was removed from the cell pellet. In parallel the cells remaining on the plate were lysed with 100 µl of 1X sample buffer (Table 6) and transferred to the corresponding eppendorf containing the pellet of floating cells from that sample which were subsequently lysed. This method ensured that all dead cells were collected and included in the protein lysate and that minimum stress was applied to the live cells still attached to the plate. Scraping of the live cells and centrifugation steps can result in stress markers being expressed and may obscure results.

The protein samples were boiled at 95 °C for 5 min and either stored at -20 °C or directly loaded on to an SDS-PAGE alongside a protein molecular weight marker. The constituents and volumes used to make these Gels are described in table 5. The SDS-Gels were placed in a tank containing running buffer and electrophoresis was carried out at 80 V for 30 min followed by 100 V for 60 min or until the samples reach the bottom of the gel.

Reagents	8 % Resolving gel (ml)	12 % Resolving gel (ml)	5 % Stacking gel (ml)
H20	4.6	3.4	3.4
30% Acrylamide	2.6	4	0.85
1.5M Tris, pH 8.8	2.6	2.6	0.65
1.0M Tris, pH 6.8	-	-	0.05
10% SDS	0.1	0.1	
10% APS	0.1	0.1	0.05
TEMED	0.006	0.004	0.005
Total Volume	**10**	**10**	**5**

Table 5: SDS-PAGE

Reagents	2X Sample buffer (IP)	1X Sample buffer (WB)
20% SDS	2 ml	1 ml
1 M Tris pH 6.8	1.2 ml	0.6 ml
Glycerol	1 ml	0.5 ml
Bromophenol blue	Dash	Dash
DTT	0.154 g	0.308 g
dH20	up to 10 ml	up to 10 ml

Table 6: Protein sample buffer

2.12 Western Blotting

For blotting of the proteins, the SDS-PAGE gel was sandwiched between a sponge, filter paper, gel**,** nitrocellulose paper, filter paper, and a sponge. The proteins were electrophoretically transferred onto the nitrocellulose paper for 90 min at 110 V in transfer buffer (10 mM CAPS at pH 11 and 20% methanol). Following transfer, the nitrocellulose membrane was blocked with 5% non-fat milk in PBS containing 0.05% Tween. The membranes were incubated with the primary antibody under the antibodies optimum conditions, described in table 7. Membrane were then washed 3 times with PBS-T (0.05% Tween in PBS) and further incubated in the appropriate horseradish peroxidase-conjugated secondary antibody for 2 h at room temperature (Table 7). Antibodies were visualized using Millipore detection reagent horseradish peroxidase substrate chemiluminescent (Millipore #11556345).

2.13 Immunoprecipitation

Cells were seeded at the appropriate density in 100 mm dishes 24 h prior to treatment. On day 0 (harvesting samples), the plates were placed on ice and the cells were washed with ice cold PBS. Next, 1 ml of ice cold NP-40 buffer (150 mM NaCl, 1% NP-40, 10% glycerol, 10 mM Tris pH8) containing protease inhibitors (Roche #11836170001, 1 tablet/10 ml) was added to the plates, on ice (Everything was kept on ice from this moment on). Plates were put on the shaker at 4 °C for 15 min. Cell lysates were scraped and added to an eppendorf, and centrifuged at 15,000 g for 10 min at 4 °C. Next, 60 µl of the supernatant was added to 60 µl of 2X Sample Buffer (Table 6); this was boiled at 95 °C for 5 min, and then put on ice. This was the pre-IP. The remainder of the lysate was subjected to the addition of 2.5 µl of antibody and overnight rotation at 4 °C. The next day, 40 µl of 50% beads slurry was added to the lysate and rotated at 4 ºC for 3 h. After incubation the beads were centrifuged at 3,000 g for 1 min at 4 °C, the supernatant was discarded. The beads were washed with 1 ml of ice cold NP-40 buffer, and then centrifuged at 3,000 g, 4 °C, for 1min. Supernatant was discarded using a vacuum and a protein tip. The washing step was repeated 10 times. After the last wash, the beads were centrifuged at 10,000 g for 30 sec. All the supernatant was discarded. 60 µl of 2X SB was added to the bead pellet and vortex briefly. Samples were boiled at 95 °C for 10 min, and then put back on ice. Samples were centrifuged at 10,000 g for 1 min. 18 µl was loaded on SDS-gel or frozen at -20 °C.

2.14 Enzyme-Linked Immunosorbent Assay (ELISA)

The ELISA plate was coated with 50 µl/well of TNF antibody (capture antibody) diluted in coating buffer (PBS), sealed and incubated overnight at 4 °C. The next day the coating buffer was aspirated off and the wells were washed 3 times for 1 min with wash buffer (PBS-T-0.05%). Excess liquid was removed by blotting plate on tissue paper. The wells were blocked with 200 µl/well of 1X Assay diluent (5% BSA in PBS-T-0.05% Tween) and incubated at room temperature (RT) for 1 h. After incubation, assay diluent was aspirated off and the wells were washed 3 times as previously described. Standards were prepared ranging from 250-1,000 pg/ml of recombinant mouse TNF. Next, 50 µl of the standards and 50 µl of the samples were added to the plate and incubated on the shaker at RT for 2 h. After incubation, wells were aspirated off and washed 3 times as previously described. The detection antibody (Avidin-HRP) was diluted in 1x assay dilutent. 50 µl of detection antibody was added to each well and incubated for 30 min at RT in a dark area (light sensitive). Following incubation, the wells were aspirated off and washed 7 times with a soak period of 1-2 min for every wash. 50 µl of substrate solution (Tetramethylbenzidine) was added to each well and incubated at RT for 15 min. The reaction was stopped after incubation with 25 µl of stop solution (1M H3PO4). The plate was read at 450 nm.

Antibody	Company	Cat No.	Poly/Mono	Species Reactivity	Raised In	Primary Dilution	Primary Incubation
Anti-Goat IgG (H+L)	Jackson	705-035-003	poly	G	donkey	1:5000 5% Milk	1 hour RT
Anti-Mouse IgG (H+L)	Thermo	#31430	poly	M	goat	1:5000 5% Milk	1 hour RT
Anti-Rabbit IgG (CS)	CST	#3678	mono	R	mouse	1:5000 5% Milk	2 hour RT
Anti-Rabbit IgG (H+L)	Jackson	111-035-003	poly	R	goat	1:5000 5% Milk	1 hour RT
ATG5	CST	#8540	mono	H, M, R, Mk	rabbit	1:1000 5% Milk	0/N 4°C
Beclin 1	Santa Cruz	sc-11427	poly	H, M, R	rabbit	1:500 5% Milk	0/N 4°C
Beta-actin	Sigma	A-5060	poly	H, M, R	rabbit	1:5000 5% Milk	1 hour RT
Caspase-3	CST	#9662 S	poly	H, M, R, Mk	rabbit	1:1000 5% Milk	0/N 4°C
Caspase-7	CST	#9492	poly	H, M, R, Mk	rabbit	1:1000 5% Milk	0/N 4°C
Caspase-8	CST	#4790 S	mono	M	rabbit	1:1000 5% Milk	0/N 4°C
Caspase-8	CST	#9746	mono	H	mouse	1:1000 5% Milk	0/N 4°C
Caspase-9	CST	#9502	poly	H	rabbit	1:1000 5% Milk	0/N 4°C
Caspase-9	CST	#9508 S	mono	H, M, R	mouse	1:1000 5% Milk	0/N 4°C
Chop	Santa Cruz	sc-793	poly	H, M, R	rabbit	1:1000 5% Milk	0/N 4°C
cIAP1/2	Santa Cruz	sc-12410	poly	H, M, R	goat	1:1000 5% Milk	0/N 4°C

cleaved caspase-3	CST	#9664 L	mono	H, M, R, Mk, Dg	rabbit	1:1000 5% Milk	0/N 4°C
cleaved-PARP	CST	#9544 S	poly	M	rabbit	1:1000 5% Milk	0/N 4°C
COX IV	CST	#4844	poly	H, M, R, Mk, B	rabbit	1:1000 5% Milk	0/N 4°C
FADD	Santa Cruz	sc-5559	poly	H, M, R	rabbit	1:1000 5% Milk	0/N 4°C
LC3	Sigma	L7543	poly	H, M, R	rabbit	1:1000 5% Milk	1 hour RT
p62 (SQSTM1)	ENZO	PW9869	poly	H	rabbit	1:1000 5% Milk	0/N 4°C
PARP	CST	#9542 L	poly	H, M, R, Mk	rabbit	1:1000 5% Milk	0/N 4°C
phospho-EIF2-□	CST	#9721 S	poly	H, M, R, Mk	rabbit	1:1000 5% BSA	0/N 4°C
RIP1K	BD biosciences	610459	mono	M, R, Dg, Ch	mouse	1:2000 5% Milk	0/N 4°C
RIP3K	Sigma	R4277	poly	M, R	rabbit	1:1000 5% Milk	0/N 4°C
sXBP1	Biolegend	619502	poly	H, M, R	rabbit	1:1000 5% Milk	0/N 4°C
Total-EIF2-a	CST	#9722	poly	H, M, R, Mk	rabbit	1:1000 5% BSA	2 hour RT
TRADD	Santa Cruz	sc-7868	poly	H, M, R	rabbit	1:1000 5% Milk	0/N 4°C
XIAP	ENZO	AD1-AAM-050	mono	H, M	mouse	1:1000 5% Milk	0/N 4°C

Table 7: Antibodies for Western blotting and Immunoprecipitation

2.15 Clonogenic Survival Assay

$C9^{-/-}$ MEFs PLKO and $C9^{-/-}$ MEFs caspase-8 shRNA were seeded at three different densities in a 6-well plate and subjected to treatment with either brefeldin A or brefeldin A and necrostatin-1, as described in the results section. After 72 h treatment the media was removed from the cells and replaced with fresh growth medium, however the cells which contained treatment in combination with necrostatin-1 continued to be maintained with necrostatin-1 in the fresh growth medium without Bfa for the first 2 days of recovery. The remaining live cells on the plate were allowed to recover and grow for 7 days. Following 7 day recovery the media was removed from the cells, the cells were washed with PBS and then stained with crystal violet solution (2.5% methylene blue, 20% methanol 77.5% dH2O) for 5 min at room temperature. Excess stain was removed by washing with dH2O.

2.16 Annexin V and Propidium Iodide Staining

Externalization of phosphatidylserine (PS) to the outer leaflet of the plasma membrane is a marker of early apoptotic cells and can be assessed using annexin V-FITC which binds to the exposed PS in the presence of calcium. Propidium Iodide (PI) is a fluorescent DNA stain which is excluded from viable cells; however, if the cell has lost its plasma membrane integrity the PI will enter the cell and bind to the DNA. PI positive cells are a marker of late apoptotic or necrotic cells.

Following treatment, cells were trypsinized and transferred to an eppendorf. Cells were let recover from trypsinization for 10 min at 37 °C. The cells were collected by centrifugation at 1000 g for 5 min at 4 °C. The supernatant was removed and the cells were resuspended in 50 µl of ice-cold calcium buffer (10 mM HEPES/NaOH, pH 7.4, 140 mM NaCl, 2.5 mM $CaCl_2$), containing annexin V-FITC (1µl sample) and incubated in the dark for 15 min on ice. Prior to analysis 300 µl of ice-cold calcium buffer containing 4 µl of PI (50 µg/ml) was added to the cells immediately before analysis, which was performed using FACS Calibur flow cytometer (Becton Dickinson).

2.17 Analysis of DEVDase Activity

The activity of effector caspases, DEVDases, was determined fluorometrically. Caspases recognize their substrates by the presence of a DEVD* peptide sequence. Effector caspases cleave their protein substrates after D*. The DEVDase assay exploits this characteristic of effector caspases in order to quantify the caspase activity in a cell population. The tetrapeptide motif DEVD has been used to develop caspase-specific fluorogenic peptide substrate Acetyl-L-Aspartyl-L-Glutamyl-L-Valyl-L-Aspartic Acid α-(4-Methyl-Coumaryl-7-Amide) (Ac-DEVD-MCA). When the effector caspases cleave the peptide substrate, AMC is released which fluoresces at 460nm.

Following treatment, cells were scraped into the media and pelleted by centrifugation at 1000 g for 5 min at 4 °C. The cell pellet was washed in PBS and centrifuged as before. The cells were re-suspended in 50 µl of PBS and 25 µl was transferred to duplicate wells of a microtiter plate and snap-frozen in liquid nitrogen. To initiate the reaction, 50 µM of the caspase substrate Ac-Asp-Glu-Val-Asp-α-(4-methyl- coumaryl- 7- amide) (DEVD-AMC, Peptide Institute Inc Cat# 3171-v) in assay buffer (100 mM HEPES, pH 7.5, 10% sucrose, 0.1% CHAPS, 5 mM DTT and 0.0001% Igepal-630, pH 7.25) was added to the cell lysates. Liberated free AMC was measured by a Wallac Victor 1420 Multilabel counter (Perkin Elmer Life Sciences) using 355 nm excitation and 460 nm emission wavelengths at 37 °C at 60 sec intervals for 25 cycles. The data was analysed by linear regression and enzyme activity was expressed as nM of AMC released × $min^{-1} \times mg^{-1}$ total cellular protein.

2.18 Statistical Analysis

Cell death data is expressed as mean ± SD for at least three independent experiments. Real-Time data is expressed as mean ± SEM for three independent experiments. Differences between the treatment groups were assessed using graph pad's Two-tailed unpaired student's t-tests. The p-values with $pV<0.05$ is considered statistically significant, values with $pV<0.01$ is considered very statistically significant and values with $pV<0.001$ is considered extremely statistically significant.

Chapter 3: Unmasking of a Novel Death Pathway

3.1 Introduction and Objectives

The ER is the site of cellular Ca^{2+} storage and maintains a rich oxidative environment which is required for the synthesis, folding and maturation of most secreted and transmembrane proteins. Physiological or pathological processes that disturb this unique environment cripple the ER's protein folding machinery, a condition referred to as ER stress [197]. The initial cellular responses to ER stress are collectively referred to as Unfolded Protein Response (UPR) [198]. The UPR sustains cell survival by attenuating protein synthesis, and restoring cellular homeostasis via the activation of a cascade of transcription factors which upregulate genes encoding chaperones, components of the ER associated degradation (ERAD) machinery [199] and components of the autophagy machinery [200]. If these cellular adaptive mechanisms fail to re-establish proper ER homeostasis, persistent ER stress induces cell death [112].

The molecular details of how the UPR switches from a pro-survival response to a pro-death response are still unclear, but it does appear to be dependent on the regulation of the Bcl-2 family proteins. The role of the Bcl-2 family in ER stress-induced apoptosis is emphasized by the fact that overexpression of Bcl-2, Bcl-xL and Mcl-1, the anti-apoptotic members of the family can repress ER stress-induced apoptosis [201,202]. Furthermore, the expression levels of the BH3-only proteins, Noxa, Puma and Bim, are increased in cells undergoing ER stress-induced apoptosis, thereby coupling ER stress to Bax/Bak mediated MOMP [201,202]. It is likely that the upstream events of the mitochondria differ in response to ER stress depending on the ER stress inducing stimuli, the cell type or the species under investigation. However, the mode of cell death executed by the cell in response to ER stress is generally quite consistent. Following Bax and Bak activation, mitochondrial outermembrane permeabilization results in the release of the mitochondrial factor, cytochrome c, stimulating the assembly of the apoptosome. The apoptosome provides a platform for caspase-9 activation, resulting in subsequent processing and activation of executioner caspases, ensuring apoptotic cell death. Although ER stress primarily uses the mitochondrial-mediated apoptotic pathway to execute cell death, conditions where this pathway is compromised does not inhibit cell death rather it only delays cell death.

Apoptosis is one of most well characterized forms of cell death; however, other forms of cell death also exist, namely necroptosis and autophagy-mediated cell death. These processes are not so well defined, therefore determining their activation can prove difficult[203].

Necroptosis is a programmed form of necrotic cell death. Like necrotic cell death, necroptosis shows similar morphological hallmarks such as rounding of the cell, enhanced cell volume, swelling of organelles, lack of inter-nucleosomal fragmentation, and plasma membrane rupture[182]. Unlike necrotic cell death, necroptosis can be regulated by the receptor-interacting protein kinase 1 (RIP1) and receptor-interacting protein kinase 3 (RIP3). RIP1 and RIP3 form a death complex referred to as the Necrosome. The assembly of the complex requires RIP1 kinase activity, thus chemical inhibition of RIP1 kinase using necrostatin-1 can inhibit the formation of the Necrosome and thus inhibit necroptosis and cell death. Although RIP1 and RIP3 act in concert to form the Necrosome, studies have shown that necroptosis can be executed by RIP3 independent of RIP1[204,205]. It is evident that RIP1 and RIP3 are major regulators of necroptosis; however, it is unclear what the downstream targets of the Necrosome are, or how the Necrosome actually results in cell death.

As discussed in the introduction, autophagic cell death (ACD) is still a controversial topic, there is no clear mechanism of ACD nor are there any hallmarks that can differentiate ACD from pro-survival autophagy signaling. The term autophagic cell death is generally not used as the resulting cell death usually shows features of apoptosis or necrosis, because of this we refer to ACD as autophagy-mediated cell death. What is clear is that in certain conditions inhibition of the autophagic pathway can result in reduced cell death. From the literature morphological descriptions of autophagy-mediated cell death include excessive levels of autophagosome formation and subsequent necrotic-like cell death or apoptotic-like cell death. Inhibition of autophagy reduces cell death in these systems. The studies described in the introduction insinuate that there seems to be no clear mechanism describing how autophagy induces cell death and indeed it may vary depending on the cellular context; however, what is

evident is that in certain conditions autophagy can act as a destructive process, enhancing the levels of cell death.

Exposure of cells to cytotoxic chemotherapeutic drugs or severe adverse conditions will eventually result in cell death. Although the dose of the drug and the time of exposure to the drug may vary depending on the cell, death will generally ensure, at least in culture conditions. The cell displays a very dynamic system; if its primary mode of cell death is compromised it will most likely use an alternative pathway to execute death. Alternative modes of cell death may not be as efficient as the primary route to cell death; however, if we can understand how the cell regulates these alternative pathways and elucidate the major components and inhibitors involved, it will make it possible to develop drugs to specifically enhance the sensitivity of highly resistant cells to these death pathways.

The aim of this study is to investigate the mode of stress induced cell death in cells whose intrinsic apoptotic machinery is compromised. We primarily investigate the effect of ER stress induced cell death in WT and $C9^{-/-}$ mouse embryonic fibroblasts (MEFs); however we extend the study using human cancer cells, different cellular stress inducing agents and different knockout models to inhibit the intrinsic pathway. Our study revealed a novel death inducing pathway which requires components of the autophagy machinery, the apoptotic machinery and the necroptosis machinery. Furthermore, inhibiting these systems individually provides increased resistance to the stress stimuli exerted on the cell; however the cell still dies, albeit at a slower rate, emphasizing how dynamic the cell can be in executing death. Only when we inhibit multiple pathways at a time do we observe a dramatic resistance to cell death.

3.2 Results

3.2.1 Mitochondrial-mediated apoptosis (MMA) compromised cells exhibit a prolonged UPR

It is well established that prolonged ER stress will result in mitochondria-mediated apoptosis (MMA) via activation of the apoptosome[206]; however, no studies have monitored the UPR when this route of cell death is compromised. Here we monitor the effect of caspase-9 deficiency on the UPR. To test whether caspase-9 deficiency resulted in a differential UPR we treated WT and $C9^{-/-}$ MEFs with the ER stress inducing agents thapsigargin (Tg), A SERCA pump inhibitor, or tunicamycin (Tm), an inhibitor of N-glycosylation, and monitored an array of UPR target genes, both at the RNA level by real time PCR (Fig 3.1) and at the protein level by Immunoblotting (Fig 3.2).

In order to obtain a direct read out of UPR signaling kinetics in WT and $C9^{-/-}$ MEFs we monitored an array of UPR target genes (EDEM1, ERP72, ATF4, Chop, HERP and P58IPK) using real time PCR (Fig 3.1). Basal transcript pools in WT and $C9^{-/-}$ MEFs were similar; however, upon Tg or Tm treatment WT MEFs showed an increase of transcript pools over the first 12 h followed by a decline over the course of 12 to 24 h. In contrast, $C9^{-/-}$ MEF transcript levels increased more gradually and levels were retained up to 24 h.

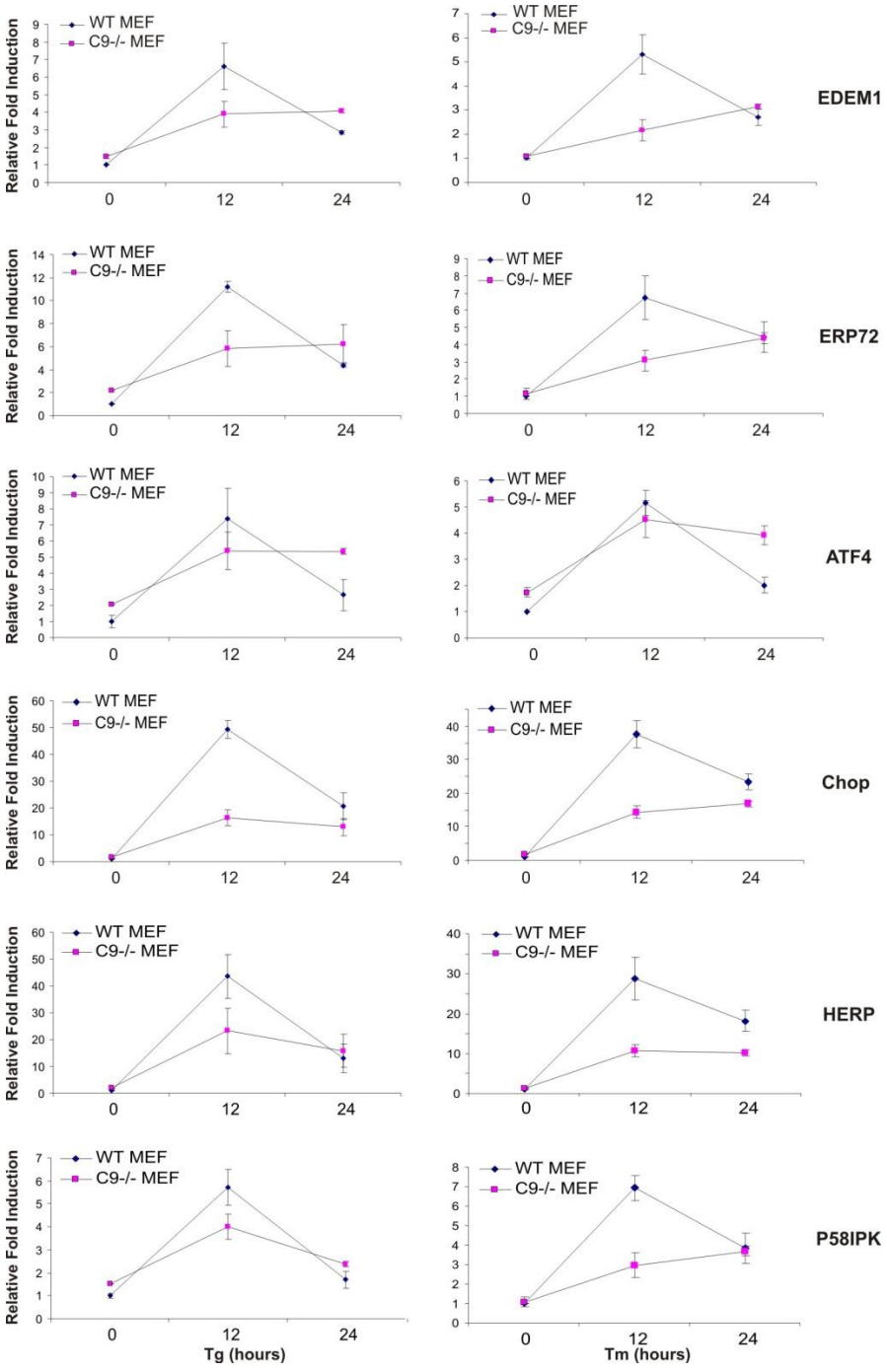

Figure 3.1: Differential kinetic of UPR induction in WT vs C9$^{-/-}$ MEFs. WT and C9$^{-/-}$ MEFs were treated with 0.5 μM Tg or 0.5 μg/ml Tm for the indicated time points. Cells were harvested in TRIzol at the indicated time points. RNA was extracted as described in the materials and methods section. 2 μg of RNA was reverse transcribed and the cDNA was diluted in ddH_2O to 1:5 ratios. Real time PCR was carried out on the cDNA using Taqman probes for EDEM1, ERP72, ATF4, Chop, HERP, P58IPK. Genes were normalized to GAPDH levels. Graphs were plotted as relative fold induction in respect to WT 0 h. Graphs represent the mean ± SEM of three independent experiments.

To ensure that this kinetic response observed at the RNA level translated at the protein level we carried out immunoblots for some of the most well established markers of the UPR, including Chop, total and phosphorylated eIF2α and spliced XBP1 (XBP1s) (Fig 3.2). Interestingly there was no attenuation of eIF2α phosphorylation in the $C9^{-/-}$ MEFs upon Tg treatment throughout the 72 h time course, and only a negligible decrease at 72 h upon Tm treatment. This also correlated with prolonged expression of Chop, a downstream transcription factor of the PERK arm of the UPR. Spliced XBP1 also exhibited a prolonged activation similar to that of Chop and eIF2α. In contrast, WT MEFs showed early attenuation of eIF2α phosphorylation and Chop expression. Studies have shown that prolonged phosphorylation of eIF2α protects cells during ER stress induced cell death which suggests that eIF2α dephosphorylation may act as a determining factor for the switch between protective and pro-death UPR signaling[207]. Our results suggest that inhibition of caspase-9 may result in prolonged eIF2α phosphorylation as well as an overall prolonged UPR response. Of course, these experiments were primarily executed to ensure that these cells actually exhibited a UPR response upon treatment with ER stress inducing drugs, as well as ensuring that the drugs remained active over the long time course of 72 h, of which we have shown in both cases; however, some interesting insights into how the UPR behaves in conditions where cell death is compromised were also revealed.

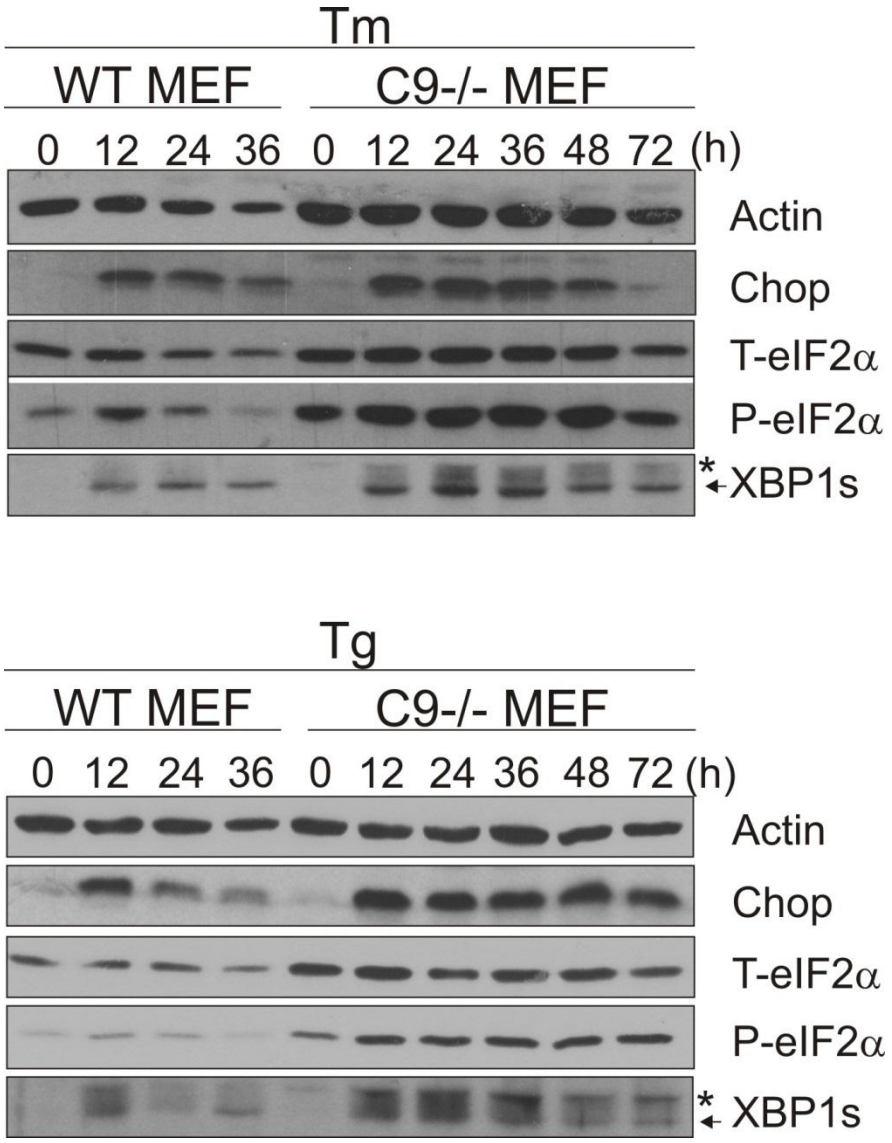

Figure 3.2: WT and C9$^{-/-}$ MEFs exhibit a functional UPR response. WT and C9$^{-/-}$ MEFs were treated with 0.5 μM Tg or 0.5 μg/ml Tm for the indicated time points. Cells were harvested in 1X sample buffer following treatment. Whole cell lysates were subjected to SDS-PAGE followed by immunoblotting. Cell lysates were assessed using antibodies against Actin, Chop, Total-eIF2α (T-eIF2α), phosphorylated-eIF2α (P-eIF2α) and spliced XBP1 (XBP1s). * is indicative of non-specific band.

3.2.2 MMA compromised cells undergo a delayed mode of cell death in response to an array of cellular stresses

Cellular stress stimuli activate an intrinsic apoptotic pathway that is mediated largely by the mitochondria and MOMP[208]. Mitochondrial release of cytochrome *c* into the cytoplasm induces the formation of a multiprotein complex called the apoptosome[163]. The apoptosome contains, among others, cytochrome *c*, pro-caspase-9 and the adaptor protein APAF-1, which supports the auto-activation of caspase-9 through enforced multimerization[163]. Caspase-9 then in turn cleaves and activates the effector caspase-3 resulting in the subsequent degradation of cellular substrates and dismantling of the cell[208].

To determine the sensitivity of WT and $C9^{-/-}$ MEFs to ER stress-induced cell death we treated the cells with the ER stress inducing drugs Tg and Tm. Bright phase microscopy images were analyzed at the indicated time points (Fig 3.3A). Moreover, following treatment, cells were stained with PI and cell viability was analyzed by flow cytometry (Fig 3.3B). We observed that when treated with Tg or Tm for a prolonged period, $C9^{-/-}$ MEFs progressively died and there was a significant loss in viability of $C9^{-/-}$ MEF cultures at 72 h. In contrast WT MEFs died much more rapidly with cell death observed as early as 12 h and almost complete loss in viability at 36 h. Thus, ER stress induces two phases of cell death, the first of which is caspase-9-dependent rapid cell death; the other is caspase-9-independent cell death that occurs at a slower rate.

(A)

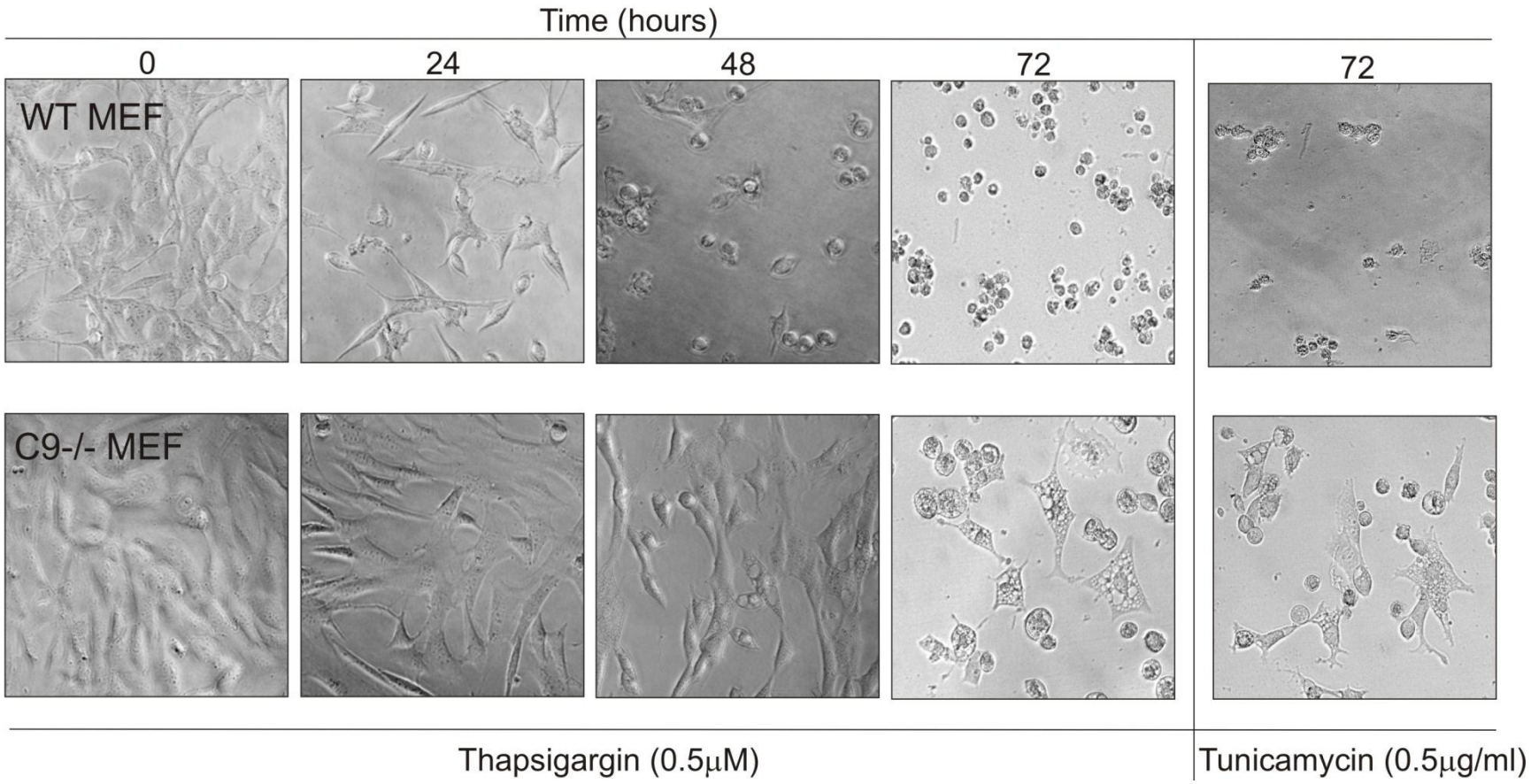
Time (hours)
0
24
48
72
72
WT MEF
C9-/- MEF
Thapsigargin (0.5μM)
Tunicamycin (0.5μg/ml)

(B)

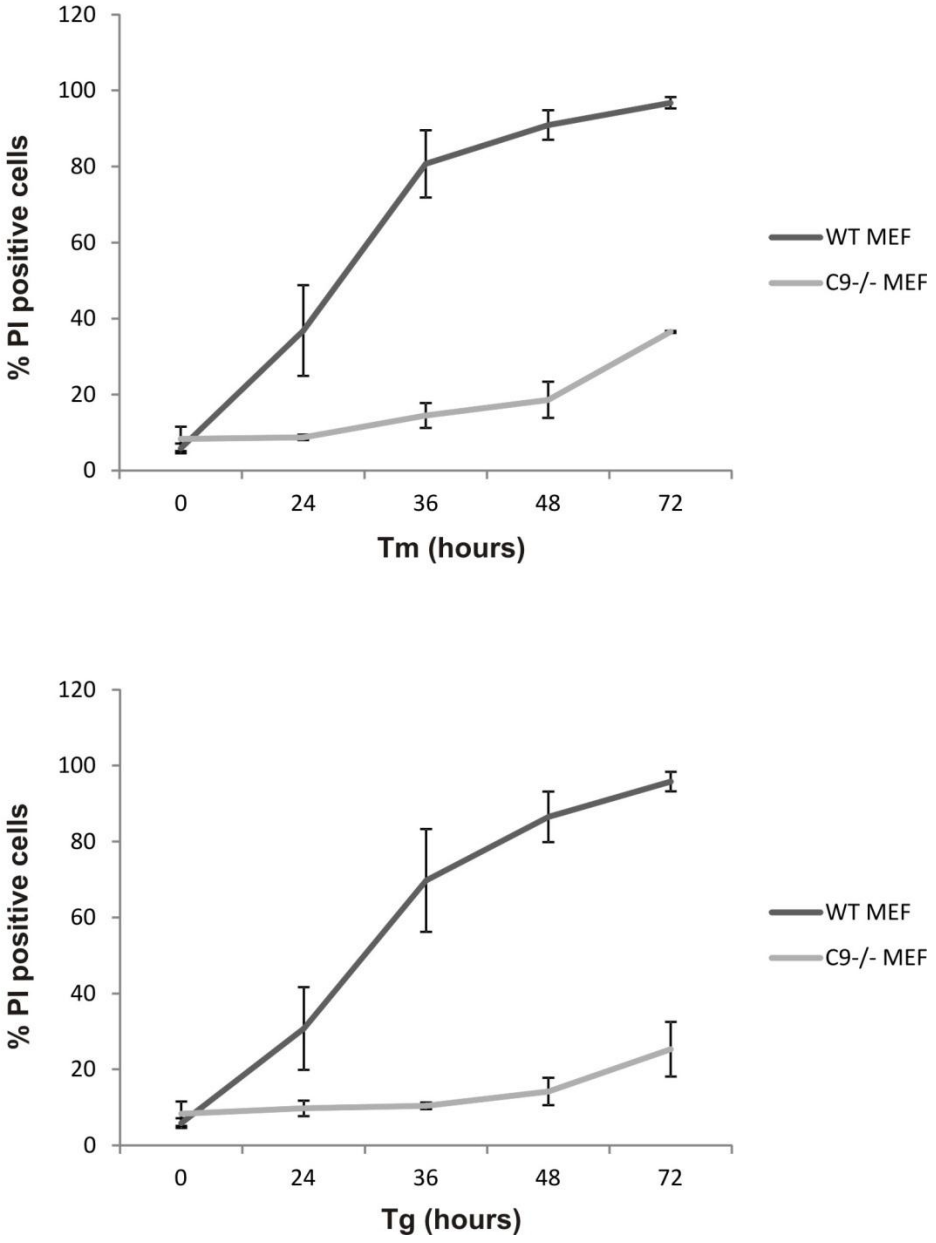

Figure 3.3: Loss of caspase-9 provides resistance to ER stress-induced cell death. **(A)** WT and $C9^{-/-}$ MEFs were treated with 0.5 μM Tg or 0.5 μg/ml Tm for the indicated time points and assessed by bright field microscopy. **(B)** WT and $C9^{-/-}$ MEFs were treated with 0.5 μM Tg or 0.5 μg/ml Tm for the indicated time points. Following treatment, loss of viability was determined with PI staining followed by FACS analysis. Graphs represent the mean ± SD of three independent experiments.

We further subjected WT and $C9^{-/-}$ MEFs to etoposide and bortezomib treatment to ensure that the loss of caspase-9 had the same effect in response to other cellular stress stimuli that use the mitochondrial intrinsic pathway as the primary mode of cell death. Loss of viability was monitored over a prolonged time course using PI staining and FACs analysis. Similar to the ER stress inducing agents Tg and Tm, both DNA damage, mediated by etoposide treatment and proteasome inhibition by bortezomib treatment resulted in a caspase-9 dependent rapid cell death and a delayed caspase-9 independent mode of cell death (Fig 3.4).

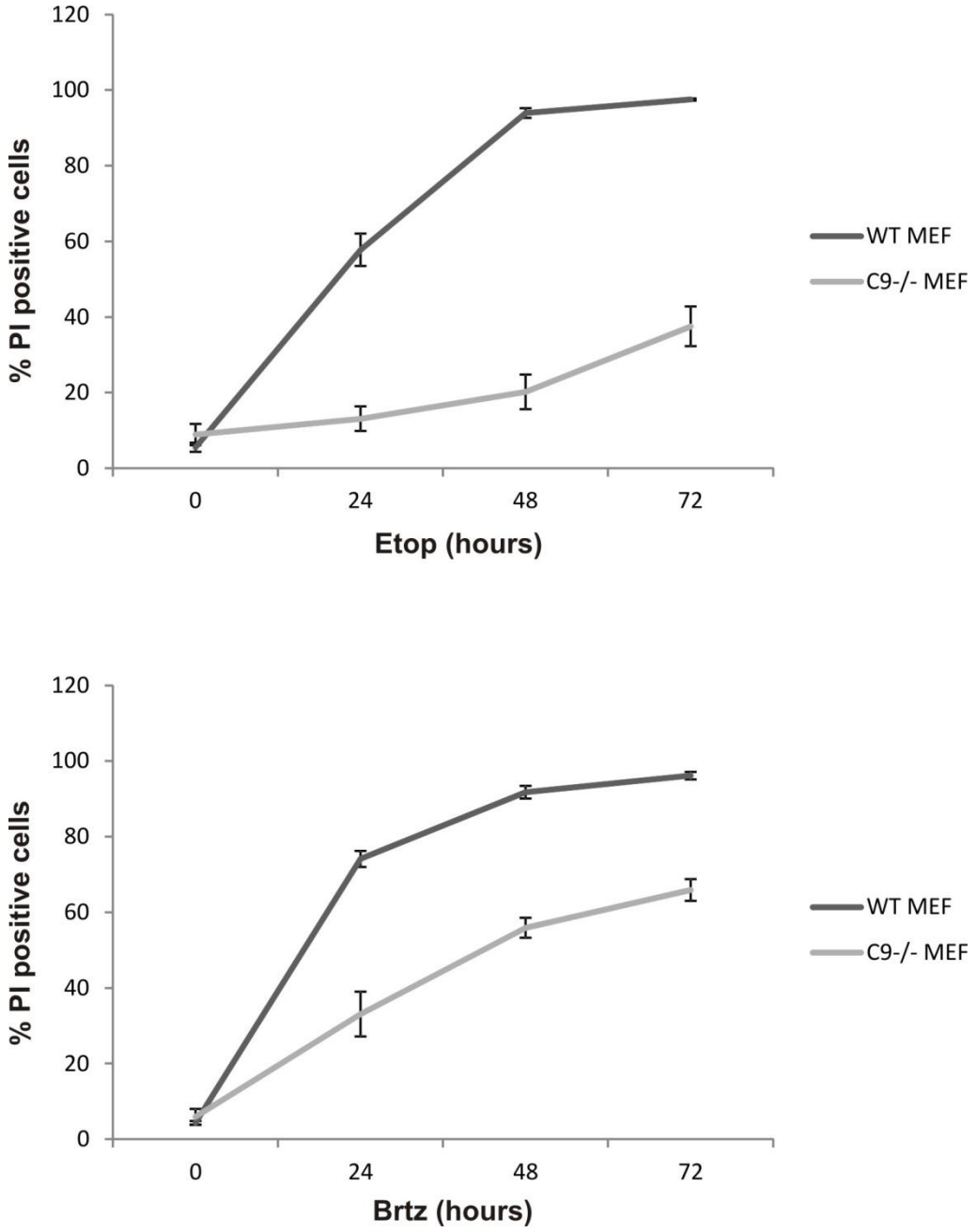

Figure 3.4: Resistance to cell death in caspase-9 deficient cells is independent of stress stimulus. WT and $C9^{-/-}$ MEFs were treated with 50 μM etoposide (Etop) or 1 μM of bortezomib (Brtz) for the indicated time points. Following treatment, loss of viability was determined with PI staining followed by FACS analysis. Graphs represent the mean ± SD of three independent experiments.

3.2.3 MMA compromised cells display apoptosome-independent activation of effector caspases in response to an array of cellular stresses

Although MMA is the primary mode of cell death executed by cells in response to intracellular stresses such as ER stress, DNA damage or proteasomal inhibition, it is well established that other forms of cell death exist, including necroptosis and autophagy-mediated cell death. It is clear that the cell is an exceptionally dynamic system and has the ability to adapt when functions fail, activating alternative signaling pathways. Insight of this we wanted to determine the type of cell death by which WT and $C9^{-/-}$ MEFs endured. One of the most well established features of apoptosis is caspase activation and subsequent cleavage of essential proteins such as PARP. As mentioned earlier, autophagy-mediated cell death and necroptosis are not well defined and thus markers for these processes are not well established. Monitoring the conversion of LC3I to LC3II will allow us to determine if autophagy is induced in our system; however, inhibition of autophagy and subsequent functional studies will be required to determine if autophagy is functioning as a protective response or if it is contributing towards cell death.

We subjected WT and $C9^{-/-}$ cells to an array of cellular stresses by treating with either Tg, Tm, Bfa, Etop or Brtz. Whole cell lysates were harvested at the indicated time points and assessed by Immunoblotting for caspase-9 activation, caspase-3 processing, cleavage of PARP and LC3I to LC3II conversion. WT MEFs displayed characteristic mitochondrial-mediated apoptotic cell death, showing early caspase-9 cleavage followed by processing of the effector caspases-3 as well as PARP cleavage in response to multiple stress inducing stimuli. Interestingly, the $C9^{-/-}$ MEFs showed processing of caspase-3 and PARP cleavage at 48-72 h time points (Fig 3.5). Since these cells have no caspase-9, processing of caspase-3 in these cells is independent of apoptosome. Induction of autophagy in response to these treatments is not surprising; however, the levels of LC3II at later time points in the $C9^{-/-}$ MEFs indicates excessively high levels of autophagy is occurring in the system. Further investigation is required to determine the role of autophagy in this system.

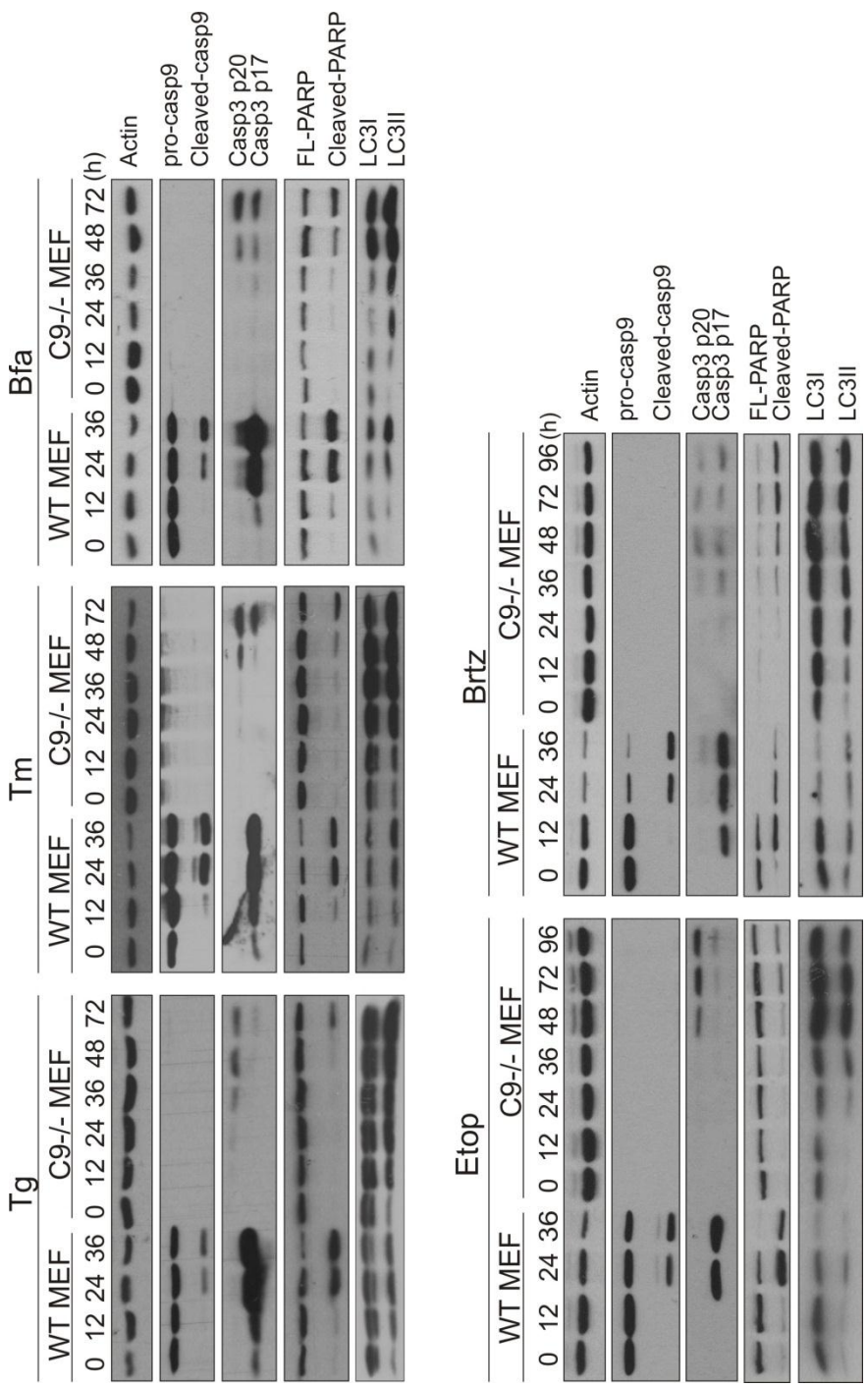

Figure 3.5: C9$^{-/-}$ MEFs display delayed caspase activation in response to multiple cellular stresses. WT and C9$^{-/-}$ MEFs were treated with 0.5 μM Tg, 0.5 μg/ml Tm, 0.5 μg/ml Bfa, 50 μM Etop or 1 μM Brtz for the indicated time points. Cells were harvested in 1X sample buffer following treatment. Whole cell lysates were subjected to SDS-PAGE followed by immunoblotting. Cell lysates were assessed using antibodies against Actin, caspase-9, cleaved caspase-3, PARP and LC3.

To ensure that the delayed cell death with features of apoptosis observed in the $C9^{-/-}$ MEFs was not a specific feature of caspase-9 deficiency and is rather a feature of a compromised mitochondrial-mediated apoptotic pathway, we used Bax/Bak double knockout (BB DKO) MEFs. A prerequisite for MOMP is Bax and Bak homo-oligomerization, resulting in formation of pores which assist cytochrome c release and subsequent apoptosome assembly. Thus BB DKO MEFs also inhibit apoptosome assembly in response to cellular stresses; however, whereas $C9^{-/-}$ MEFs inhibit apoptosome formation downstream of the mitochondria and MOMP, BB DKO MEFs inhibit upstream of the mitochondria.

We show that BB DKO MEFs display a similar response to the $C9^{-/-}$ MEFs. BB DKO MEFs underwent a delayed cell death compared to their WT counterpart; however, although delayed, similar to that of their WT counterpart, BB DKO MEFs displayed features of apoptosis assessed by DEVDase activity of whole cell lysates (Fig 3.6A) as well as caspase-3 processing and PARP cleavage determined by Immunoblotting (Fig 3.6B). Again autophagy levels seem to be quite excessive at later time points in the BB DKO MEFs, indicated by the levels of LC3II. Chop is used here as a marker of ER stress in this system, ensuring that Tm remained active over the prolonged time course.

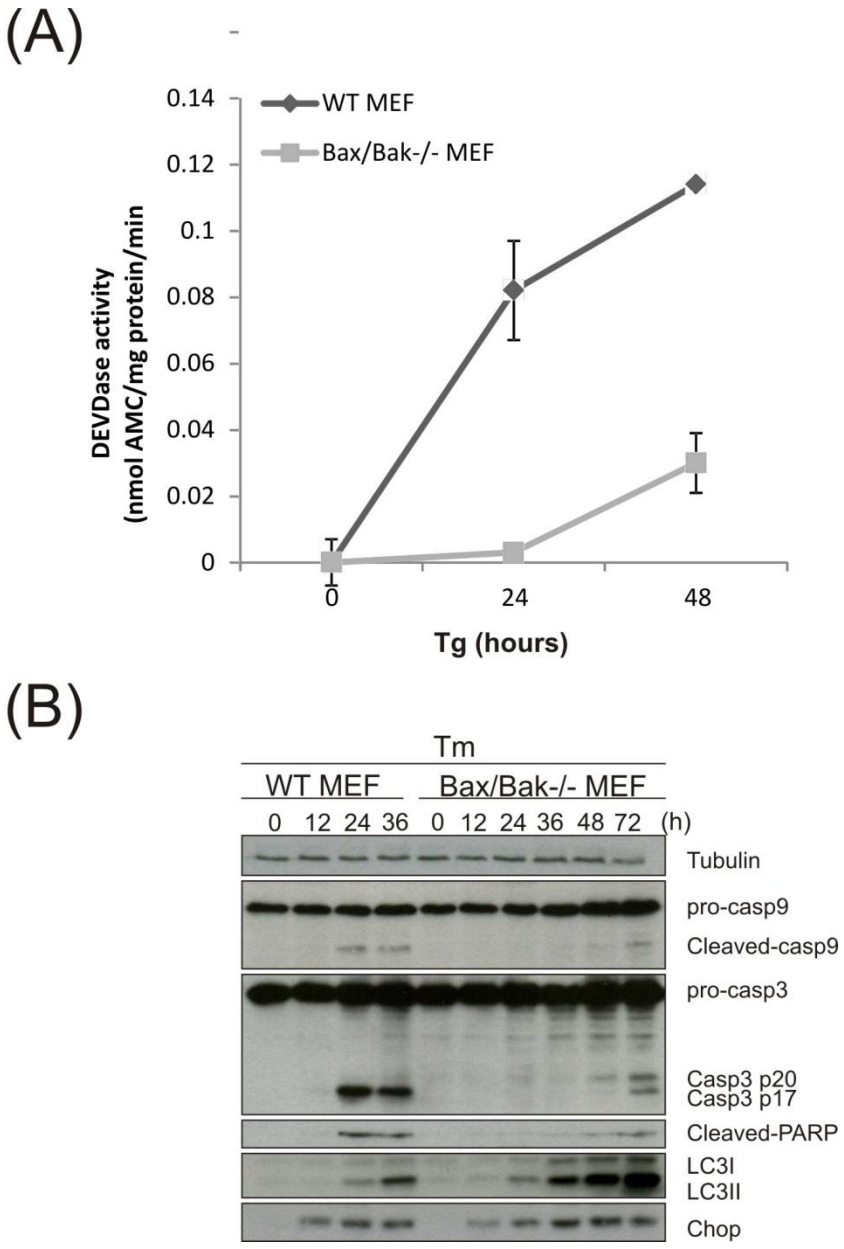

Figure 3.6: Delayed caspase activation is displayed in Bax/Bak$^{-/-}$ MEFs in response to ER stress. WT and Bax/Bak$^{-/-}$ MEFs were treated with 0.5 μM Tg, or 0.5 μg/ml Tm for the indicated time points. **(A)** Caspase activity was determined by DEVD-AMC cleavage activity which was measured in whole cell extracts. The rate of DEVDase activity was normalized to the amount of protein. Graphs represent the mean ± SD of three independent experiments. **(B)** WT and Bax/Bak$^{-/-}$ MEFs were harvested in 1X sample buffer at the indicated time points. Whole cell lysates were subjected to SDS-PAGE followed by immunoblotting. Cell lysates were assessed using antibodies against tubulin, caspase-9, caspase-3, cleaved PARP, LC3 and Chop.

To further confirm that this delayed mode of cell death in MMA compromised cells is conserved, we used human derived WT and $Bax^{-/-}$ HCT116 colon cancer cell line. WT and $Bax^{-/-}$ HCT116 cells were treated with the ER stress inducing agent Bfa, DNA damage inducer etoposide and proteasome inhibitor bortezomib for the indicated time points. Whole cell lysates were assessed by immunoblotting for caspase-9 and caspase-3 processing as well as PARP cleavage. Analogous to the MEFs, the WT HCT116 cells demonstrated a characteristic mitochondrial-mediated cell death showing early caspase-9 activation, caspases-3 processing and PARP cleavage in response to multiple stress-inducing stimuli (Fig 3.7). Yet again the $Bax^{-/-}$ HCT116 cells were less sensitive to the stress stimuli, however at later time points caspase-3 was processed and PARP cleavage was observed. $Bax^{-/-}$ HCT116 also showed some cleavage of caspase-9, more evident in Brtz and Etop treatment; however, caspase-9 was not processed as evidently as in the WT model. The caspase-9 processing is most likely a result of other caspases; thus, although caspase-9 may contribute to caspase-3 processing, it is not the apical caspase in this cascade of events.

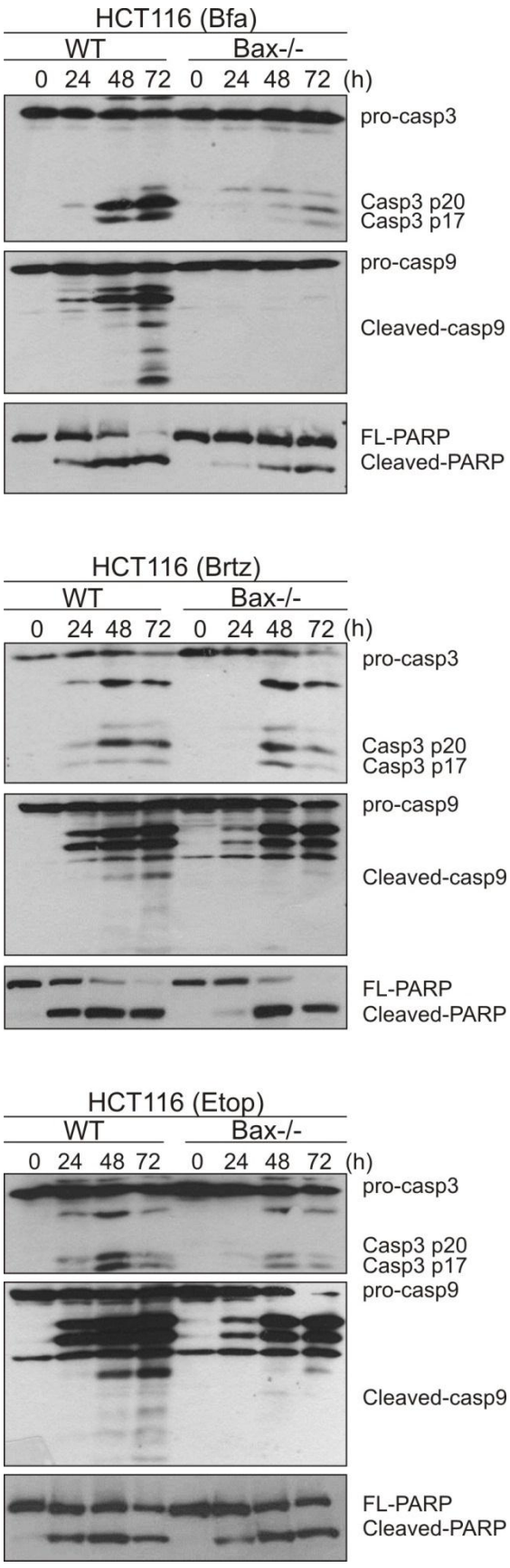

Figure 3.7: Bax$^{-/-}$ HCT116 colon cancer cells display MOMP independent caspase activation in response to cellular stresses. WT and Bax$^{-/-}$ HCT116 cells were treated 0.5 μg/ml Bfa, 50 μM Etop or 1 μM Brtz for the indicated time points. Cells were harvested in 1X sample buffer following treatment. Whole cell lysates were subjected to SDS-PAGE followed by immunoblotting. Cell lysates were assessed using antibodies against actin, caspase-9, caspase-3 and PARP.

3.2.4 Processing of caspase-3 and PARP cleavage is Initiator caspase mediated

To determine if caspase-3 processing and PARP cleavage was mediated by an initiator caspase and not through other proteolytic enzymes such as calpains, we used the caspase-specific inhibitor Boc-D-FMK. The $C9^{-/-}$ MEFs were treated with Tg alone for the first 36 h which was followed by the addition Boc-D-FMK for the remaining 36 h with harvests at 48 and 72 h post Tg treatment. The addition of Boc-D-FMK at 36 h was to ensure that the drug remained active at the late time points of 48 and 72 h. The addition of Boc-D-fmk at 36 h was decided due to the fact that caspase activity was not evident in the $C9^{-/-}$ MEFs until 48 h. We observed that Boc-D-FMK prevented ER stress-induced caspase-3 processing and PARP cleavage in $C9^{-/-}$ MEFs (Fig 3.8). Taken together these results suggest that ER stress induced activation of caspase-3 in $C9^{-/-}$ MEFs is dependent on Boc-D-FMK-inhibited cysteine proteases.

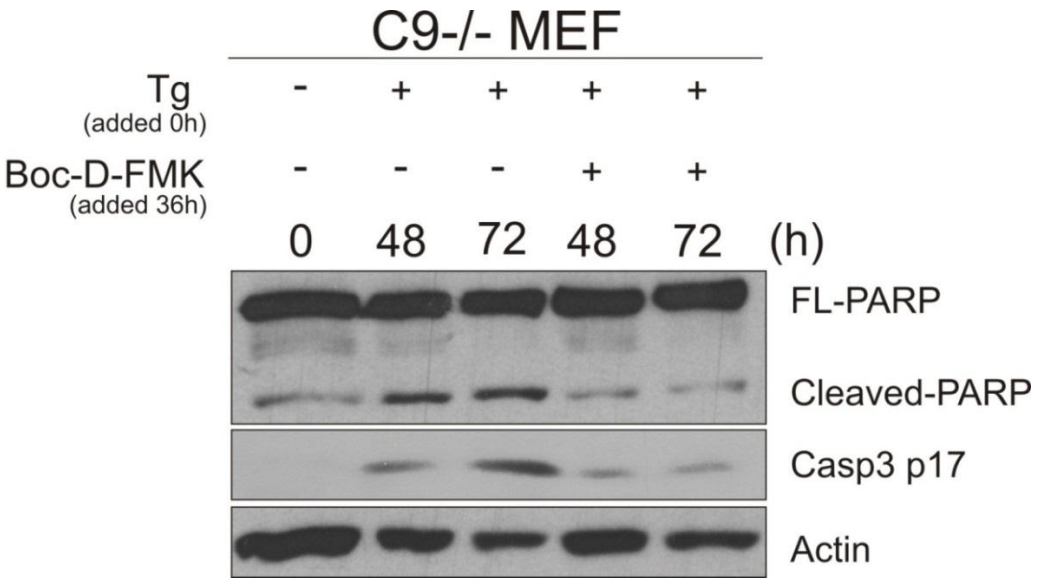

Figure 3.8: Caspase-3 processing and PARP cleavage is impeded by caspase inhibitor. $C9^{-/-}$ MEFs were treated with 0.5 μM Tg or 0.5 μM Tg in combination with 20 μM Boc-D-Fmk for the indicated time points. Tg was added at 0 h whereas Boc-D-FMK was added 36 h post Tg treatment. Cells were harvested in 1X sample buffer following treatment. Whole cell lysates were subjected to SDS-PAGE followed by immunoblotting. Cell lysates were assessed using antibodies against actin, caspase-3 and PARP

3.2.5 Inhibition of the intrinsic pathway unmasks a delayed caspase-8 mediated apoptotic program in response to cell stress

Thus far we have demonstrated that blocking the mitochondrial intrinsic pathway both upstream and downstream of the mitochondria results in the activation of an alternative apoptotic pathway characterized by the activation of effector caspases which lead to PARP cleavage. We further demonstrate that this event is not cell type or cell stress specific and that it requires the activation of an apical caspase as determined from the Boc-D-FMK study.

With this in mind, we next wanted to determine which apical caspase was involved in activating caspase-3. With the exception of caspase-9, caspase-8 has been the only other apical caspase which has been convincingly shown to result in caspase-3 processing. To determine the role of caspase-8 in our system we generated lentivirus expressing either caspase-8 shRNA or a PLKO control (ctrl) vector, and generated stable WT and $C9^{-/-}$ MEFs expressing caspase-8 shRNA. Knockdown of caspase-8 was confirmed by immunoblotting.

$C9^{-/-}$ MEFs PLKO (ctrl transduced cell line) and $C9^{-/-}$ MEFs caspase-8 shRNA were treated with the ER stress inducing agents Tm and Bfa for the indicated time points. Whole cell lysates were assessed by immunoblotting for caspase-3 processing and PARP cleavage. As predicted, caspase-8 knockdown resulted in the complete inhibition of caspase-3 processing and PARP cleavage (Fig 3.9A). This confirmed that the effector caspase-3 was activated by caspase-8 in the $C9^{-/-}$ MEFs; however, to show that these caspases actually contributed towards the death of the cell we carried out PI staining and FACs analysis of $C9^{-/-}$ MEFs PLKO and $C9^{-/-}$ MEFs caspase-8 shRNA at the indicated time points following treatment of Tm or Bfa (Fig 3.9B). Knockdown of caspase-8 in the $C9^{-/-}$ MEFs resulted in an extremely significant rescue from cell death indicating that the activation of caspases are essential for catalyzing this delayed form of cell death.

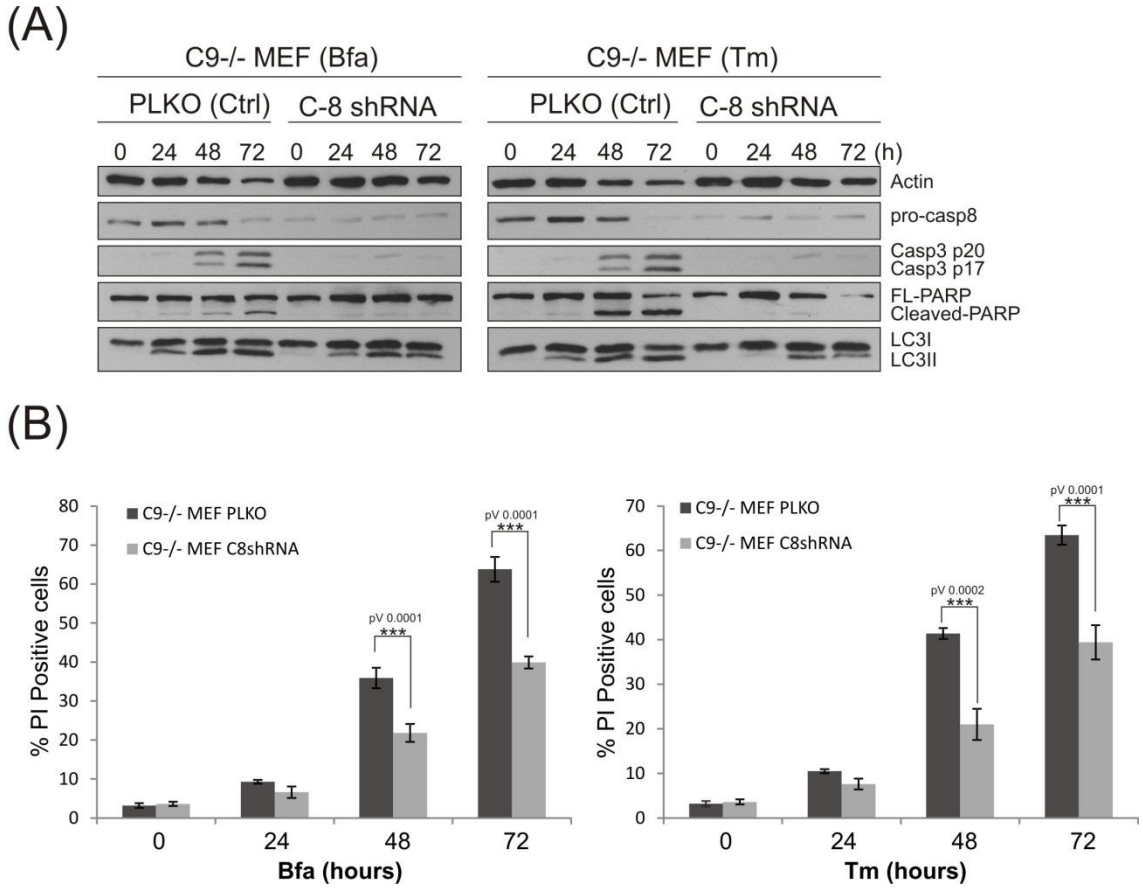

Figure 3.9: Caspase-8 knockdown reduces cell death in C9$^{-/-}$ MEFs. C9$^{-/-}$ MEFs were transduced with a caspase-8 shRNA containing lentivirus or the corresponding PLKO empty vector containing lentivirus as a control. C9$^{-/-}$ MEFs PLKO and C9$^{-/-}$ MEFs caspase-8 shRNA, were treated with 0.5 μg/ml Tm or 0.5 μg/ml Bfa for the indicated time points. **(A)** Following treatment, cells were harvested in 1X sample buffer. Whole cell lysates were subjected to SDS-PAGE followed by immunoblotting. Cell lysates were assessed using antibodies against actin, caspase-8, caspase-3, PARP and LC3. **(B)** Following treatment for the indicated time points, loss of viability was determined with PI staining followed by FACS analysis. Graphs represent the mean ± SD of three independent experiments. Unpaired student *t* test was used to determine the P-value (pV<0.05*, pV<0.01**, pV<0.001***)

We also wanted to determine the role of caspase-8 in conditions where the intrinsic pathway was not compromised. We used WT MEFs transduced with either control PLKO vector or with caspase-8 shRNA to generate stable cell lines, knockdown was validated by immunoblotting. The transduced WT MEFs were treated with ER stress inducing agents, Tm and Bfa. Whole cell lysates were assessed by immunoblotting for the processing of caspase-9, caspase-3 and PARP cleavage (Fig 3.10). In this system

caspase-8 knockdown had no obvious effect on the processing of caspase-9, caspase-3 or PARP cleavage. It is likely that the effects of caspase-8 on cell death are concealed by the potent effect of the apoptosome mediated processing of caspase-3 and apoptosis. The MMA pathway is an exceptionally efficient mode of effector caspase activation and cell death, for this reason cells primarily execute death via this pathway. Thus caspase-8 mediated apoptosis becomes most apparent in conditions where the MMA pathway is compromised.

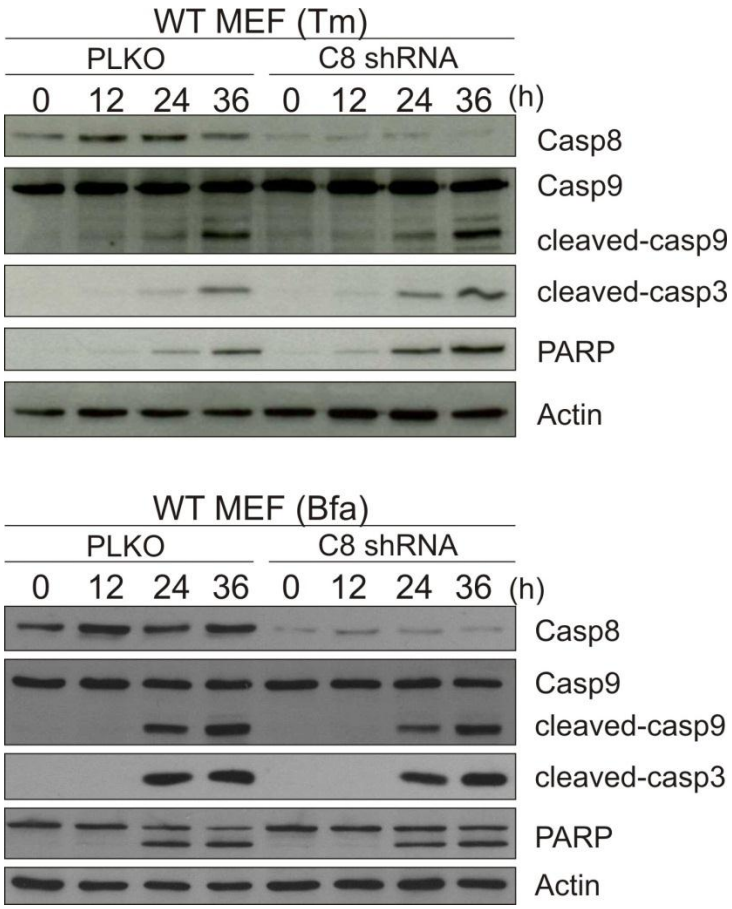

Figure 3.10: Caspase-8 is not required for the processing of caspase-3 and cleavage of PARP in WT MEFs. WT MEFs were transduced with a caspase-8 shRNA containing lentivirus or the corresponding PLKO empty vector containing lentivirus as a control. WT MEFs PLKO and WT MEFs caspase-8 shRNA were treated with 0.5 μg/ml of Tm or 0.5 μg/ml of Bfa for the indicated time points. Following treatments, cells were harvested in 1X sample buffer. Whole cell lysates were subjected to SDS-PAGE followed by immunoblotting. Cell lysates were assessed using antibodies against actin, caspase-8, caspase-9, caspase-3 and PARP.

Next, we wanted to investigate how caspase-8 gets activated in response to intracellular stress stimuli. Caspase-8 is an initiator caspase and thus requires a platform for its activation. Generally caspase-8 activation is observed at the plasma membrane in response to death ligand-mediated activation of death receptors, resulting in the formation of the DISC and recruitment of caspase-8. Less well studied forms of caspase-8 activation include the formation of the ripoptosome as well as the formation of the iDISC on the autophagosome (described in the introduction). To elucidate the mechanism of caspase-8 activation in our system we investigated these different modes of caspase-8 activation.

3.2.6 Caspase-8 requires a RIP1-complex for its activation

We first investigated the possibility of a RIP1-containing complex forming in our system. As discussed in the introduction, the ripoptosome is a newly discovered death inducing signaling complex, which has been described to assemble in response to genotoxic stress or IAP depletion. The unraveling of this complex is still in the early stages. We have yet to understand how cellular stress results in the formation of this complex and the fact that this complex was described to be 2 MDa in size suggests that there are of yet many interacting partners to be discovered. However, what is clear about this complex is that it requires the core proteins RIP1, FADD and caspase-8 for its formation and it forms independent of death receptor activation. It has also been well demonstrated that the complex is regulated by both the inhibitor of apoptosis (IAP) protein family and the FLICE-inhibitory proteins (FLIP) family; depending on the cellular content, the ripoptosome can result in apoptosis, survival or necroptosis (see introduction for more detail).

To determine if a RIP1-containing complex is required for caspase-8 activation in our system we generated lentivirus containing a RIP1 miRNA. $C9^{-/-}$ MEFs were transduced with either pLENTI ctrl lentivirus or RIP1 miRNA containing lentivirus to generate stable cell lines. Knockdown of RIP1 was demonstrated by immunoblotting. $C9^{-/-}$ MEFs pLENTI ctrl and $C9^{-/-}$ MEFs RIP1 miRNA were treated with the ER stress inducing compound Bfa for the indicated time points. Our results show that the knockdown of

RIP1 inhibits caspase-3 processing and PARP cleavage, instigating RIP1 as a major player for caspase-8 activation in our system (Fig 3.11).

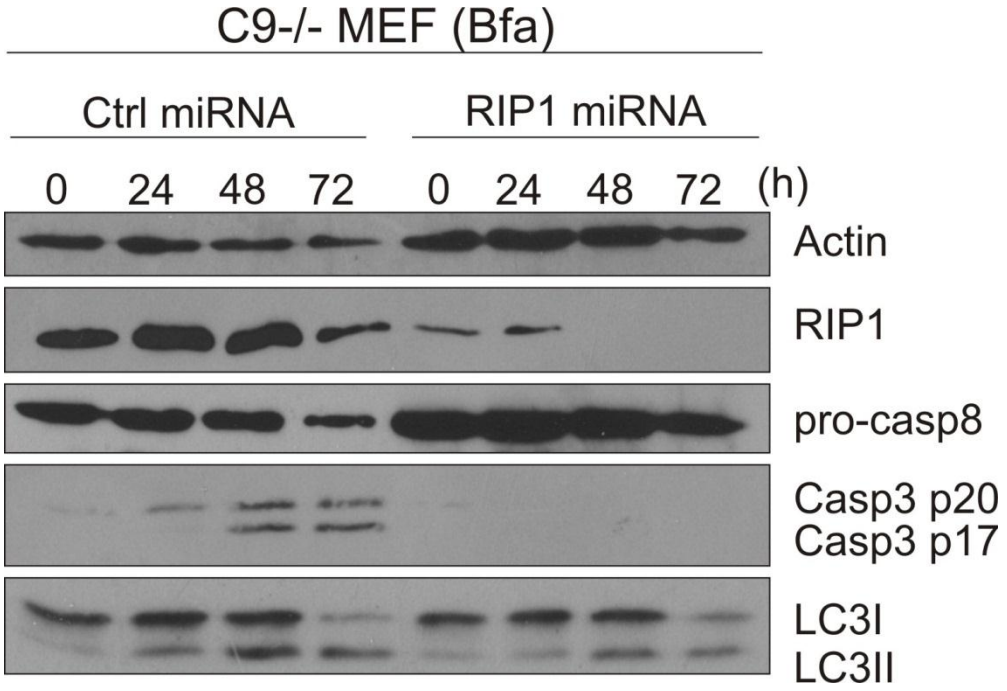

Figure 3.11: RIP1 is required for caspase-3 processing in C9$^{-/-}$ MEFs. C9$^{-/-}$ MEFs were transduced with a RIP1 miRNA containing lentivirus or the corresponding pLENTI empty vector containing lentivirus as a control. C9$^{-/-}$ MEFs pLENTI and C9$^{-/-}$ MEFs RIP1 miRNA, were treated with 0.5 μg/ml of Bfa for the indicated time points. Following treatment, cells were harvested in 1X sample buffer. Whole cell lysates were subjected to SDS-PAGE followed by immunoblotting. Cell lysates were assessed using antibodies against actin, caspase-8, caspase-3, PARP and LC3.

3.2.7 Caspase-8 is activated by a RIP1-containing complex, caspase-8 knockdown switches cell death to necroptosis

Next we wanted to determine whether RIP1 functioned as a scaffolding protein in the caspase-8 activating complex or if it also required its kinase activity for the activation of caspase-8 and subsequent caspase-3 processing. To differentiate between RIP1 scaffolding function and RIP1 kinase function we specifically inhibited RIP1 kinase with necrostatin-1. $C9^{-/-}$ MEFs were treated with Bfa in the absence or presence of necrostatin-1 for the indicated time points. Whole cell lysates were assessed by Immunoblotting for caspase-3 processing and PARP cleavage (Fig 3.12). Our results show that there is only a negligible reduction in caspase-3 processing and PARP cleavage. These results indicate that RIP1 is required as a scaffold protein for the activation of caspase-8 and that its kinase domain is not essential for complex formation however may catalyze its formation as indicated by the slight delay in caspase-3 processing and PARP cleavage.

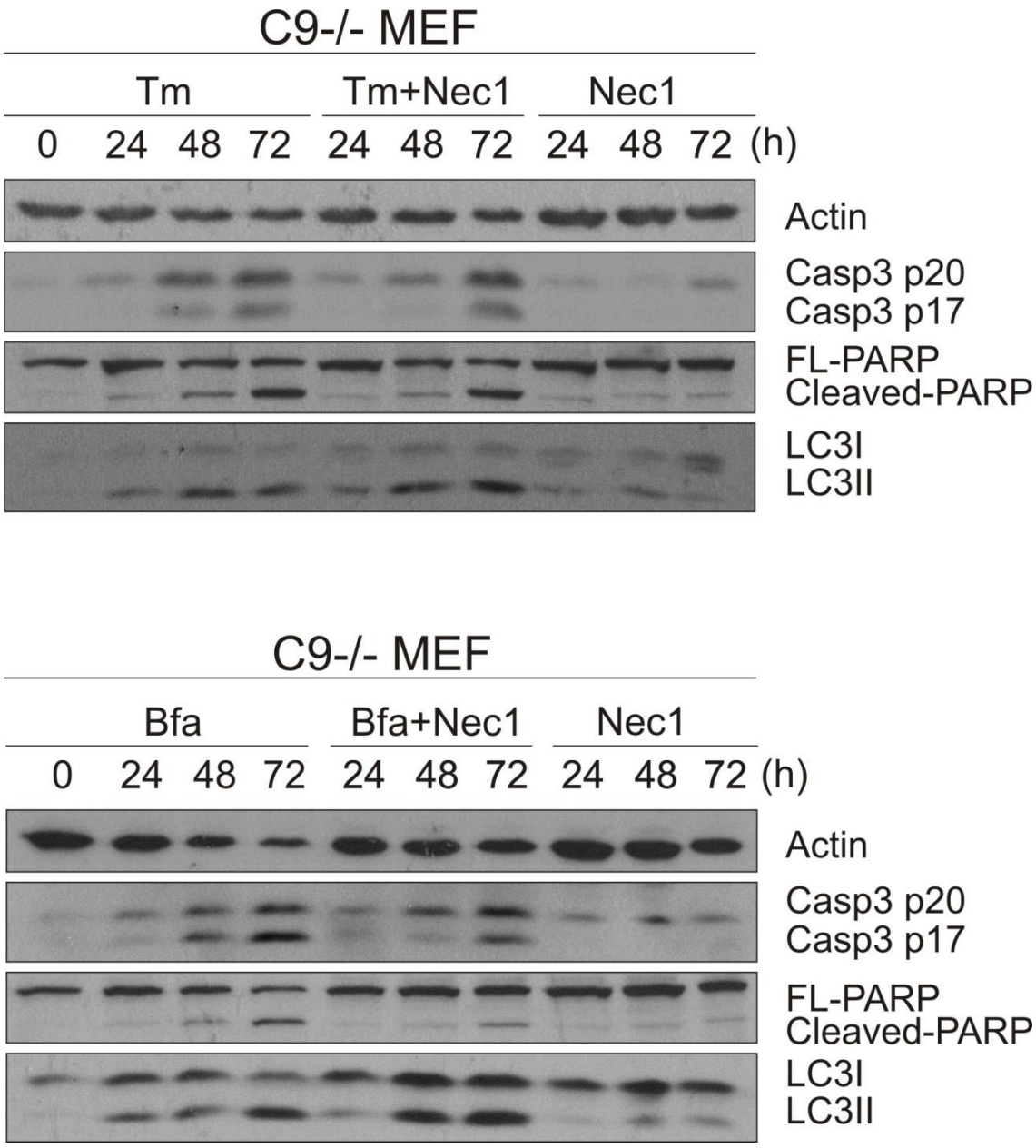

Figure 3.12: C9$^{-/-}$ MEFs requires RIP1 kinase activity for optimal caspase-3 processing in response to ER stress. C9$^{-/-}$ MEFs were treated with 0.5 μg/ml of Tm, 0.5 μg/ml of Bfa, 50 μM of necrostatin-1 (Nec-1), Tm+Nec1 and Bfa+Nec-1 for the indicated time points. Following treatment, C9$^{-/-}$ MEFs were harvested in 1X sample buffer. Whole cell lysates were subjected to SDS-PAGE followed by immunoblotting. Cell lysates were assessed using antibodies against actin, caspase-3, PARP and LC3.

We furthered this study to monitor the effects of necrostatin-1 on cell death in $C9^{-/-}$ MEFs PLKO ctrl and $C9^{-/-}$ MEF caspase-8 shRNA. While we showed that RIP1 kinase domain only had a negligible effect on caspase-3 processing, it did however have a significant effect on cell viability. We further demonstrated that the combination of caspase-8 and necrostain-1(nec-1) resulted in almost complete inhibition from cell death (Fig 3.13).

These results suggest a model similar to that of the ripoptosome or complex II. In conditions where caspase-8 is removed or down regulated the cells can no longer undergo apoptotic cell death; however, because caspase-8 can no longer cleave RIP1in complex, RIP1 phosphorylates RIP3 and subsequently inducing necroptosis. However if in addition to inhibiting caspase-8, we inhibit RIP1 kinase activity we are able to block both modes of cell death.

The effect that nec-1 and caspase-8 knockdown exerts on cell viability was very evident; however, for this effect to have relevance we wanted to demonstrate that the surviving cells could survive and proliferate if treatment was removed. To this end we carried out a clonogenic survival assay on $C9^{-/-}$ MEFs PLKO and $C9^{-/-}$ MEFs caspase-8 shRNA, treated with Bfa or Bfa and nec-1 for 72 h (Fig 3.14). Following the 72 h treatment the drugs were removed and replaced with fresh growth medium. However, in addition to growth medium nec-1 was added in the case of the cells that had been treated with Bfa and nec-1. Nec-1 was only added for the first 2 days of recovery to allow the cell to reinstate a homeostatic environment before RIP1 inhibition was relieved. The cells were given a further 5 day recovery subsequent to nec-1 removal. The rationale for the addition of nec-1 for the first 2 days of recovery came from the fact that although the cells death pathway was blocked with nec-1over the period of Bfa treatment the cells would still be quite stressed upstream of necroptosis or apoptosis. Thus removal of nec-1 would allow activation of RIP1 kinase activity, catalyzing the formation of the RIP1-containing death complex.

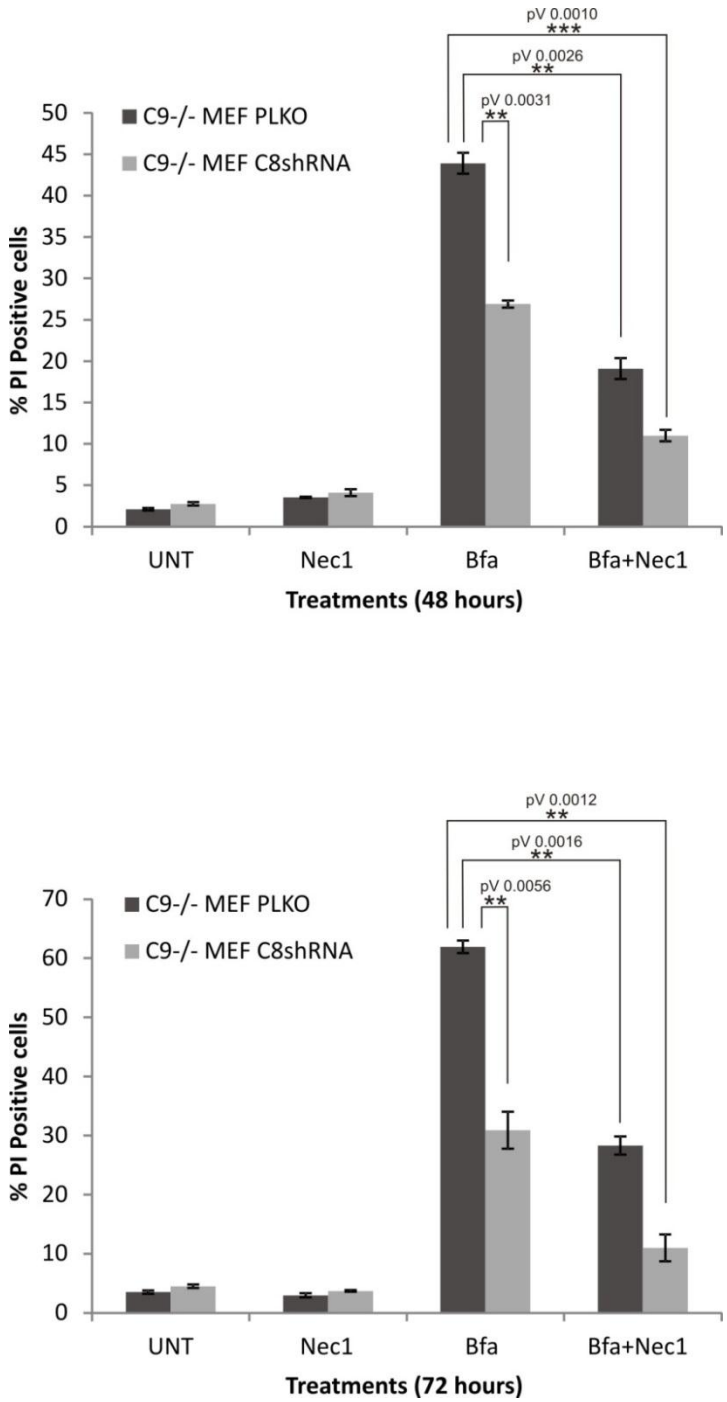

Figure 3.13: C9$^{-/-}$ MEFs undergo a caspase-8 and RIP1 kinase dependent cell death in response to ER stress. C9$^{-/-}$ MEFs PLKO and C9$^{-/-}$ MEFs caspase-8 shRNA were treated with 0.5 μg/ml Tm, 0.5 μg/ml Bfa, 50 μM necrostatin-1 (Nec-1), Tm+Nec1 and Bfa+Nec-1 for the indicated time points. Following treatment, loss of viability was determined with PI staining followed by FACS analysis. Graphs represent the mean ± SD of three independent experiments. Unpaired student *t* test was used to determine the P-value (pV<0.05*, pV<0.01**, pV<0.001***).

Our results confirm what was observed in the viability assays. Caspase-8 knockdown resulted in a significant protection in the $C9^{-/-}$ MEFs and showed a significant amount of colony formation compared to $C9^{-/-}$ MEFs PLKO which resulted in virtually no colony formation. The addition of nec-1 to $C9^{-/-}$ MEFs resulted in an even more pronounced recovery suggesting that RIP1 kinase also significantly contributed to cell death in our system. However addition of nec-1 to the $C9^{-/-}$ MEFs caspase-8 shRNA resulted in even further colony formation.

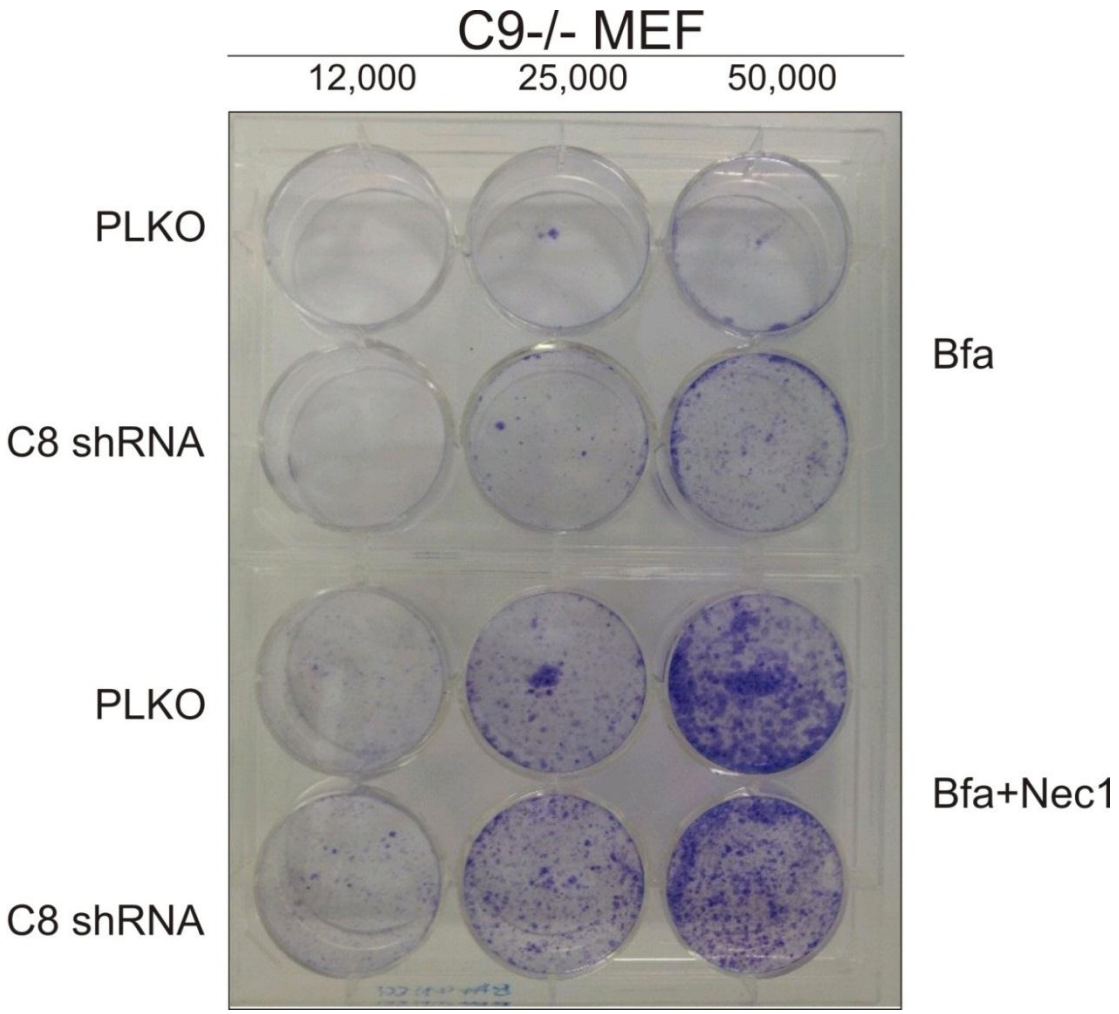

Figure 3.14: Clonogenic survival of $C9^{-/-}$ MEFs is observed subsequent to ER stress inducing treatment. $C9^{-/-}$ MEFs PLKO and $C9^{-/-}$ MEFs caspase-8 shRNA were seeded in a 6 well plate at the indicated densities. Cells were treated with 0.5 μg/ml Bfa or 0.5 μg/ml Bfa+ 50 μM of Nec-1 for 72 h. Following treatment, culture medium was removed and replaced with fresh growth medium or growth medium+50 μM of Nec-1. Cells were left to proliferate for 7 days. After 7 days of recovery cells were stained with crystal violet dye.

Together, these results suggest that in our system we get the formation of a RIP1-containing complex which reflects dynamics similar to that of the ripoptosome and complex II. As described earlier these RIP1-containing death complexes such as the ripoptosome and complex II are quite dynamic, depending on the cellular content they can either induce cell death through apoptosis or necroptosis. In our system it may be the case that a population of the cell culture is undergoing apoptosis as this population may have low FLIP protein levels allowing for caspase-8 activation, conversely the culture may also contain a population of cells that have high FLIP protein levels and thus the RIP1-containing complex signals cell death through necroptosis. Cells with in the same culture having different protein ratios and concentrations is well accepted, it may be for reasons such as stage of cell cycle or possibly sites where cells have more contact with each other in the culture dish, it is for these reasons why cells gradually die in response to a drug over a time course and not all at the same time point.

Alternatively the cells could be dying primarily through apoptosis, however when we knockdown caspase-8 the RIP1-containing complex now switches to necroptosis.

3.2.8 C9$^{-/-}$ MEFs mode of cell death is depicted by its cellular content

To try and determine the primary mode of cell death in C9$^{-/-}$ MEF we treated the cells with Tm or Bfa for the indicated time points followed by co-staining of the cells with Annexin V and PI (Fig 3.15). Annexin V binds to externalized phosphatidylserine on the cell membrane. Positive Annexin V cells indicate early apoptotic cell, at this stage the cells still maintain their plasma membrane integrity and thus PI cannot penetrate. Cells stained Annexin V and PI positive indicates either late apoptotic or secondary necrotic cells, and PI alone indicates late necrotic.

Our results indicate that the C9$^{-/-}$ MEFs seem to be primarily undergoing apoptotic cell death. The dying cells are migrating into the Annexin V + channel (early apoptosis) and up into the Annexin V+/PI+ channel (secondary necrosis). However, because Annexin V+/PI+ channel can be indicative of late apoptosis or necrotic cells it is still possible that some cells are undergoing necroptosis. The cell death profile of the C9$^{-/-}$ MEFs is similar to the WT MEFs, although with slower kinetics, suggesting that the C9$^{-/-}$MEFs are dying by similar means, in contrast, the H_2O_2 treated cells are a positive marker for

necrotic cell death which displays a completely different profile. However, because this experiment only catches cell death at defined time points, it is impossible to determine if cells in the Annexin V+/PI+ channel migrated from the Annexin V+ channel or directly from the Annexin V- /PI – channel.

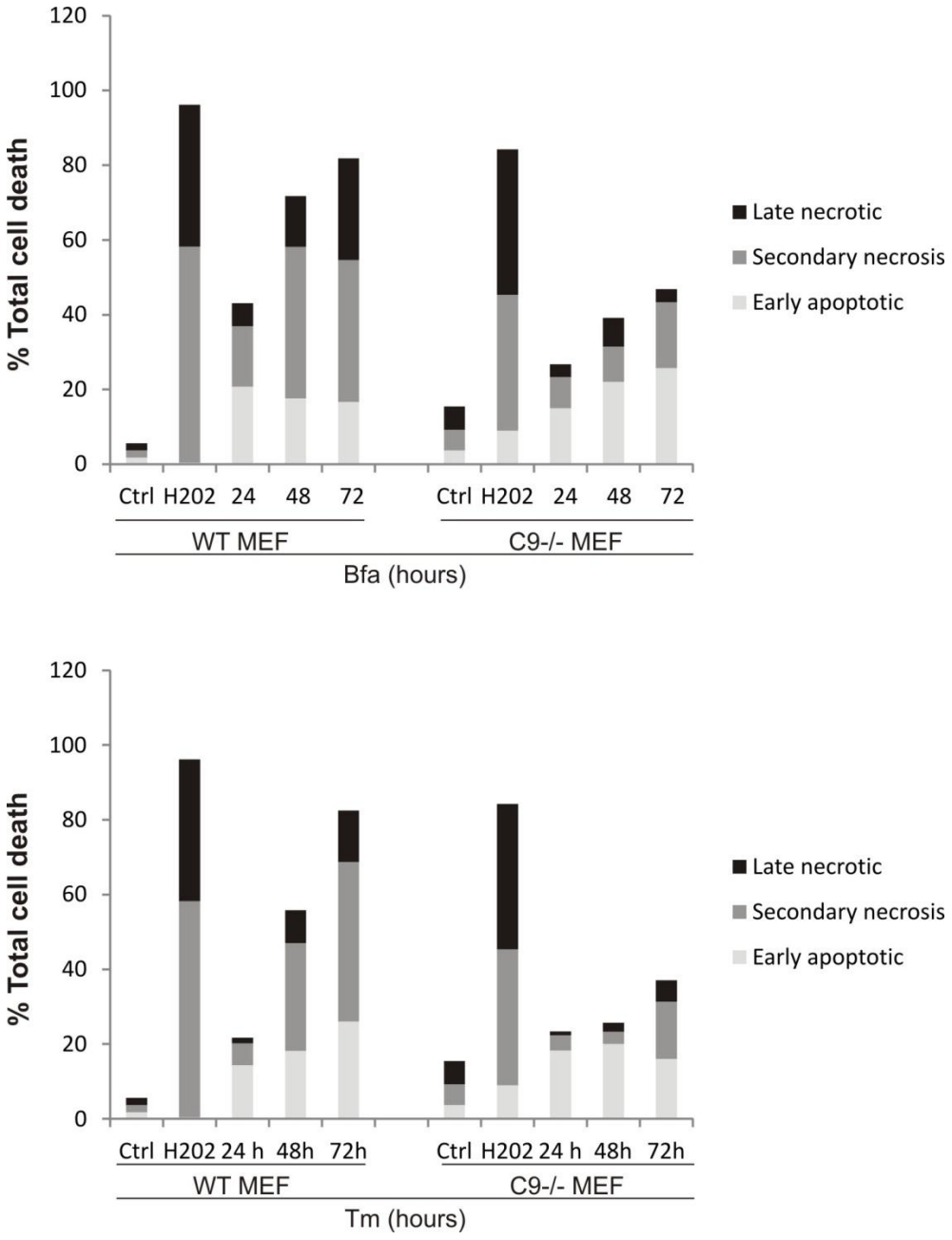

Figure 3.15: Annexin V/PI staining of WT and C9-/- MEFs. WT and $C9^{-/-}$ MEFs were treated with 0.5 μg/ml of Tm or 0.5 μg/ml of Bfa for the indicated time points. Following treatment, cell death was determined with Annexin V/PI staining followed by FACS analysis. Graphs represent the mean of three independent repeats.

To try and resolve this question, we attempted to uncouple apoptosis and necroptosis in the $C9^{-/-}$ MEFs. Necroptosis occurs through the activation of the Necrosome, a complex which consists of the core proteins RIP1 and RIP3. If caspase-8 is inhibited in the ripoptosome or complex II, RIP1 phosphorylates RIP3 to induce necroptosis. With this in mind, knocking down RIP3 should inhibit necroptosis and not affect the apoptotic signaling of the RIP1-containing, caspase-8 activating complex in our system. To this end we generated lentivirus containing RIP3 miRNA and the corresponding control vector pLENTI. $C9^{-/-}$ MEFs were transduced with either pLENTI ctrl lentivirus or RIP3 miRNA containing lentivirus to generate stable cell lines. Knockdown of RIP3 was confirmed by Immunoblotting (Fig 3.16). $C9^{-/-}$ MEFs pLENTI ctrl and $C9^{-/-}$ MEFs RIP3 miRNA were treated with the ER stress inducing compound Bfa or Tm for the indicated time points. Our results show that the knockdown of RIP3 enhanced the levels of caspase-3 processing suggesting that the knockdown of RIP3 pushes the cells into apoptosis (Fig 3.16).

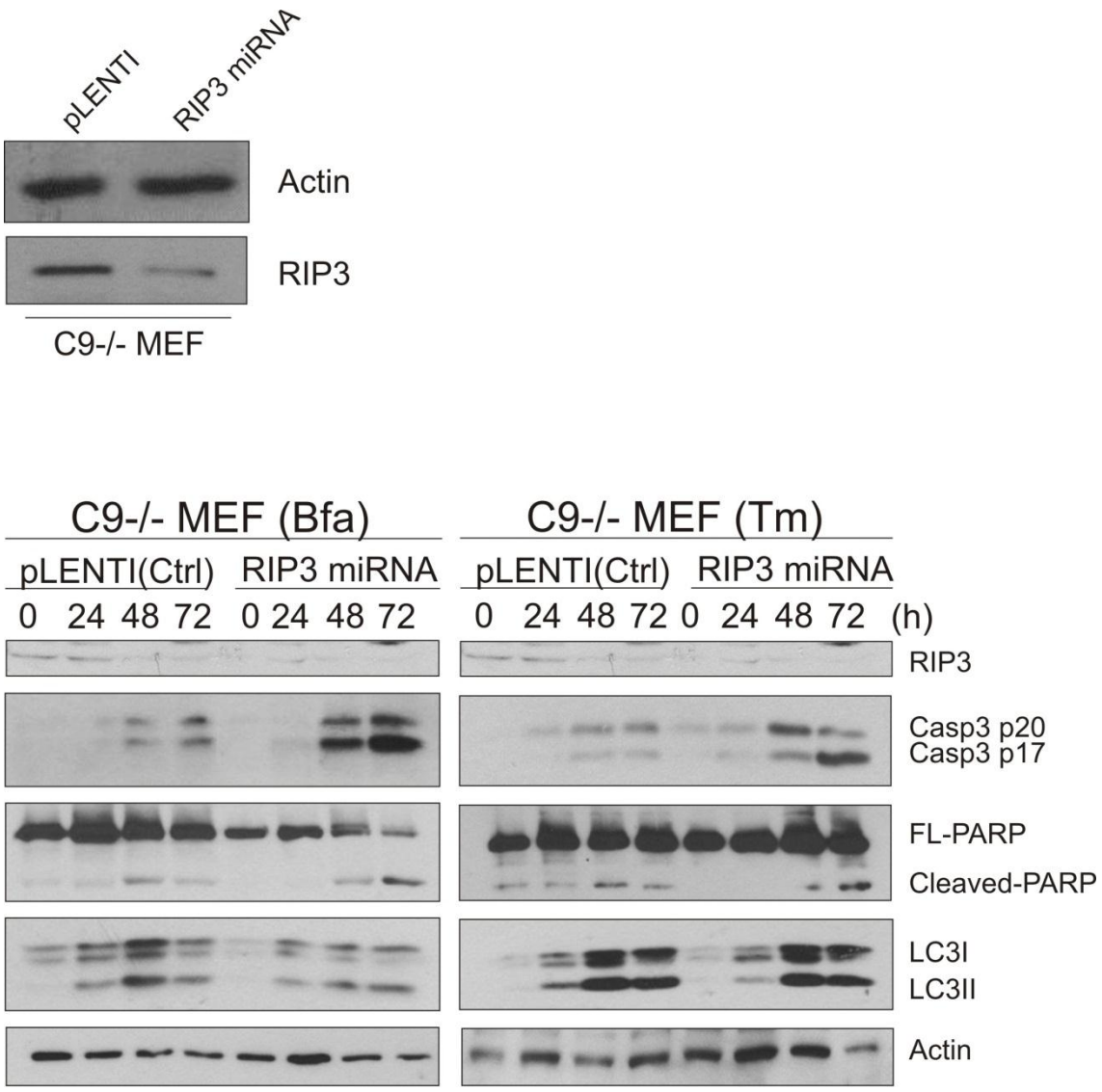

Figure 3.16: Knockdown of RIP3 in C9$^{-/-}$ MEFs enhances caspase-3 processing. C9$^{-/-}$ MEFs were transduced with a RIP3 miRNA containing lentivirus or the corresponding pLENTI empty vector containing lentivirus as a control. C9$^{-/-}$ MEFs pLENTI and C9$^{-/-}$ MEFs RIP3 shRNA, were treated with 0.5 μg/ml of Tm or 0.5 μg/ml of Bfa for the indicated time points. Following treatment, cells were harvested in 1X sample buffer. Whole cell lysates were subjected to SDS-PAGE followed by immunoblotting. Cell lysates were assessed using antibodies against actin, RIP3, caspase-3, PARP and LC3.

To determine if RIP3 had any effect on cell viability we treated the cells with Bfa or Tm. At the indicated time points, the cells were stained with PI and cell viability was analyzed by flow cytometry (Fig 3.17). Our results indicate that the knockdown of RIP3 and thus the inhibition of necroptosis has no effect on overall cell death (Fig 3.17),

however it does enhance caspase-3 processing (Fig 3.16), thus indicating that C9$^{-/-}$ MEFs may undergo both apoptosis and necroptosis in response to cellular stress; however, knockdown of RIP3 in cells undergoing necroptosis switches their mode of cell death to apoptosis.

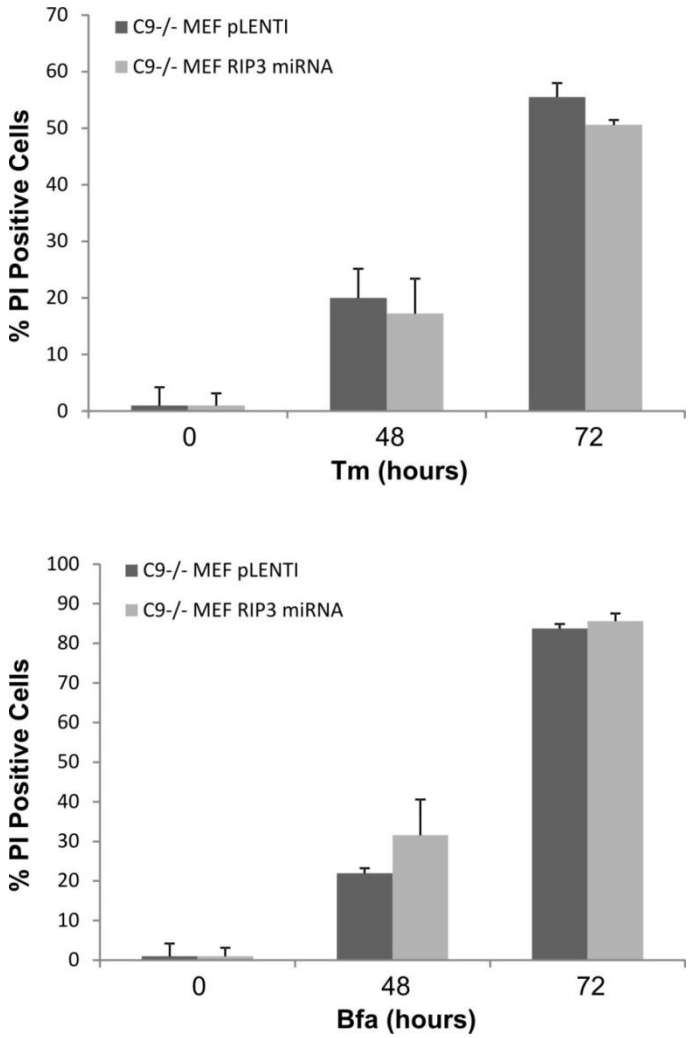

Figure 3.17: Knockdown of RIP3 in C9$^{-/-}$ MEFs has no effect on cell death. C9$^{-/-}$ MEFs were transduced with a RIP3 miRNA containing lentivirus or the corresponding pLENTI empty vector containing lentivirus as a control. C9$^{-/-}$ MEFs pLENTI and C9$^{-/-}$ MEFs RIP3 miRNA, were treated with 0.5 μg/ml of Tm or 0.5 μg/ml of Bfa for the indicated time points. Following treatment for the indicated time points, loss of viability was determined with PI staining followed by FACS analysis. Graphs represent the mean ± SD of three independent experiments.

3.2.9 TNF signaling is not involved in the formation of the RIP1-containing complex

Although the complex in our system meets many of the characteristics of the ripoptosome, the ripoptosome tends to have the same dynamic characteristic of the TNF mediated Complex II (discussed in the introduction). To rule out the possibility of TNF secretion and subsequent autocrine signaling we carried out an ELISA assay for the secretion of TNF in response to Tm, Eto and Brtz for the indicated time points in both WT and $C9^{-/-}$ MEFs (Fig 3.18). Our results showed that there were no detectable levels of TNF secreted into the media in response to multiple cellular stresses.

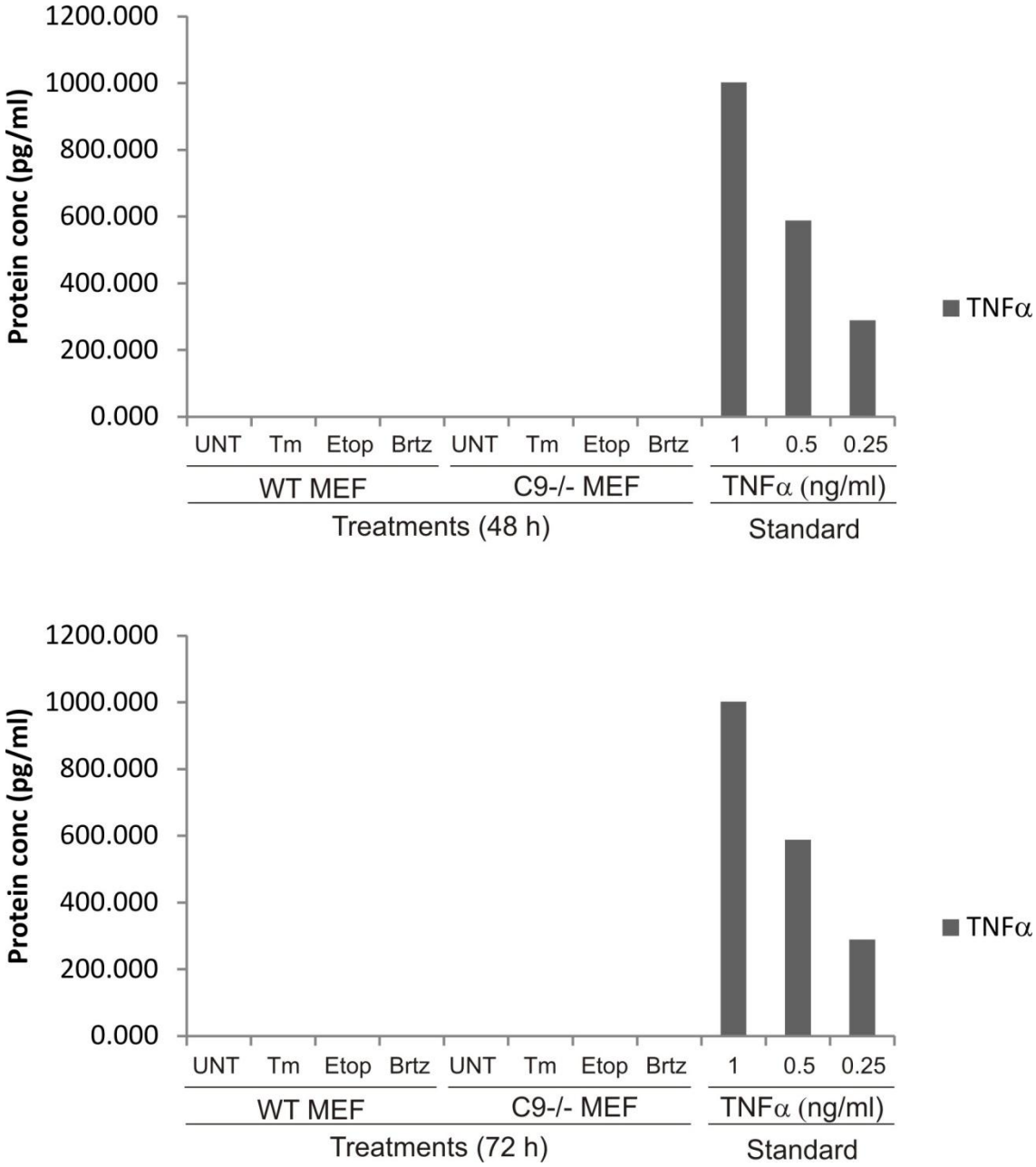

Figure 3.18: WT and C9$^{-/-}$ MEFs do not secrete TNFα in response to cellular stress. WT and C9$^{-/-}$ MEFs were treated with 0.5 μg/ml Tm, 50 μM Etop or 1 μM Brtz for the indicated time points. Following treatment, the medium was removed from the cells, centrifuged to remove dead cells and debris, supernatant was transferred to new eppendorf and stored at -20 °C until required. ELISA was carried out on the harvested medium for the detection of secreted TNFα. Secretion of TNFα from the MEFs was measured against a standard generated from a serial dilution of recombinant TNFα.

Studies have demonstrated that TNFR1 can also signal from IRE1 at the ER[209]. To be confident that TNFR1 signaling was playing no role in the activation of the caspase-8 activating complex in our system, we generated a lentivirus containing TNFR1 shRNA and a lentivirus containing PLKO ctrl vector. We transduced $C9^{-/-}$ MEFs with these lentiviruses to generate stable cell lines. TNFR1 knockdown was validated by conventional PCR against a small sequence of TNFR1 mRNA (Fig 3.18A). To confirm that the knockdown of TNFR1 was sufficient enough to have a functional consequence we treated $C9^{-/-}$ MEFs PLKO and $C9^{-/-}$ MEFs TNFR1 shRNA with the SMAC mimetic (BV6) alone and with BV6 and TNF-α in combination. Addition of BV6 is required for IAP depletion, If IAPs are not depleted TNF-α will only stimulate the activation of the NFκB pathway. Following treatment, cell death was assessed by PI staining and FACS analysis (Fig 3.18B). Our results confirm that TNFR1 knockdown inhibits TNF-α mediated cell death.

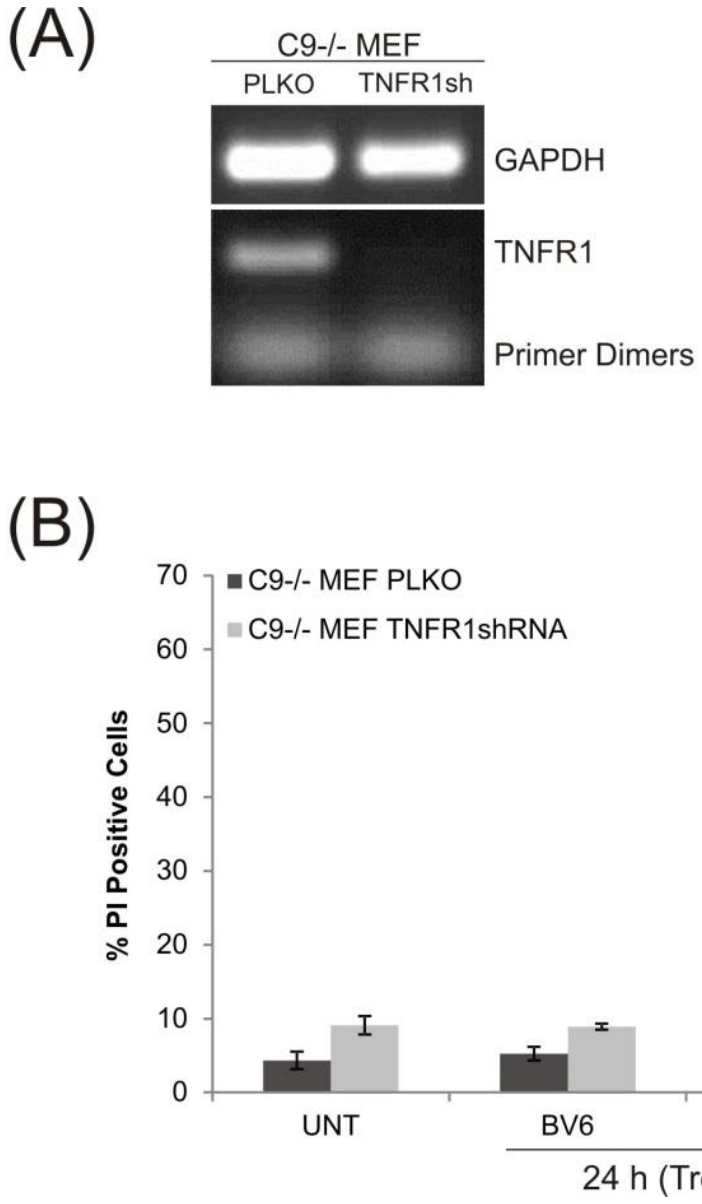

Figure 3.18: Knockdown of TNF Receptor 1 in C9$^{-/-}$ MEFs provides resistance against TNFα stimulation. C9$^{-/-}$ MEFs were transduced with a TNFR1 shRNA containing lentivirus or the corresponding PLKO empty vector containing lentivirus as a control **(A)** RNA was extracted from the generated stable cell lines. cDNA synthesis was performed on 2 μg of extracted RNA. Knockdown was determined by conventional PCR using primers designed against a small region of TNFR1 cDNA, GAPDH was used as control. **(B)** C9$^{-/-}$ MEFs PLKO and C9$^{-/-}$ MEFs TNFR1 shRNA were treated with 10 μM of the SMAC mimetic (BV6) or 200 ng/ml of TNFα + 10 μM BV6 for 24 h. Cell viability was assessed by PI staining and FACS analysis.

To determine if TNFR1 knockdown had any effect on caspase-3 processing in response to ER stress in the C9$^{-/-}$ MEFs, cells were treated with Tm or Bfa for the indicated time points. Whole cell lysates were assessed by Immunoblotting for caspase-3 processing and PARP cleavage (Fig 3.19A). Furthermore we carried out PI staining and FACS analysis to determine if there was any effect on overall cell death (Fig 3.19B). Our results confirm that TNFR1 has no contribution to the processing of capase-3 or PARP cleavage in our system, nor does it affect the viability of the cells in response to ER stress.

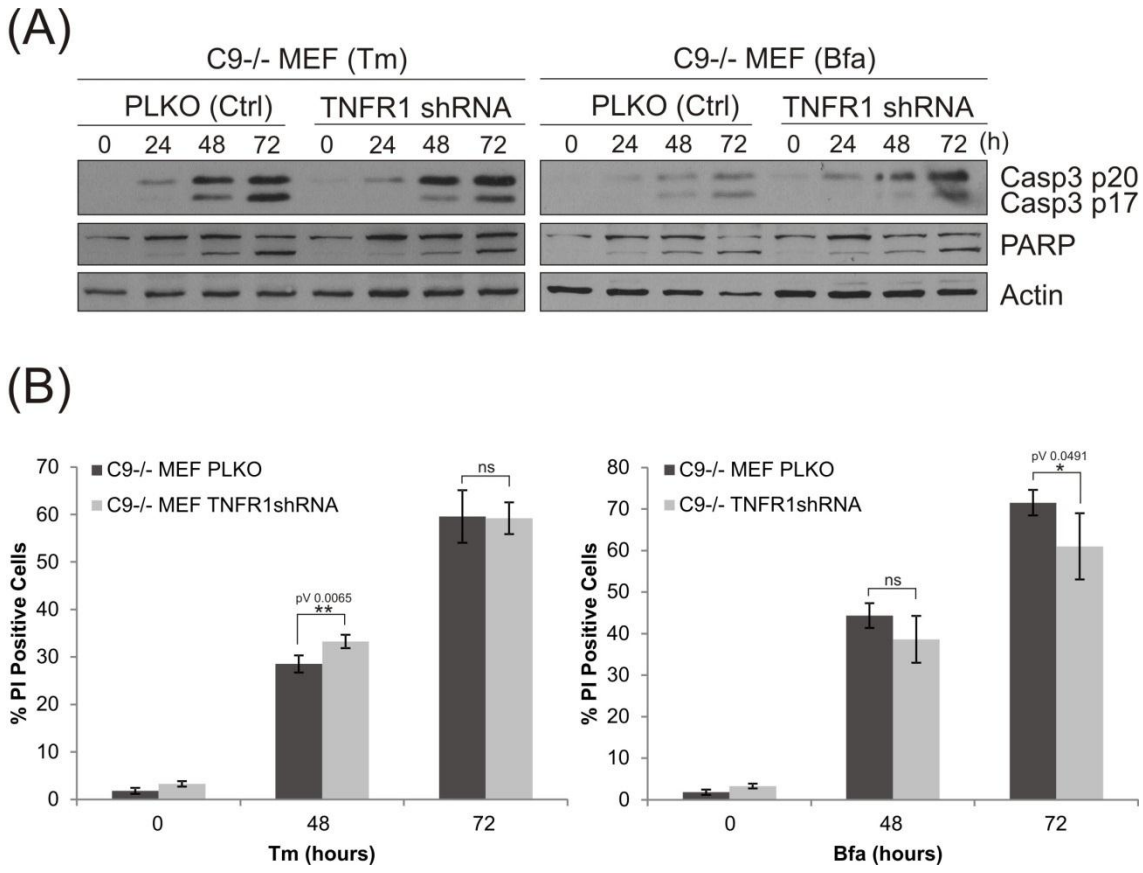

Figure 3.19: Knockdown of TNF Receptor 1 in C9$^{-/-}$ MEFs has no effect on caspase-3 processing or cell viability. C9$^{-/-}$ MEFs PLKO and C9$^{-/-}$ MEFs TNFR1 shRNA were treated with 0.5 μg/ml of Tm or 0.5 μg/ml of Bfa for the indicated time points. **(A)** Following treatment for the indicated time points, C9$^{-/-}$ MEFs PLKO and C9$^{-/-}$ MEFs TNFR1 shRNA were harvested in 1X sample buffer. Whole cell lysates were subjected to SDS-PAGE followed by immunoblotting. Cell lysates were assessed using antibodies against actin, caspase-3 and PARP. **(B)** Following treatment for the indicated time points, loss of viability was determined with PI staining followed by FACS analysis. Graphs represent the mean ± SD of three independent experiments. Unpaired student *t* test was used to determine the P-value (pV<0.05*, pV<0.01**, pV<0.001***).

3.2.10 Assessing the role of the adaptor proteins TRADD and FADD in assembly of the caspase-8 activating complex

The assembly of a caspase activating platform requires adaptor proteins for the recruitment of the initiator caspase. In our case, caspase-8 requires an adaptor protein which contains a death effector domain (DED) for its recruitment to the complex. The most well established platforms which recruit caspase-8 require the adaptor protein FADD for its recruitment, i.e. DISC formation in response to Fas ligand stimulation of the Fas receptor or TRAIL stimulation of the TRAIL receptors. In some cases TRADD acts as an intermediate adaptor protein, binding FADD via its death domain (DD) and FADD subsequently recruiting caspase-8 via its DED, i.e. formation of complex II in response to TNF stimulation.

To determine if FADD was required for caspase-3 processing in our system we again generated lentivirus containing either PLKO or FADD shRNA. Although we obtained a substantial knockdown of FADD, determined by immunoblotting, we found that there was no inhibition of caspase-3 processing in the $C9^{-/-}$ MEFs FADD shRNA compared to PLKO ctrl in response to Bfa treatment (Fig 3.20A). To ensure that the amount of FADD knocked down was sufficient we carried out a functional test similar to that of $C9^{-/-}$ MEF TNFR1 shRNA (Fig 3.18B). $C9^{-/-}$ MEFs PLKO ctrl and $C9^{-/-}$ MEF FADD shRNA were treated with the SMAC mimetic (BV6) alone and with BV6 and TNF-α in combination. $C9^{-/-}$ MEFs PLKO and $C9^{-/-}$ MEFs FADD shRNA showed no difference in sensitivity to treatments, thus indicating that the amount of FADD knockdown obtained was not sufficient (Fig 3.20B).

Upon discussions with other groups we learned that FADD knockdown required almost undetectable levels by Immunoblotting as it can still carry out its function at low levels. To this end we tried a further round of lentivirus transduction; however the shRNA was not capable of lowering the levels of FADD any further.

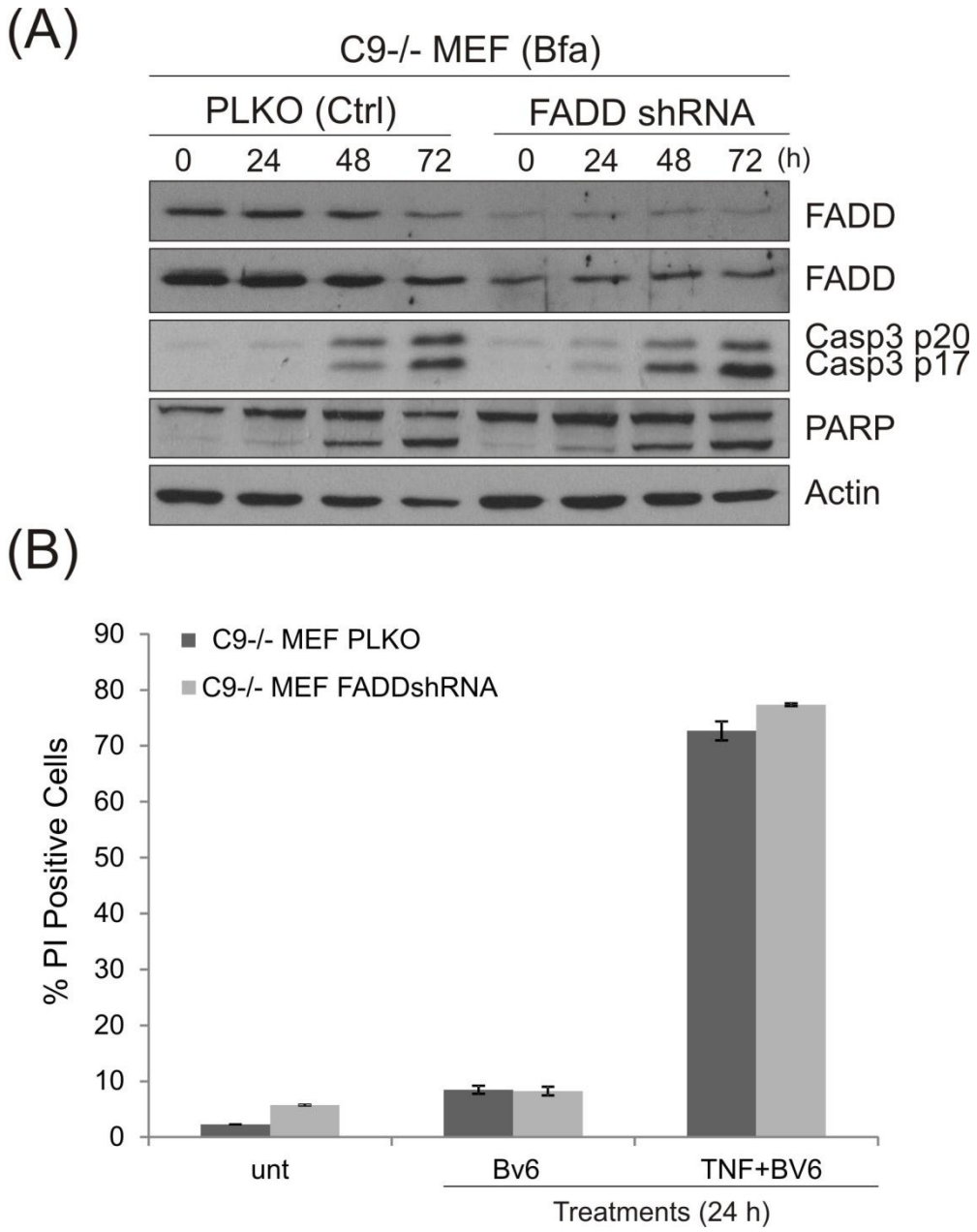

Figure 3.20: Knockdown of FADD in C9$^{-/-}$ MEFs was insufficient to provide a functional effect. C9$^{-/-}$ MEFs were transduced with a FADD shRNA containing lentivirus or the corresponding PLKO empty vector containing lentivirus as a control. Knockdown was determined by immunoblotting. **(A)** C9$^{-/-}$ MEFs PLKO and C9$^{-/-}$ MEFs FADD shRNA were treated with 0.5 μg/ml of Tm or 0.5 μg/ml of Bfa for the indicated time points. Following treatment, cells were harvested in 1x sample buffer. Whole cell lysates were subjected to SDS-PAGE followed by Immunoblotting. Cell lysates were assessed using antibodies against actin, caspase-3, PARP and FADD. **(B)** C9$^{-/-}$ MEFs PLKO and C9$^{-/-}$ MEFs TRADD shRNA were treated with 10μM of the SMAC mimetic (BV6) or 200 ng/ml of TNFα + 10 μM BV6 for 24 h. Cell viability was assessed by PI staining and FACS analysis.

To evaluate the role of TRADD in our system we generated lentivirus containing either PLKO ctrl vector or TRADD shRNA. $C9^{-/-}$ MEFs were transduced with these lentiviruses to generate stable cell lines. TRADD knockdown was confirmed by immunoblotting. $C9^{-/-}$ MEFs PLKO ctrl and $C9^{-/-}$ MEFs TRADD shRNA were treated with Tm or Bfa for the indicated time points. Whole cell lysates were assessed by Immunoblotting for the processing of caspase-3 and PARP cleavage (Fig 3.21A). Furthermore, following treatment with Tm or Bfa at the indicated time points, we carried out PI staining and FACS analysis to determine if there was any effect on overall cell death (Fig 3.21B).

Our results are somewhat confusing. TRADD seems to have only a negligible effect on caspase-3 processing and PARP cleavage; however, TRADD shows a significant protection against cell death. This may suggest that TRADD knockdown is affecting both apoptosis and necroptosis in this system.

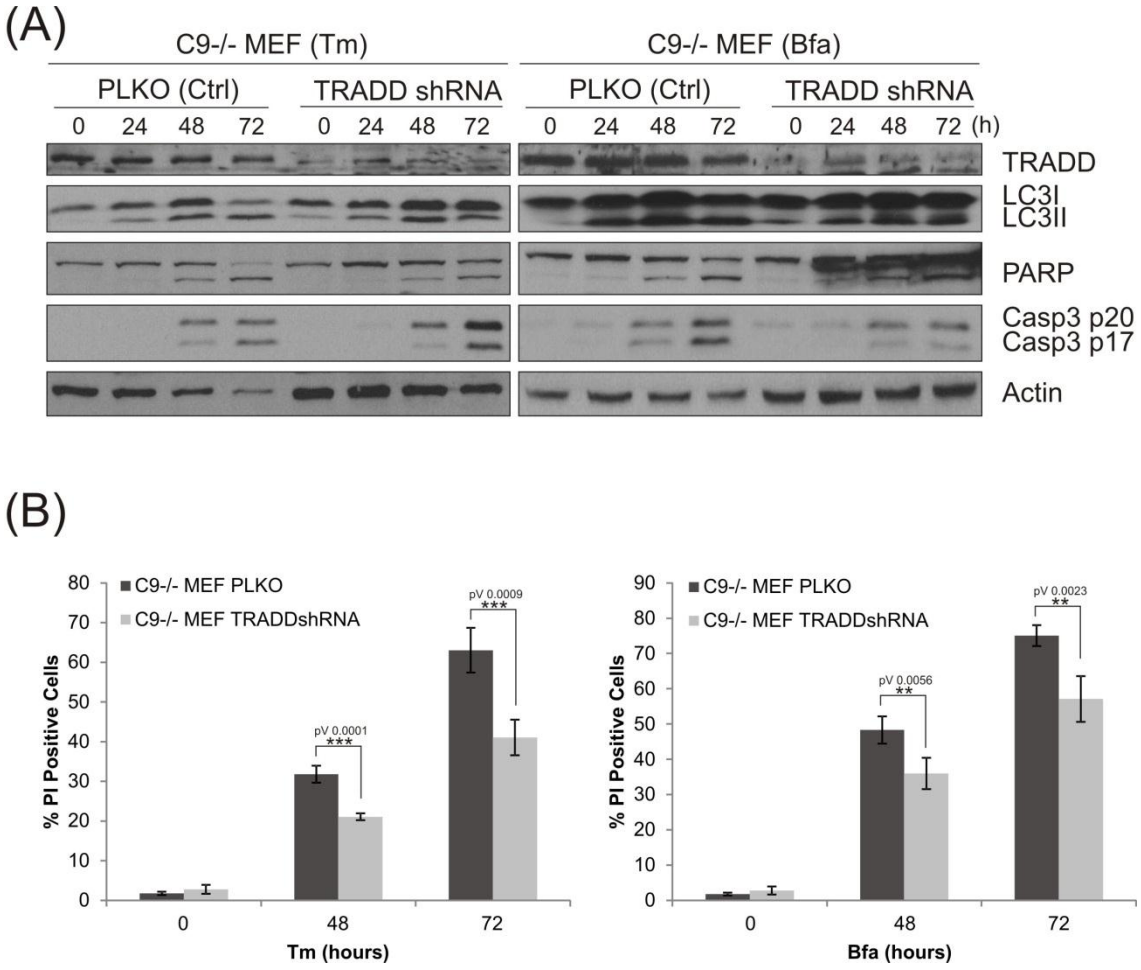

Figure 3.21: Loss of TRADD in C9$^{-/-}$ MEFs has a negligible effect on caspase-3 processing, but a pronounced effect on cell viability. C9$^{-/-}$ MEFs were transduced with a TRADD shRNA containing lentivirus or the corresponding PLKO empty vector containing lentivirus as a control. Knockdown was determined by immunoblotting. C9$^{-/-}$ MEFs PLKO and C9$^{-/-}$ MEFs TRADD shRNA were treated with 0.5 μg/ml of Tm or 0.5 μg/ml of Bfa for the indicated time points. **(A)** Following treatment, cells were harvested in 1X sample buffer. Whole cell lysates were subjected to SDS-PAGE followed by immunoblotting. Total protein was assessed using antibodies against actin, caspase-3 and PARP, LC3 and TRADD. **(B)** Following treatment for the indicated time points, loss of viability was determined with PI staining followed by FACS analysis. Graphs represent the mean ± SD of three independent experiments. Unpaired student *t* test was used to determine the P-value (pV<0.05*, pV<0.01**, pV<0.001***)

3.2.11 The autophagy gene ATG5 is required for caspase-8 activation in MMA compromised cells, however protects WT cells from ER stress induced cell death

As described in the introduction, accumulating evidence is building to suggest that the autophagosome may act as a signaling platform for assembly of a caspase activating complex. Also the connection between autophagy, FADD, caspase-8 and RIP1 in T-cell proliferation insinuates that these proteins can communicate amongst each other in the same pathway or possibly the same complex[210]. Furthermore it is clear that autophagy and ER stress are tightly connected processes, and like the UPR, autophagy can have pro-survival and pro-death consequences if the stress exerted on the cell becomes too extreme.

To demonstrate that autophagy was induced in WT and $C9^{-/-}$ MEFs in response to ER stress, cells were treated with Tm or Tg with or without chloroquine (CQ). Cells were harvested at the indicated time points and whole cell lysates were assessed by Immunoblotting for LC3I and LC3II (Fig 3.22). As described in the material and methods CQ inhibits the final degradation step of the autophagosome at the lysosome. CQ is used to provide evidence to suggest that autophagy is in constant flux in the cell. Thus, if Tm or Tg is inducing autophagosome biogenesis then inhibition of lysosomal degradation should result in enhanced levels of autophagosomes in the cell. The conversion of LC3I to LC3II is used as a marker of autophagosome biogenesis.

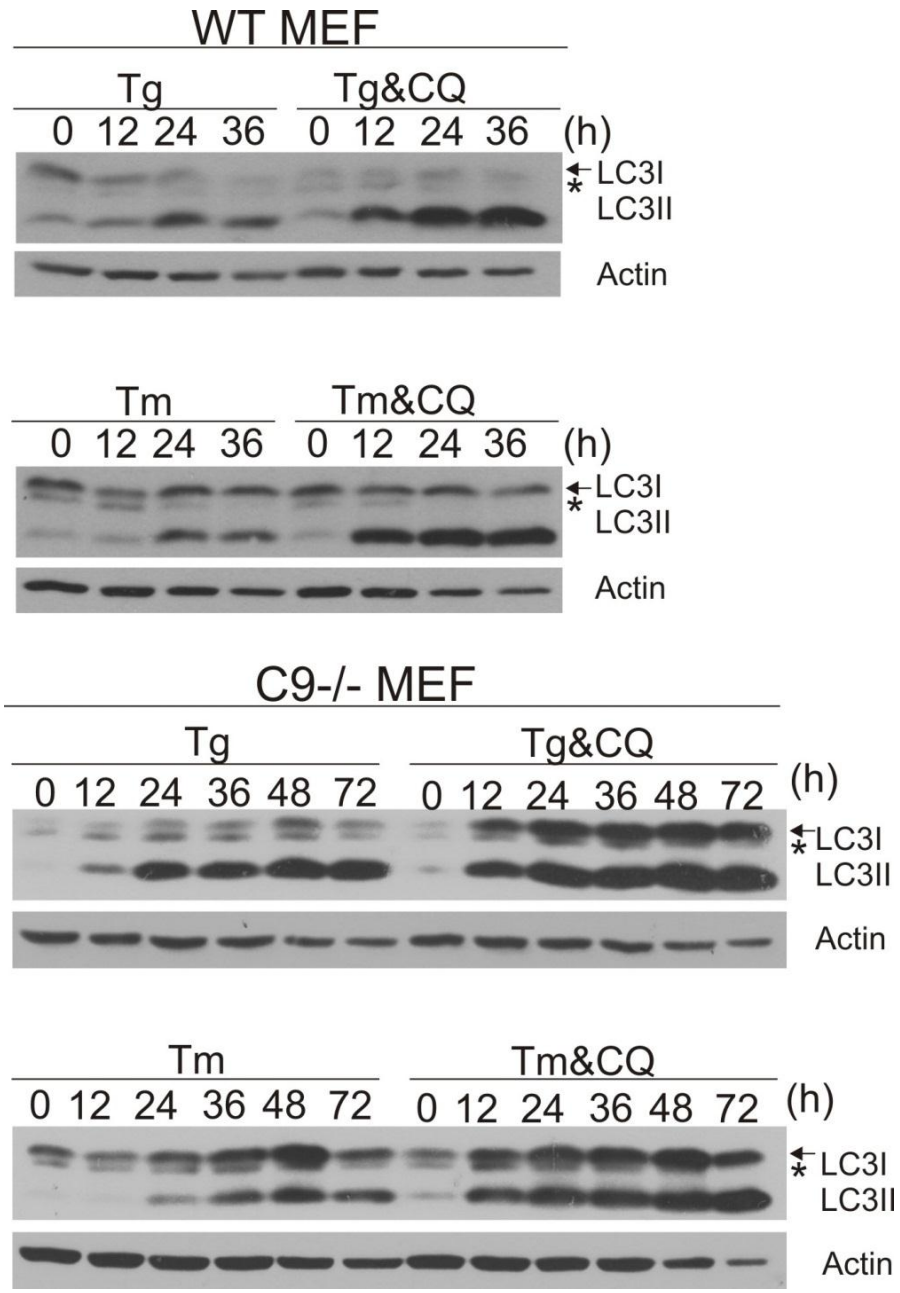

Figure 3.22: ER stress induces autophagy flux in WT and C9$^{-/-}$ MEFs. (A) WT and C9$^{-/-}$ MEFs were treated with 0.5 μM Tg or 0.5 μg/ml Tm, in the presence or absence of 60 μM of chloroquine (CQ) to monitor the autophagy flux at indicated time points. Following treatment, WT MEFs and C9$^{-/-}$ MEFs were harvested in 1X sample buffer. Whole cell lysates were subjected to SDS-PAGE followed by immunoblotting. Cell lysates were assessed using antibodies against actin and LC3. * is indicative of non-specific band.

To further provide evidence that autophagosome biogenesis was occurring, we transfected the MEFs with GFP-LC3 expression construct. During resting condition GFP-LC3 remains dispersed throughout the cell; however, in response to ER stress GFP-LC3 is recruited to the autophagosome. This results in the accumulation of GFP-LC3 to a distinct site (the autophagosomes) which was then observed by confocal microscopy (Fig 3.23A).

We also carried out transmission electron microscopy (TEM). We observed cytosolic dense double membrane vacuoles in WT and $C9^{-/-}$ MEFs in response to Tm treatment. The autophagosomes contained mitochondrial shaped structures as well as other unidentifiable substrates, most likely protein aggregates and damaged organelles (Fig 3.23B).

Our results confirm that autophagy is functional and is capable of engulfing large cytosolic substrates, confirming the role for autophagy in response to cellular stress.

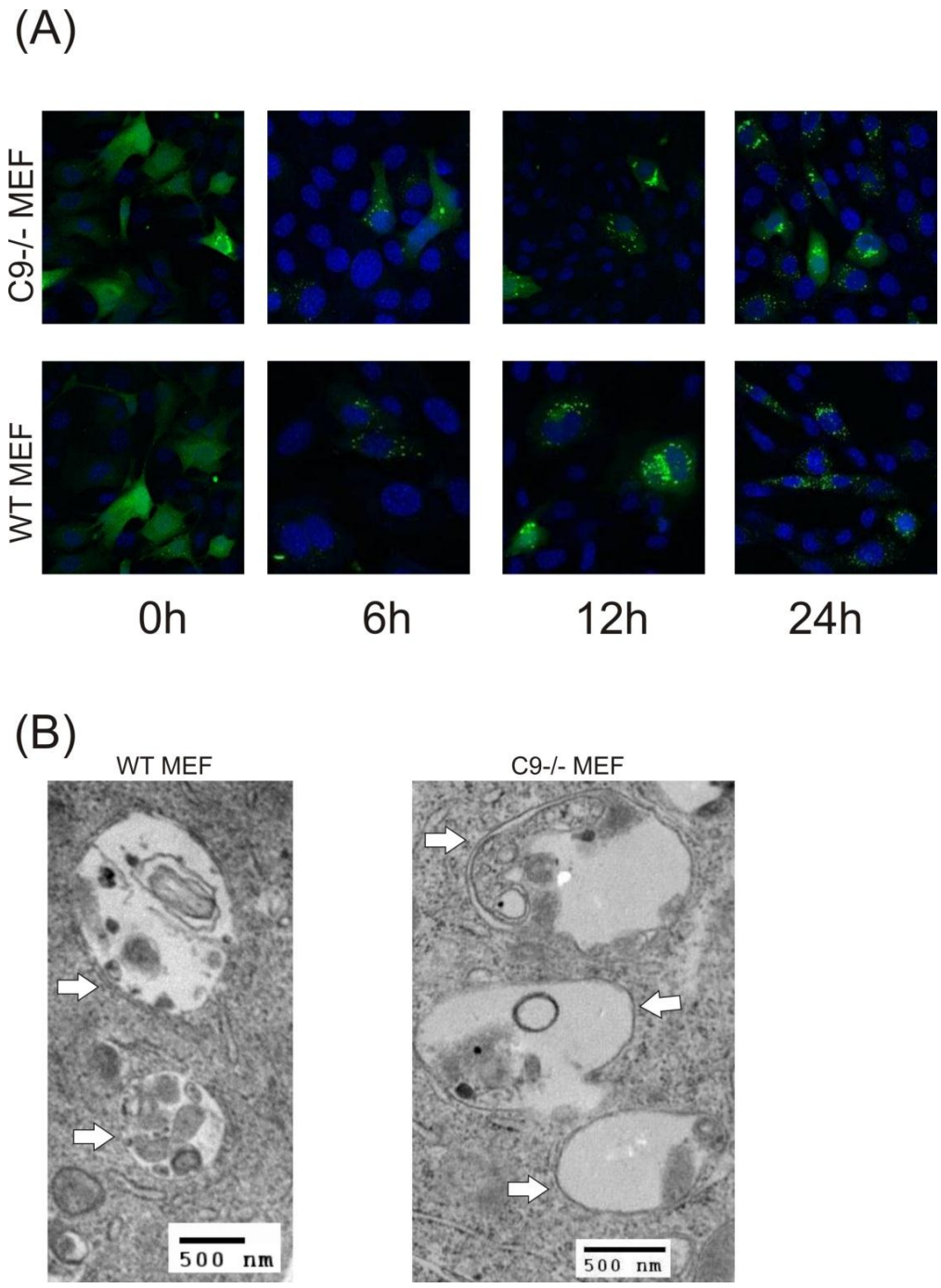

Figure 3.23: Monitoring autophagosome formation in WT and C9$^{-/-}$ MEFs in response to ER stress. (A) WT and C9$^{-/-}$ MEFs were transfected with GFP-LC3 plasmid. 24 h post-transfection, WT and C9$^{-/-}$ MEFs were treated with 0.5 μM Tg for the indicated time points. The punctation of GFP-LC3 was assessed by confocal microscopy. **(B)** WT and C9$^{-/-}$ MEFs were treated with 0.5 μM Tg for 24 h and subjected to electron microscopy after fixing. A representative morphology of autophagic vacuoles is shown.

To determine if autophagy contributes to cell death in $C9^{-/-}$ MEFs we generated lentivirus containing ATG5 shRNA and a corresponding pGIPZ ctrl lentivirus. Autophagy is well established in providing a protective role during cellular stress in conditions where mitochondrial-mediated apoptosis is functional; thus, we also inhibited the autophagy process in WT MEFs as a control to demonstrate that autophagy is functioning normally in these cells. WT and $C9^{-/-}$ MEFs were transduced with ATG5 shRNA lentivirus or pGIPZ empty lentivirus. To validate knockdown of ATG5 in the MEFs we carried out RT-PCR with primers specific for mouse ATG5 mRNA (Fig 3.24A). To determine the role of ATG5 in ER stress induced cell death we carried out PI staining on WT and $C9^{-/-}$ MEFs expressing ATG5 shRNA or pGIPZ control subjected to Tg treatment (Fig 3.24B). In WT MEFs ATG5 knockdown enhanced the rate of cell death, confirming autophagy as a protective response during ER stress under normal conditions; however, in $C9^{-/-}$ MEFs ATG5 knockdown enhanced cell survival.

We further validated this result using multiple ER stress-inducing agents. To monitor cell survival we fixed the cells with formalin and stained them with hematoxylin and eosin for visualization under bright field microscopy (Fig 3.24C). In response to all three ER stress-inducing agents, Bfa, Tg and Tm we observed that ATG5 knockdown increased cell death in WT MEFs and decreased the rate of cell death in $C9^{-/-}$ MEFs.

(A)

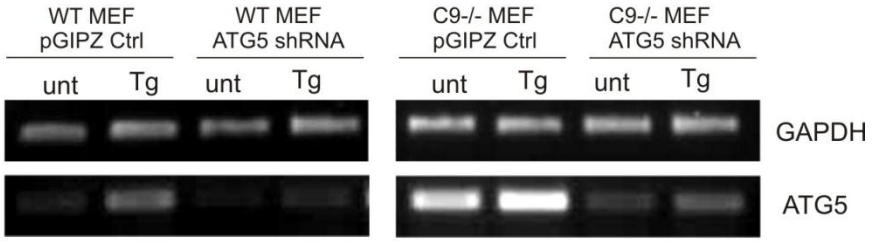
WT MEF pGIPZ Ctrl
WT MEF ATG5 shRNA
C9-/- MEF pGIPZ Ctrl
C9-/- MEF ATG5 shRNA
unt
Tg
unt
Tg
unt
Tg
unt
Tg
GAPDH
ATG5

(B)

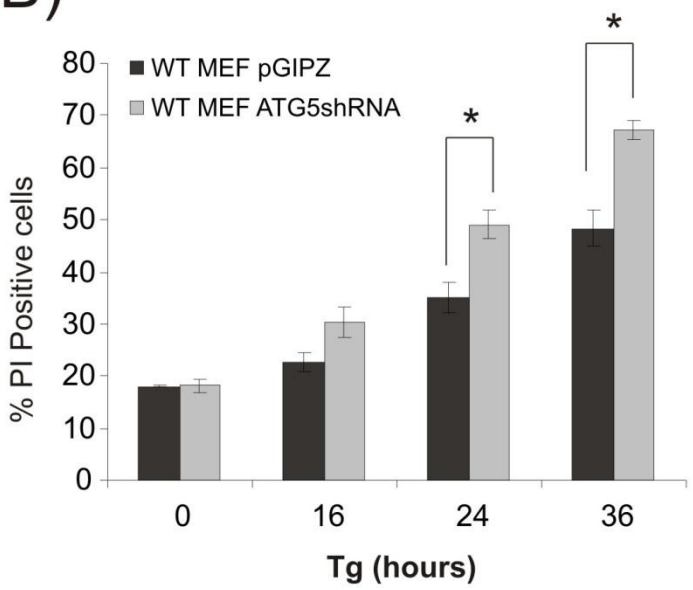
WT MEF pGIPZ
WT MEF ATG5shRNA
% PI Positive cells
80
70
60
50
40
30
20
10
0
*
*
0
16
24
36
Tg (hours)

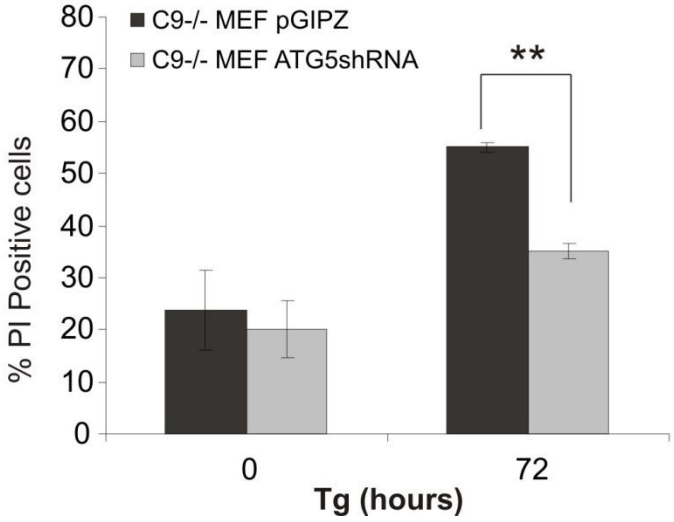
C9-/- MEF pGIPZ
C9-/- MEF ATG5shRNA
% PI Positive cells
80
70
60
50
40
30
20
10
0
**
0
72
Tg (hours)

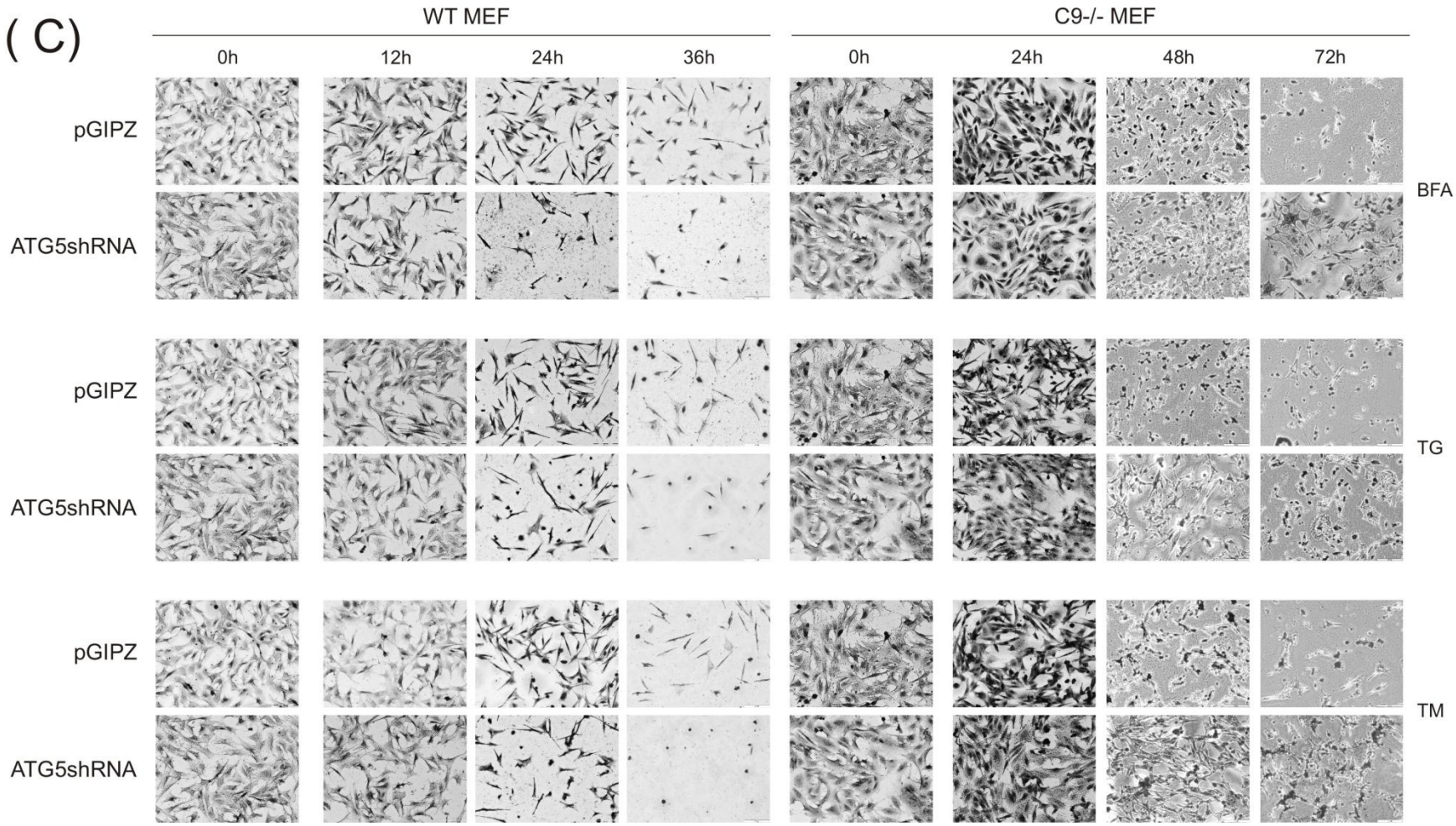
(C)
WT MEF
C9-/- MEF
0h
12h
24h
36h
0h
24h
48h
72h
pGIPZ
ATG5shRNA
BFA
pGIPZ
ATG5shRNA
TG
pGIPZ
ATG5shRNA
TM

Figure 3.24: Opposite effect of Atg5 Knockdown on ER stress-induced cell death in WT MEFs vs C9$^{-/-}$ MEFs. WT and C9$^{-/-}$ MEFs were transduced with an ATG5 shRNA containing lentivirus or the corresponding pGIPZ empty vector containing lentivirus as a control. **(A)** WT and C9$^{-/-}$ MEFs expressing Atg5 shRNAs or empty pGIPZ vector were treated with 0.5 μM Tg for 12 h. RT-PCR analysis was carried out to validate ATG5 knockdown. Total RNA was reverse transcribed and PCR of the cDNA was carried out to detect Atg5 and GAPDH. **(B)** WT and C9$^{-/-}$ MEFs expressing Atg5 shRNAs were treated with 0.5 μM Tg for indicated time points. The reduction in cell viability was determined with PI staining followed by FACS analysis. Graphs represent the mean ± SD of three independent experiments. Unpaired student *t* test was used to determine the P-value (pV<0.05*, pV<0.01**, pV<0.001***). **(C)** WT and C9$^{-/-}$ MEFs were treated with 0.5 μM Tg, 0.5 μg/ml Tm or 0.5 μg/ml of Bfa. The WT and C9$^{-/-}$ MEFs were fixed at the indicated time points in 10% formalin and stained with Hematoxylin and Eosin stain. Images of the cells were taken using bright phase microscopy

These results confirmed that ATG5 contributed to cell death in C9$^{-/-}$ MEFs; however, this could be an independent event to the formation of the caspase-8 activating complex. Therefore, to determine if compromised autophagy affected caspase-3 processing in C9$^{-/-}$ MEFs we treated C9$^{-/-}$ MEF pGIPZ and C9$^{-/-}$ MEF ATG5 shRNA with Tm or Bfa for the indicated time points and assessed whole cell lysates by Immunoblotting for the processing of caspase-3 and the conversion of LC3 I to LC3 II. Interestingly ATG5 knockdown resulted in no caspase-3 processing in response to Bfa and Tm, and LC3 blots confirmed autophagy knockdown (Fig 3.25).

These results suggest that ATG5 is essential for the activation of caspase-8 and the subsequent processing of caspase-3.

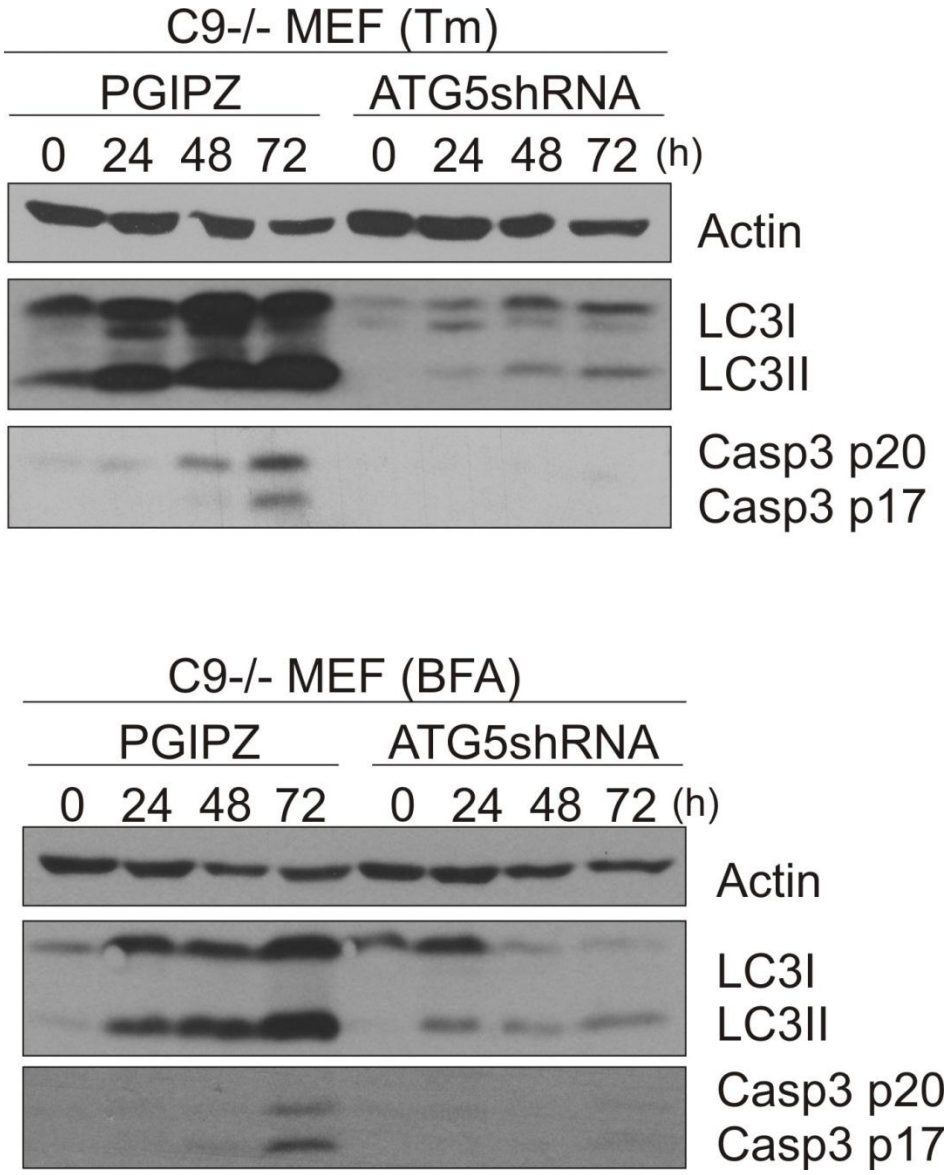

Figure 3.25: ATG5 is essential for caspase-3 processing in C9$^{-/-}$ MEFs. C9$^{-/-}$ MEFs pGIPZ and C9$^{-/-}$ MEFs ATG5shRNA were treated with 0.5 μg/ml of Tm or 0.5 μg/ml of Bfa for the indicated time points. Following treatment, cells were harvested in 1X sample buffer. Whole cell lysates were subjected to SDS-PAGE followed by Immunoblotting. Cell lysates were assessed using antibodies against actin, caspase-3 and LC3.

3.2.12 Immunoprecipitation of ATG5 in C9$^{-/-}$ MEFs co-precipitates with caspase-8, RIP1 and FADD

To demonstrate that an actual complex exists in our system consisting of RIP1, caspase-8 and ATG5, and that these are not just individual events that converge on caspase-3 processing, we had to IP one of the proteins involved and show that the other potential interacting partners co-IP.

C9$^{-/-}$ MEFs were treated with Bfa in combination with Boc-D-Fmk. Boc-D-Fmk is required to stabilize the complex by preventing caspase-8 processing. Once caspase-8 is processed the complex will most likely dissociate. We immunoprecipitated ATG5 at 0, 24 and 48 hours and probed for the RIP1, ATG5, caspase-8 and FADD. We used IgG conjugated to beads as a control to ensure that there was no non-specific binding to the beads (Fig 3.26). Our results show that RIP1, FADD and caspase-8 co-precipitated with ATG5. Moreover these results suggest that this complex associates over time as there is an accumulation of these proteins interacting with one another over the time course.

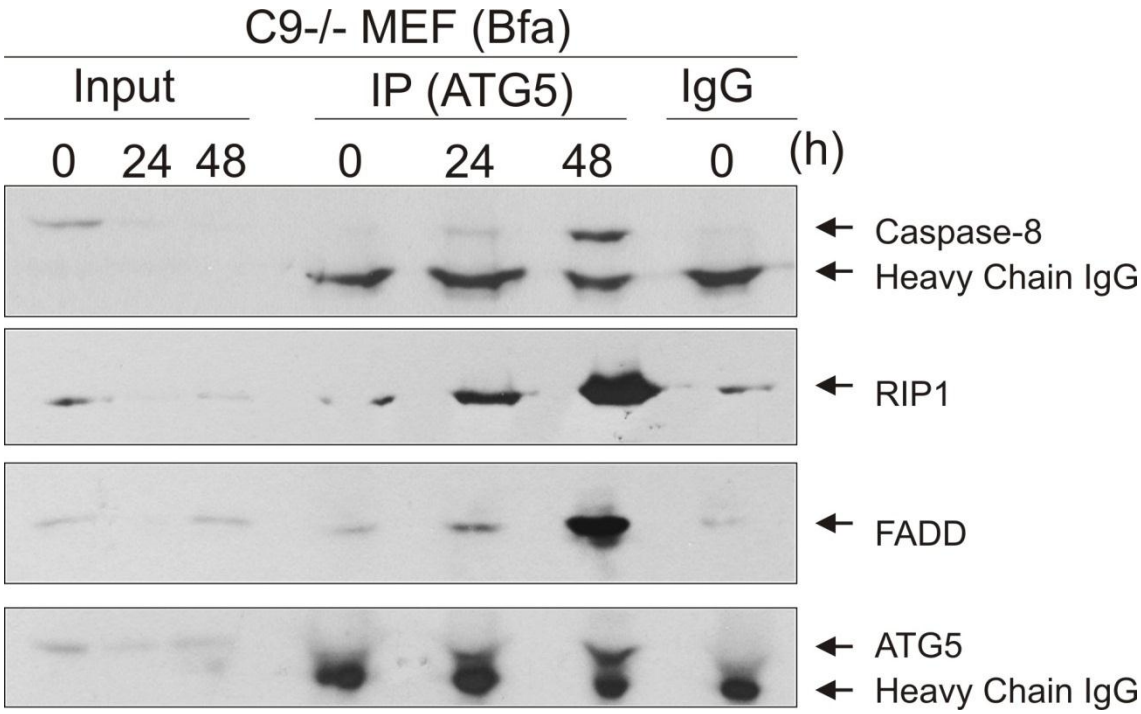

Figure 3.26: Immunoprecipitation of ATG5 results in the co-precipitation of FADD, RIP1 and Caspase-8. $C9^{-/-}$ MEFs were treated with 0.5 μg/ml of Bfa for the indicated time points. Following treatment, cells were lysed in NP40 IP buffer. Lysates were incubated with beads and antibody as described in materials and methods. Following incubation, beads were centrifuged and washed. The beads (IP) was lysed in 60μl of 2X sample buffer. The remainder of the cell extract was used as the input. 60μl of 2X sample buffer was added to 60μl of input. Lysates were subjected to SDS-PAGE and assessed by Immunoblotting for caspase-8, RIP1, FADD and ATG5.

3.3 Discussion

Cell death is an essential part of an organism's survival. The generation of new cells requires old cells to die for homeostasis to be met in the body. If old or damaged cells do not undergo cell death mutations can arise resulting in increased resistance to cell death stimuli and uncontrolled proliferation in the body resulting in the formation of carcinomas. In light of this it is important that the cell can execute death through multiple pathways. The most well used route of programmed cell death in organisms is apoptosis as this is a clean and highly efficient program in the removal of old or damaged cells without initiating an immune response.

Although apoptosis is the most widely used form of programmed cell death other forms of programmed cell death also exist such as autophagic cell death (ACD) and necroptosis. Unlike apoptosis, these pathways are not well characterized and often only activated in conditions where apoptosis is compromised. To better understand these alternative modes of cell death we used cells compromised in the mitochondrial-mediated intrinsic apoptotic pathway. The results in this chapter show that the mitochondrial mediated apoptotic pathway is the primary and most efficient mode of cell death in response to multiple stress inducing stimuli; however, in conditions where this pathway is compromised cells can use an alternative death pathway albeit at a slower, less efficient rate. The mode of cell death used when the mitochondria-mediated apoptotic (MMA) pathway is compromised shows features of all three forms of programmed cell death, apoptosis, autophagic cell death and necroptosis. Furthermore, individual inhibition of these pathways only delays cell death but does not completely inhibit the process insinuating that the cell will be pushed in the direction of cell death that it is most effectively able to execute. Only in conditions where we knockdown multiple pathways do we observe a considerable protection against cell death that would be worthy of using the term 'resistant to cell death'.

ER stress inducing agents were used as the primary stimuli in this study; however it was demonstrated that similar results were obtained using chemotherapeutic drugs such as etoposide and bortezomib. The models used in this study were primarily WT and $C9^{-/-}$ MEFs as caspase-9 is the essential apical caspase in the intrinsic apoptotic pathway.

Furthermore, our studies in $Bax^{-/-}/Bak^{-/-}$ double knockout MEFs and $Bax^{-/-}$ HCT116 human colon carcinoma cells confirmed that our observations were not caspase-9, cell type or species specific.

Exposure of WT and $C9^{-/-}$ MEFs to the ER stress inducing compounds tunicamycin (0.5mg/ml Tm) and thapsigargin (0.5Mm Tg) resulted in cell death, measured, by Propidium Iodide (PI) staining and FACs analysis. However, although cell death occurred in WT and $C9^{-/-}$ MEFs, WT MEFs underwent cell death as early as 12 h and almost 100% cell death was observed at 36-42 h. In contrast, $C9^{-/-}$ MEFs only began to show features of cell death at 36-48 h and considerable cell death was observed at 72 h. The results suggested that ER stress induces two phases of cell death, a rapid caspase-9 dependent cell death and acaspase-9 independent cell death, albeit at a slower rate. These results were also observed in response to the DNA damage inducing agent etoposide (Etop) and the proteasome inhibitor bortezomib (Brtz), suggesting that this is not an ER stress specific effect.

To elucidate the mode of cell death being executed by WT and $C9^{-/-}$ MEFs in response to the stress inducing agents Tm, Bfa, Tg, Etop and Brtz, cells were treated for 3-4 days and whole cell lysates were assessed by immunoblotting for processing of caspases. Our results demonstrated that WT MEFs underwent rapid caspase-9 processing, caspase-3 processing and PARP cleavage, indicating that these cells executed cell death through the canonical intrinsic apoptotic pathway in response to the different stress inducing agents. $C9^{-/-}$ MEFs surprising underwent caspase-3 processing and PARP cleavage at later time points where cell death is observed. As these cells were deficient in the apical caspase-9, the processing of caspase-3 was a result of another protease.

These results were validated in Bax and Bak double knockout MEFs ($BB^{-/-}$ MEFs) to confirm that this was not an effect only observed when the intrinsic pathway is inhibited post-MOMP but also pre-MOMP. WT and $BB^{-/-}$ MEFs demonstrated a similar caspase profile as WT and $C9^{-/-}$ MEFs, as demonstrated by immunoblot, in response to Tm treatment. Moreover, DEVDase activity assay confirmed that WT and $BB^{-/-}$ MEFs displayed caspase activity in response to ER stress; however, $BB^{-/-}$ MEF caspase activation was delayed compared to its WT counterpart. Furthermore, to demonstrate

that this effect also translated to a human cell line we used WT and $Bax^{-/-}$ HCT116 colon cancer cells. Exposure of WT and $Bax^{-/-}$ HCT116 to Bfa, Eto and Brtz, again correlated with previous data obtained in WT and $C9^{-/-}$ MEFs. WT HCT116 cells underwent rapid processing of caspase-9 and caspase-3 as well as PARP cleavage, indicative of mitochondrial-mediated apoptosis; however, $Bax^{-/-}$ HCT116 cells also showed processing of caspase-3 and PARP cleavage, although at a later time point. Minimal levels of caspase-9 cleavage were evident in the $Bax^{-/-}$ HCT116 cells. The caspase-9 processing observed was not as extensive as in the WT cells and is most likely a downstream event in the apoptotic cascade due to activation of the executioner caspases.

Together, our data confirmed that the late caspase-3 processing and PARP cleavage observed in cells compromised in intrinsic apoptosis, was not MOMP dependent, nor was it stimulus, cell type or species specific.

We confirmed that the processing of caspase-3 in the $C9^{-/-}$ MEFs was a result of an initiator caspase, and not due to the activation of other proteases such as calpains. $C9^{-/-}$ MEFs treated with the broad spectrum caspase inhibitor, Boc-D-Fmk, resulted in attenuation of caspase-3 processing and PARP cleavage in response to the ER stress inducing agent Tg, suggesting that this processing of caspase-3 is mediated by an apical caspase.

Our results suggested that in response to death inducing stimuli in conditions where the intrinsic apoptotic pathway is compromised, another apical caspase is activated to compensate for caspase-9 deficiency. Although there are a number of apical caspases, caspase-8 is the only one that has been well established to lead to the processing of caspase-3 independent of the intrinsic apoptotic pathway. To determine if caspase-8 was involved in this MOMP independent caspase-3 processing, $C9^{-/-}$ MEFs were transduced with caspase-8 (C-8) shRNA containing lentivirus. Knockdown of caspase-8 completely blocked caspase-3 processing in the $C9^{-/-}$ MEFs and reduced the amount of ER stress induced cell death. Knockdown of caspase-8 in WT MEFs had no obvious effect on caspase-9 and caspase-3 processing, confirming that caspase-9 is the dominant apical

caspase activated in response to ER stress in conditions where the apoptotic machinery is intact.

Our results confirmed that caspase-3 processing in $C9^{-/-}$ MEFs is a result of caspase-8 activation; however, for apical caspases to be activated the formation of a death inducing signaling platform is required[211]. Studies show, many types of caspase-8 activating platforms exist, i.e. Fas ligand (Fas L) and TRAIL ligand, mediate the activation of their respective receptors, resulting in the formation of the death inducing signaling complex (DISC) at the plasma membrane[212-214], TNFα induced activation of the TNF receptor 1(TNFR1) in the absence of IAPs results in complex II formation[215], genotoxic stress or IAP depletion results in the spontaneous assembly of the ripoptosome[136,181] and treatment of cells with sphingosone kinase inhibitor (SKI-I) leads to the formation of the intracellular DISC (iDISC)[130], an intracellular death inducing signaling complex that has been proposed to signal from the autophagosomal membrane.

The ripoptosome is a relatively new complex which was identified through the collaboration of Pascal Meiers group[136] and Martin Leverkus group[181]. As described in the introduction, the current studies have shown that the ripoptosome forms spontaneously in response to IAP depletion or upon genotoxic stress as demonstrated by etoposide treatment. The complex is a massive 2 MDa structure, and consists of the core components, RIP1, FADD and caspase-8. This complex is negatively regulated by the IAP family cIAP1, cIAP2 and XIAP, most likely through the ubiquitination and subsequent degradation of important components of the complex. Furthermore the caspase inhibitor cFLIP isoforms are involved in the regulation of the ripoptosome, with $cFLIP_L$ preventing ripoptosome assembly, whereas $cFLIP_s$ promotes ripoptosome assembly and favors necroptosis signaling (see introduction).

Knockdown of RIP1 in $C9^{-/-}$ MEFs completely abrogated caspase-3 process providing evidence that RIP1 is required for the activation of caspase-8. Furthermore inhibition of RIP1 kinase activity using necrostatin-1 rescued $C9^{-/-}$ MEFs PLKO from cell death; however, only a negligible decrease in caspase-3 processing was observed. Furthermore the combination of caspase-8 knockdown and RIP1 kinase inhibition in $C9^{-/-}$ MEFs

resulted in a substantial inhibition from cell death in response to ER stress inducing agents. Moreover, clonogenic survival assays confirmed that the surviving cells subsequent to treatment were able to proliferate. The results obtained from these experiments resembled the dynamics of both complex II and the ripoptosome. Our data shows that RIP1 is required for the formation of the caspase-8 activating complex; however, RIP1 kinase activity is not essential but does enhance its formation. RIP1 kinase activity may be required to bring multiple complexes together forming a hierarchy structure which is more active due to the close proximity of caspase-8 and RIP proteins. Furthermore, these results indicate that the cell may be undergoing either apoptosis or necroptosis depending on the cellular context. If caspase-8 is knocked down, RIP1 can still form the Necrosome and signal cell death through necroptosis. On the other hand, inhibition of RIP1 kinase activity can still result in ripoptosome formation, although less efficient, and induce apoptotic cell death. Moreover, RIP1 and RIP1 kinase activity has been shown in multiple studies to be dispensable for necroptosis in response to TNFα stimulation; however, RIP3 is essential[204,205].

Although we observe caspase activation in $C9^{-/-}$ MEFs, it is difficult to differentiate whether the cells are primarily undergoing apoptosis in response to treatment, or if some cells are undergoing apoptosis and some are undergoing necroptosis, depending of their cellular context. As mentioned in the introduction, if the cell contains high levels of FLIP proteins, the ripoptosome will primarily signal through necroptosis however if FLIP levels are low the ripoptosome will recruit caspase-8 and signal through apoptosis. Because there is no direct read out of necroptosis it is not possible to say if necroptosis is occurring; however we have carried out a couple of strategies to try and address this question.

Annexin V/PI staining showed that $C9^{-/-}$ MEFs treated with ER stress inducing drugs, Tm and Bfa, migrated into the Annexin V positive channel (early apoptosis) and subsequently into the Annexin V/PI positive channel (late apoptosis, secondary necrosis). The results indicate that at the onset of cell death in the $C9^{-/-}$ MEF, cells are showing markers of apoptosis, as the treatment progresses the cells migrate into the Annexin V/PI positive channel suggesting that the cells are in late stages of apoptosis;

however, cells undergoing necrosis also migrate to the Annexin V/PI positive channel and subsequently into the PI only channel. Hydrogen peroxide treatment was used as a positive control for necrosis in the $C9^{-/-}$ MEFs. The dot plots of the $C9^{-/-}$ MEFs are similar to that of WT MEFs, although with delayed kinetics of cell death, suggesting that the cells seem to be, at least in part, primarily undergoing apoptosis. However, because the Annexin V/PI positive channel can be indicative of late apoptosis and early necrosis it is still possible that within the same culture some cells are undergoing apoptosis and other may be dying through necroptosis.

To try and resolve this issue RIP3 was knocked down in $C9^{-/-}$ MEFs. RIP3 is required for the formation of the Necrosome and is essential in the execution of necroptosis[204,205,216]. This strategy will not affect RIP1s involvement in the formation of the ripoptosome and thus only inhibits ripoptosome-mediated necroptosis signaling but not ripoptosome-mediated apoptosis signaling. The data revealed that knockdown of RIP3 did not have a significant effect on ER stress induced cell death in $C9^{-/-}$ MEFs; however, it did seem to enhance the levels of caspase-3 processing suggesting that knockdown of RIP3 pushes the cells into apoptosis. This data suggests that there may indeed be some cells undergoing apoptosis and some cells undergoing necroptosis within the same culture; however, in conditions where RIP3 is not available to assemble the Necrosome, increased free RIP1protein is available to form the ripoptosome, providing more surfaces for caspase-8 to signal from. This dynamic effect of the ripoptosome allows for the cell to compensate cell death in condition where one pathway may be compromised.

Although the system under investigation correlates with the dynamics of the ripoptosome, Complex II also displays similar kinetics. What differentiates these two complexes is that the ripoptosome forms independently of TNF stimulation, whereas TNF stimulation and formation of complex I is a pre-requisite for complex II formation[136,181]. Reports have shown that in response to ER stress, NFκB activation can result in TNFα secretion and subsequent autocrine signaling to induce TNF mediated complex II formation[217]. ELISA assays confirmed that WT and $C9^{-/-}$ MEFs do not secrete TNF in response to ER stress, DNA damage or proteasome inhibition. To add

further complexity, studies of TNF receptor-associated periodic syndrome (TRAPS), have shown that due to a mutation in the TNFR1 gene, TNFR1 proteins are unable to translocate from the ER to the golgi and subsequently to the surface of the cell membrane. Consequently, TNFR1 can accumulate in the ER, oligomerize through disulphide bonds and signal from the ER membrane independent of TNFα. Because ER stress can disrupt ER trafficking to the golgi it has been speculated that a similar event could occur. To ensure that similar events as described in TRAPS models did not occur, TNF receptor 1was stably knocked down in $C9^{-/-}$ MEFs using lentivirus. TNFR1 knockdown in $C9^{-/-}$ MEFs had no effect on ER stress induced caspase-3 processing or on cell death as monitored by immunoblotting and PI staining respectively. These results suggest that caspase-8 activation in our system is independent of TNFR1 signaling.

To further identify other crucial partners, such as adaptor proteins, involved in the assembly of the caspase-8 activating platform, both FADD and TRADD were knocked down in $C9^{-/-}$ MEFs using lentivirus containing FADD or TRADD shRNA.

Knockdown of FADD showed no effect on caspase-3 processing. This was a surprising result as FADD is required in all well-established caspase-8 activating platforms. However, following a TNF stimulation functional test, it was confirmed that the knockdown of FADD was not sufficient to provide a functional effect. Further rounds of lentiviral transduction did not improve the knockdown thus the rate limiting effect was the efficiency of the shRNA not the lentivirus. Two studies examining the stoichiometry of the DISC were released this year by the MacFarlane group[218] and the Lavrik group[219] demonstrating that small amount of FADD is capable of activating substantial amounts caspase-8. They proposed that unlike the hypothetical model of a FADD and caspase-8 interaction at a 1:1 ratio, that in fact 1 FADD molecule can recruit chains of caspase-8 molecules through a stacking effect via the DED of the caspase-8 molecules. This could explain why no effect was observed with what seems to be quite an adequate knockdown in our system.

TRADD is another adaptor protein most well known to be required for the formation of complex II, however; it has been described to play a role in the formation of the

ripoptosome in certain conditions, although no published data confirms this stipulation. Knockdown of TRADD in $C9^{-/-}$ MEFs caused a negligible reduction in caspase-3 processing and PARP cleavage. Furthermore TRADD knockdown led to a considerable amount of protection in response to ER stress induced cell death. It is unclear what TRADDs role is in the complex. Caspase-3 reduction did not seem to correlate with the highly efficient knockdown of TRADD, indicating that it may also contribute towards necroptosis. Our results clearly demonstrate that TRADD contributes to cell death and caspase-3 processing but it is not clear what role TRADD plays in the formation of the caspase-8 activating complex or how it enhances its activity. It would be plausible that there may be more than just one type of caspase-8 activating platform, there may be multiple platforms which consist of similar core components; however, they may recruit different interacting partners required for their activity. Alternatively TRADD may result in a higher order assembly of these caspase-8 activating complexes, enhancing their activity, be it though caspase-8 mediated apoptosis or RIP1-RIP3 mediated necroptosis.

Finally we tested the hypothesis that the autophagosome may be acting as a signaling platform for the formation of a death inducing signaling complex. As described in the introduction links between autophagy and apoptosis have been proposed over the last decade. Publications throughout the years have suggested that autophagy can mediate cell death through apoptosis. In 2005, the Jung group identified a direct interaction between FADD and ATG5[184]. Treatment of HeLa cells with IFNγ resulted in a caspase dependent cell death which was dependent on an interaction between FADD and ATG5. This data was the first to suggest that the autophagosome could act as a signaling platform for caspase-8 activation. The following years resulted in only a few publications which strengthened this hypothesis[190,210]. It was only in 2012 that the Wang group coined this complex the iDISC[130], a structure capable of activating caspase-8 from the autophagosomal membrane and inducing apoptotic cell death.

ER stress and in fact most cellular stresses are potent inducers of autophagy, demonstrated by the conversion of LC3I to LC3II. To determine the role of autophagy in our system we took a genetic approach to knockdown the autophagic pathway.

Knockdown of the autophagy gene ATG5 inhibited the conversion of LC3 I to LC3 II, a key marker of autophagy. Furthermore this also abrogated caspase-3 processing and reduced cell death, as determined by PI staining and FACs analysis, in response to ER stress induced cell death. Knockdown of ATG5 in WT MEFs provided the opposite effect as seen in $C9^{-/-}$ MEFs. ATG5 knockdown in WT MEFs enhanced cell death as determined by PI staining and FACs analysis. These results provide evidence to suggest that the autophagosome may act as a platform for the formation of a ripoptosome-like death inducing signaling complex. Alternatively ATG5 in itself could be playing an independent role to autophagy and be an essential partner in the formation of the caspase-8 activating platform.

To provide evidence that there is indeed a complex formed in our system that comprises of RIP1, caspase-8 and ATG5, an immunoprecipitation was performed. ATG5 was precipitated from C9-/- MEF cell extract in non-stressed conditions and in response to Bfa treatment for 24 and 48 h. The addition of the caspase inhibitor Boc-D-Fmk was required along with the treatment to stabilize the complex once assembled. Once caspase-8 is activated and processed it is likely the signaling complex will disassemble. Our result confirmed the co-precipitation of RIP1, FADD and caspase-8 with ATG5. The formation of this complex was enhanced throughout the treatment, showing increased binding of the interacting proteins over time.

Together our results provide evidence of a novel complex which contains components of the apoptotic, necroptotic and autophagic machineries (Fig. 3.27). In conditions where the intrinsic apoptotic pathway is compromised cell death is executed through a ripoptosome-like death complex which requires ATG5 for its assembly. This is the first time a complex consisting of these components has been shown to induce cell death in response to ER stress. We show that this complex can signal cell death through apoptosis or necroptosis depending on its cellular context. Furthermore the formation of this complex requires the autophagy protein ATG5. Several studies investigating autophagic cell death show different read outs of death. Some studies show that autophagy results in a necrotic-like cell death, while others show that autophagy mediates apoptotic like cell death. This complex may be able to explain these

variations. Depending on the cellular context or the stress stimulus this complex can execute cell death through apoptosis or necroptosis.

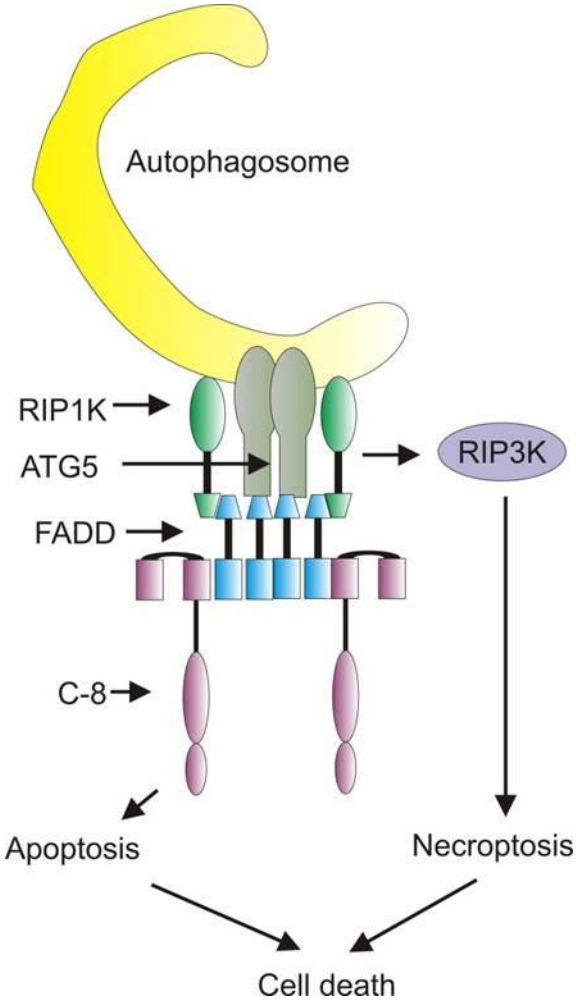

Figure 3.27: Here we present a hypothetical model of a complex which we predict assembles in response to cellular stress. In conditions where the intrinsic apoptotic pathway is compromised cell death is executed through a ripoptosome-like death complex which requires the autophagosomal membrane for its assembly. We predict that in response to cellular stress, the upregulation of autophagy provides a platform for the assembly of a caspase-8 activating complex. ATG5 interacts with the adaptor protein FADD which subsequently recruits caspase-8 and RIP1 kinase to the complex. Similar to the dynamics of the ripoptosome, depending on the cellular content, this complex can induce caspase-8 mediated apoptosis or RIP1 mediated necroptosis.

Chapter 4: Transcriptional Regulation of the Autophagy Receptors by the UPR

4.1 Introduction and Objectives

In the previous chapter we have demonstrated a pro-death role for autophagy; however, as discussed this is often only seen in conditions where the mitochondrial-mediated apoptotic pathway is compromised. Autophagy, in general, is considered to aid in the relief of cellular stress by degrading unfolded proteins, large protein aggregates and damaged organelles such as ER and mitochondria[87,220]. ER stress can lead to all of the above mentioned conditions. With this in mind it would seem reasonable that ER stress-induced autophagy would aid in the removal of these substrates and contribute to reinstating homeostasis. Although it is well established that autophagy is induced in response to ER stress[116,221] there is a lack of data on the function of autophagy in response to ER stress, or how autophagy is regulated by ER stress and the UPR.

There are many indirect and some direct connections that can link ER stress and autophagy, yet there are many questions that need to be addressed[38]. With over 34 proteins required for the autophagy pathway to function correctly it would seem likely that for autophagy to be upregulated in response to cellular stress a massive transcriptional cascade would need to be executed.

The objective of this study was to investigate the connection between the UPR and how it regulates the autophagy machinery. To do this, we carried out a microarray analysis in HCT116 cells treated with the ER stress inducing agents, brefeldin A and tunicamycin. The screen identified the transcriptional upregulation of a number of autophagy-related genes involved in many aspects of the autophagy pathway. Of these genes we identified the upregulation of the recently characterized autophagy receptors, NIX/BNIP3L, p62 and NBR1, which specifically target damaged organelles and ubiquitinated proteins and aggregates to the autophagosome[47]. Although these autophagy receptors have been well characterized both structurally and functionally, not much is known about their regulation. Furthermore, whether ER stress induced autophagy is a selective process or a non-selective process remains a question of debate. In light of this we wanted to first confirm the regulation of the autophagy receptors by the UPR and determine which UPR arm is involved in there regulation.

4.2 Results

4.2.1 Activation of the UPR in HCT116 cells results in the upregulation of autophagy

To confirm that both the UPR and the autophagy pathway were functional in HCT116 cells, we treated the cells with the ER stress inducing agent brefeldin A (Bfa, 0.5 μg/ml) or with 0.5 μg/ml Bfa in combination with the lysosomotropic agent chloroquine (60 μM CQ) over an extensive time course of 0, 6, 12, 24, 32, 36 hours. Cells were harvested in 1X sample buffer and whole cell lysates were assessed by Immunoblotting for markers of the UPR (Chop, spliced XBP1, total and phosphorylated eIF2α) and autophagy (the conversion of LC3I to LC3II).

The results show that in response to Bfa treatment, HCT116 cells induce a typical UPR response, with target genes of all three UPR sensors being induced, including Chop, spliced XBP1, total and phosphorylated eIF2α (Fig 4.1A).

To confirm that autophagy is induced in HCT116 cells in response to ER stress, and that it is in a constant state of flux, i.e., a constant state of autophagosome biogenesis and autophagosome degradation, we treated cells with Bfa or Bfa in combination with CQ. Chloroquine inhibits the degradation of the autophagosome at the lysosomal compartment, thus if autophagy is in a constant flux of biogenesis and degradation, blocking the degradation step should result in the accumulation of autophagosomes in the cytosol. Our read out for autophagosome biogenesis is the immunoblot detection of LC3I to LC3II conversion. Cells were harvested at the indicated time points, lysed and whole cell lysates were assessed by immunoblotting for the conversion of LC3I to LC3II. Our results show that autophagy is induced in response to Bfa treatment; however, the addition of CQ to Bfa dramatically increases the levels of LC3I and LC3II, confirming that autophagosomes are in a constant flux of biogenesis and degradation (Fig 4.1B).

Together the results here confirm that in response to ER stress inducing agents, HCT116 cells activate the UPR and enhances autophagy flux in the cell.

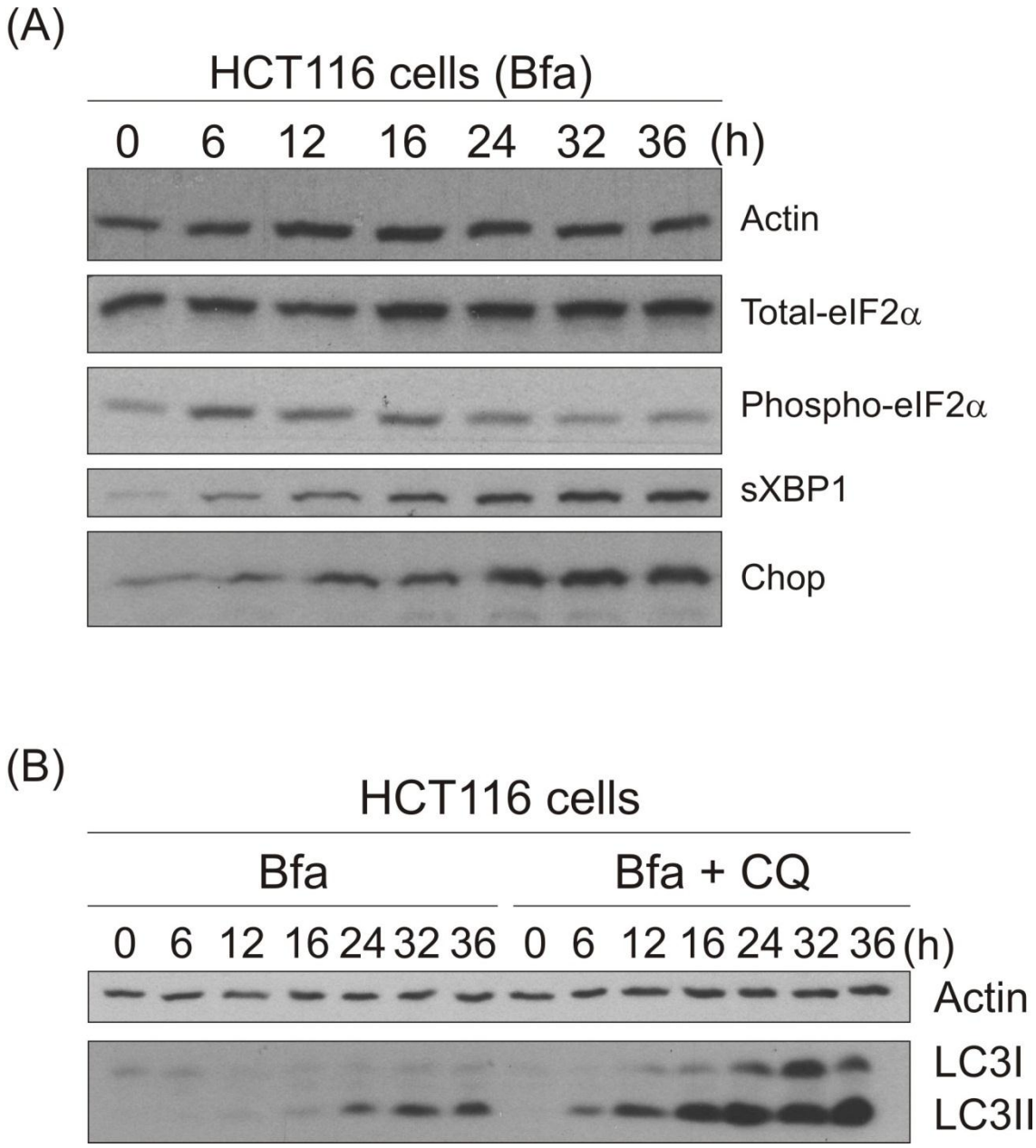

Figure 4.1: HCT116 cells exhibit a functional UPR and enhanced autophagy flux in response to ER stress. (A) HCT116 cells were treated with 0.5 μg/ml of Bfa for the indicated time points. Cells were harvested in 1X sample buffer following treatment. Whole cell lysates were subjected to SDS-PAGE followed by immunoblotting. Total protein was assessed using antibodies against Chop, spliced XBP1, total-eIF2α, phospho-eIF2α. **(B)** HCT116 cells were treated with 0.5 μg/ml of Bfa, in the presence or absence of 60 μM of chloroquine (CQ) to monitor autophagy flux at the indicated time points. Following treatment, cells were harvested in 1X sample buffer. Whole cell lysates were subjected to SDS-PAGE followed by Immunoblotting. Cell lysates were assessed using antibodies against actin and LC3.

4.2.2 ER stress induces autophagy-mediated degradation of mitochondria and ubiquitinated proteins

ER stress induced autophagy is generally thought of as a protective response, required for the degradation of unfolded proteins, protein aggregates and damaged organelles such as the ER and the mitochondria. Although autophagy has been shown to be capable of all these functions, very little evidence exists to support that autophagy is actually required for these processes in response to ER stress. Here we used wild-type mouse embryonic fibroblasts (WT MEFs) co-transfected with GFP-LC3 and Mito-RFP to monitor mitochondria and autophagosome co-localization as a marker of mitophagy in response to ER stress. Furthermore, we carried out transmission electron microscopy (TEM) on WT MEFs treated with Tm to observe mitochondria containing autophagosomes. To monitor the effect of autophagy on the degradation of ubiquitinated proteins we used HCT116 cells treated with 0.5 μg/ml of Bfa or with 0.5 μg/ml of Bfa in combination with 60 μM CQ. If autophagy is required for the degradation of ubiquitinated proteins, the inhibition of autophagosome degradation should result in the accumulation of ubiquitinated substrates.

To monitor autophagy-mediated mitochondrial degradation "Mitophagy" in response to ER stress, WT MEFs were co-transfected with a GFP-LC3 expression construct as a marker for autophagosomes and a Mito-RFP expression construct as a marker for mitochondria. 24 h post transfection, the cells were treated with 0.5 μM thapsigargin (Tg) for the indicated time points. Following treatment, cells were fixed in a 10% formalin solution and images were taken with a confocal microscope at a 40x magnification (Fig 4.2A).

Here we show that during resting conditions GFP-LC3 is dispersed in the cell and resides mainly in the nucleus[222]. Upon ER stress stimulation GFP-LC3 gets processed to GFP-LC3 II which binds to the autophagosomes resulting in punctate formation. Mito-RFP is a fusion protein which binds specifically to the mitochondria irrespective of membrane potential. In response to ER stress inducing agent Tg, GFP-LC3 translocates to the cytosol and is incorporated into the autophagosome, forming bright green punctates. Some co-localization of the mitochondria and the autophagosomes is

observed in response Tg treatment (Fig 4.2A). However this was by no means extensive, nor was there a time dependent increase in the amount of co-localization of the mitochondria and the autophagosomes. Although the amount of co-localization was minimal, it still may be enough to delay cell death. Furthermore electron microscopy images of WT MEFs treated with Tm confirmed that mitochondrial degradation occurs in response to ER stress, observing mitochondrial structures in double membrane vacuoles (Fig 4.2B).

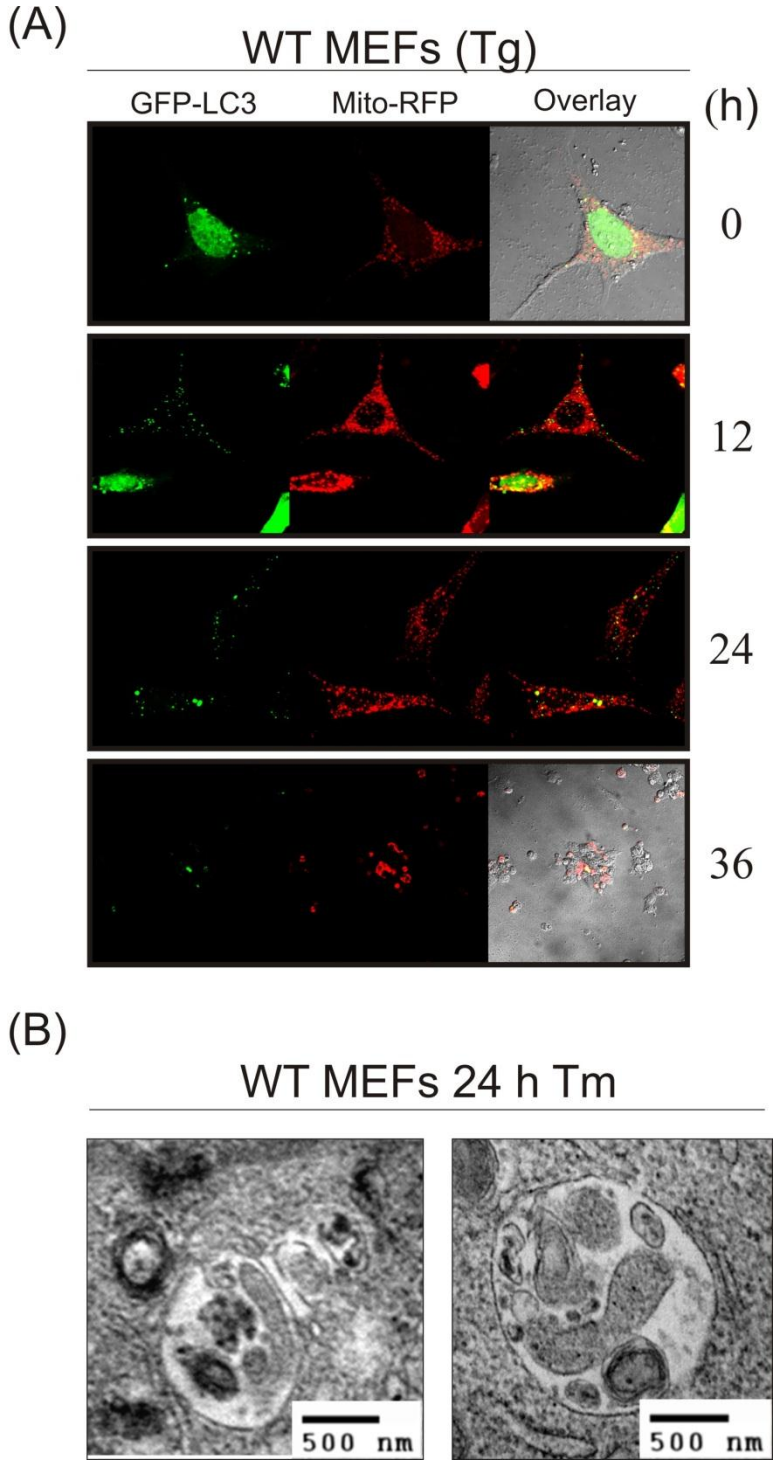

Figure 4.2: Monitoring mitochondrial degradation in response to ER stress. (A)WT MEFs were co-transfected with GFP-LC3and Mito-RFP plasmid. 24 h post-transfection, WT MEFs were treated with 0.5 μM Tg for the indicated time points. Following treatment cells were fixed in a 10% formalin solution and the co-localization of GFP-LC3 and Mito-RFP was assessed by confocal microscopy. **(B)** WT MEFs were treated with 0.5 μM Tg for 24 h and subjected to electron microscopy after fixing. Images show morphology of autophagic vacuoles.

To determine if autophagy was involved in the removal of ubiquitinated proteins from the cell in response to ER stress we treated WT HCT116 cells with either Bfa or Bfa in combination with CQ. As discussed earlier CQ blocks autophagosome degradation in turn preventing the degradation of its contents. Following treatment, cells were lysed in 1X sample buffer. Whole cell lysates were assessed by Immunoblotting for ubiquitinated proteins (Fig 4.3).

Our results demonstrated that in response to ER stress, ubiquitinated protein levels do not increase over time; however, blocking autophagosome degradation by means of CQ treatment resulted in the accumulation of ubiquitinated proteins throughout treatment indicating that autophagy mediates the degradation of ubiquitinated proteins in response to ER stress. The ubiquitinated proteins appeared quite high on the membrane, indicating that these substrates are large protein aggregates. Smaller soluble ubiquitinated proteins did not appear and are most likely removed via the proteasome.

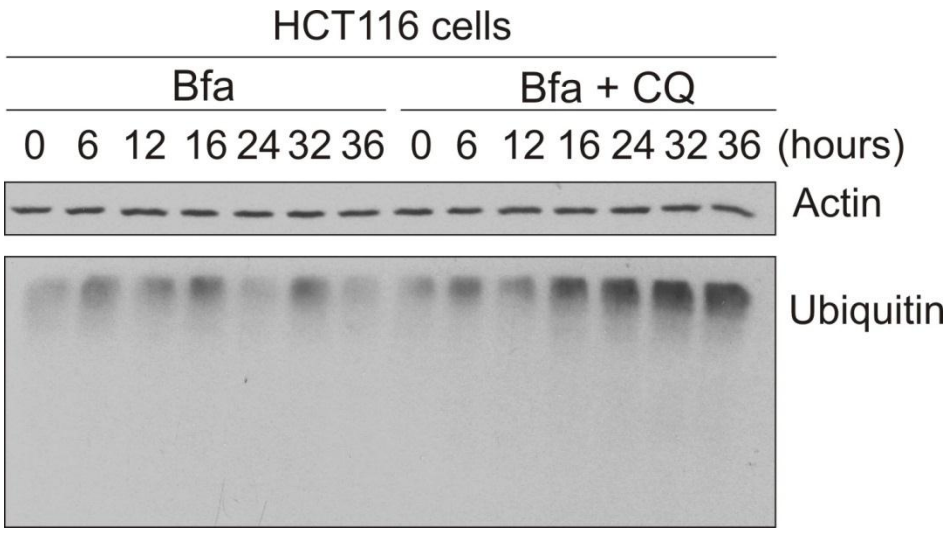

Figure 4.3: Inhibition of autophagosome degradation results in the accumulation of ubiquitinated proteins in response to ER stress. HCT116 cells were treated with 0.5 μg/ml of Bfa in the presence or absence of 60 μM of chloroquine (CQ) for the indicated time points. Cells were harvested in 1X sample buffer following treatment. Whole cell lysates were subjected to SDS-PAGE followed by Immunoblotting. Cell lysates were assessed using antibodies against actin and ubiquitin.

4.2.3 Microarray analysis of HCT116 cells reveals an array of autophagy-related genes transcriptionally upregulated in response to ER stress

As discussed previously the connection between the UPR and its regulation of the autophagy pathway remains vague. Here we aimed to shine some light on this connection by carrying out a microarray analysis of HCT116 cells treated with ER stress inducing agents brefeldin A and tunicamycin to identify autophagy related genes transcriptionally upregulated in response to ER stress.

Wild-type (WT), $p53^{-/-}$ and $dicer^{-/-}$ HCT116 colon cancer cells were treated with 0.5 μg/ml Bfa or 2 μg/ml Tm for 24 h. Following treatment, cells were lysed in TRIzol and RNA was extracted. The RNA samples were sent to DNA vision, a company which specializes in performing microarrays. The $p53^{-/-}$ and $dicer^{-/-}$ HCT116 cells were included in this study to ensure that the transcriptional upregulation of the autophagy genes were a direct target of the UPR. The transcription factor p53 has been described to be upregulated at later stages during ER stress of which we have also observed in our hands[223]. Many autophagy related genes which are involved in modulating the induction of autophagy, such as Sestrin2[224], REDD1[225], DRAM[226] and NIX/BNIP3L[227], have been described to be a target of p53, thus $p53^{-/-}$ cells should be able to differentiate between UPR indirect transcriptional upregulation of autophagy-related genes by p53. There is mounting evidence to suggest that micro-RNAs (miRNAs) are regulated by the UPR[228]; therefore, to rule out miRNAs playing a role in the regulation of the autophagy-related genes at the mRNA level we used $dicer^{-/-}$ cells.

The data obtained from the microarray analysis was immense; however, as my interest lied in the connection between ER stress and autophagy, I screened the thousands of hits for any autophagy related gene upregulated greater than a 3 fold induction compared to the untreated sample. Furthermore, these genes were also transcriptionally upregulated to a similar extent in all three cell lines, WT, $p53^{-/-}$ and $dicer^{-/-}$ HCT116 cells, therefore indicating that there upregulation was not an artifact as it was essentially repeated under three different conditions, nor was it dependent on p53 or microRNA regulation. From this we identified an array of autophagy related genes upregulated in response to ER stress (Fig 4.4).

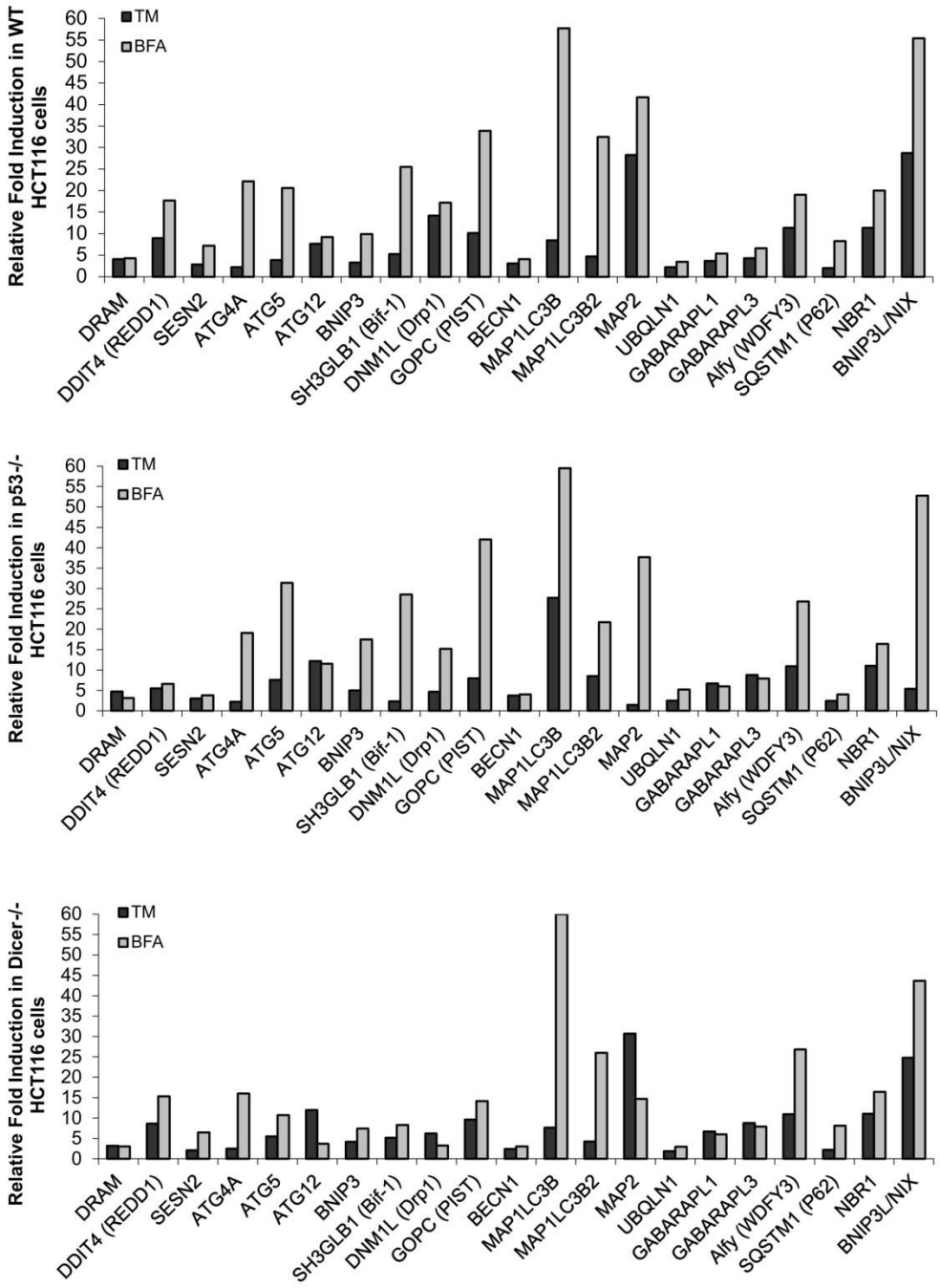

Figure 4.4: Microarray analysis of HCT116 identifies the transcriptional upregulation of an array of autophagy-related genes in response to ER stress. WT, $p53^{-/-}$ and $dicer^{-/-}$ HCT116 cells were treated with 0.5 μg/ml of Bfa or 2 μg/ml of Tm for 24 h. Following treatment cells were harvested and lysed in TRIzol reagent and RNA was extracted. RNA was sent to DNA vision, a company that specializes in microarray analysis. The data received was screened for the transcriptional upregulation of autophagy-related genes in response to both Tm and Bfa in all 3 cell lines which had a relative fold induction of 3 or more compared to untreated sample.

Gene	Description
DRAM	(DAMAGE-REGULATED AUTOPHAGY MODULATOR): DRAM is a p53 target gene involved in autophagy, activates autophagy via beclin1.
DDIT4(REDD1)	(REGULATED IN DEVELOPMENT AND DNA DAMAGE RESPONSES 1): REDD1 is a transcriptional target of p53 induced following DNA damage, activates TSC and thus inhibits mTOR.
Sestrin2	SEST2: is a transcriptional target of p53 induced following hypoxia, activates AMPK and thus inhibits mTOR.
BNIP3	(ADENOVIRUS E1B 19-KD PROTEIN-INTERACTING PROTEIN 3) upregulated in response to hypoxia, required for hypoxia induced autophagy.
ATG4A	Protease required for the cleavage of LC3I.
ATG5	Binds ATG12 and ATG16 to form a complex involved in the elongation and maturation of the autophagosome.
ATG12	Binds ATG5 and ATG16 to for a complex involved in the elongation and maturation of the autophagosome
Ubiquilin	(PLIC) Ubiquilins (UBQLNs) are adaptor proteins, they bind to protein aggrgates and generate aggresomes, they then act as adaptor proteins for autophagy receptors to target the aggresome to the autophagosome.
SQSTM1(p62)	Sequestosome 1/p62 Is a Polyubiquitin Chain Binding Protein, can bind to ubiquitinated substrates and targets them to the autophagosme via interaction with LC3 family proteins.
BNIP3L/NIX	BCL2/ADENOVIRUS E1B 19-KD PROTEIN-INTERACTING PROTEIN 3-LIKE: binds to mitochondria and act as an autophagy receptor for the selective degradation of mitochondria (mitophagy)
SH3GLB1 (Bif-1)	Bif-1 (also known as Endophilin B1) interacts with Beclin 1 through ultraviolet irradiation resistance-associated gene (UVRAG) and functions as a positive mediator of the class III PI(3) kinase (PI(3)KC3).
DNM1L	Dynamin-1-like protein is a member of the dynamin superfamily of GTPases, required for mitochondrial fission, a pre-requisite for mitophagy.
GOPC(PIST)	PIST is a PDZ domain-containing Golgi protein. It has been shown to directly bind to beclin1 and modulate its activity.
Beclin1	Beclin-1 is also known as autophagy-related gene (Atg) 6. Beclin-1 and its binding partner class III phosphoinositide 3-kinase (PI3K), also named Vps34, are required for the initiation and the formation of the autophagosome in autophagy.
MAP1LC3B	Microtubule-associated proteins 1A/1B light chain 3B, required for autophagosome elongation, autophagosome translocation and binding of autophagy receptors.
MAP1LC3B2	Microtubule-associated proteins 1A/1B light chain 3B 2, required for autophagosome elongation, autophagosome translocation and binding of autophagy receptors.
MAP2	Microtubule-associated protein 2, required for autophagosome translocation.
NBR1	Next to BRCA1 gene 1 protein, binds ubiquitinated proteins and aggresomes

	and acts as an autophagy receptor for the selective degradation of protein aggregates.
GABARAPL1	Member of the LC3 family, component of the autophagosome, binds to NIX mediating mitochondrial specific autophagy (mitophagy)
GABARAPL3	Member of the LC3 family, component of the autophagosome, binds to NIX (less affinity then L1) mediating mitochondrial specific autophagy (mitophagy)
Alfy (WDFY3)	WDFY3 is also known as autophagy-linked FYVE protein (Alfy). Acts as a scaffolding protein for p62 and LC3, ATG5, ATG12, ATG16 to mediate selective degradation of aggregates.

4.2.4 ER stress results in the transcriptional upregulation of the autophagy receptor genes

The microarray analysis identified an array of autophagy-related genes upregulated in response to ER stress. Many of these genes are involved in the induction of autophagy or are involved in the biogenesis of the autophagosome. These genes provide interesting insights into the close connection between the UPR and the autophagy pathway; furthermore it indicates that many factors can result in autophagy induction in response to ER stress. Investigation of these genes will further help unravel how the UPR regulates the induction of autophagy and how it contributes to the biogenesis of the autophagosome. Although investigation into these genes will further our understanding of ER stress induced autophagy and autophagy biogenesis in response to ER stress, it still however remains unclear whether autophagy is a selective or non-selective process during ER stress. The idea that autophagy is a non-selective process seems uncharacteristic of such a complex and highly regulated pathway. The identification of the autophagy receptor proteins shed new light on the whole concept of autophagy degradation. These receptors clearly demonstrate that for a substrate to be taken up by the autophagosome it must undergo some modification that is recognized by these autophagy receptors and thus targeting them to the autophagosome[47]. Although the autophagy receptor proteins have been well characterized both structurally and functionally, not much is known about their regulation.

The HCT116 cells were exposed to Tm and Bfa for 24 h before RNA was harvested and sent for microarray analysis. The treatments, Tm and Bfa, resulted in different severities of stress, where Tm was only resulting in 20% cell death; Bfa resulted in around 60%

cell death (Fig 4.5A). This would allow us to determine if the transcriptional upregulation of the genes was an early or late event in the ER stress response and would also determine if it was a drug specific response or a general ER stress response. The microarray analysis identified the transcriptional upregulation of the three autophagy receptors, Nix/Bnip3L, p62 and Nbr1, which was evident with both treatments insinuating that this upregulation was a general ER stress response (Fig 4.5B).

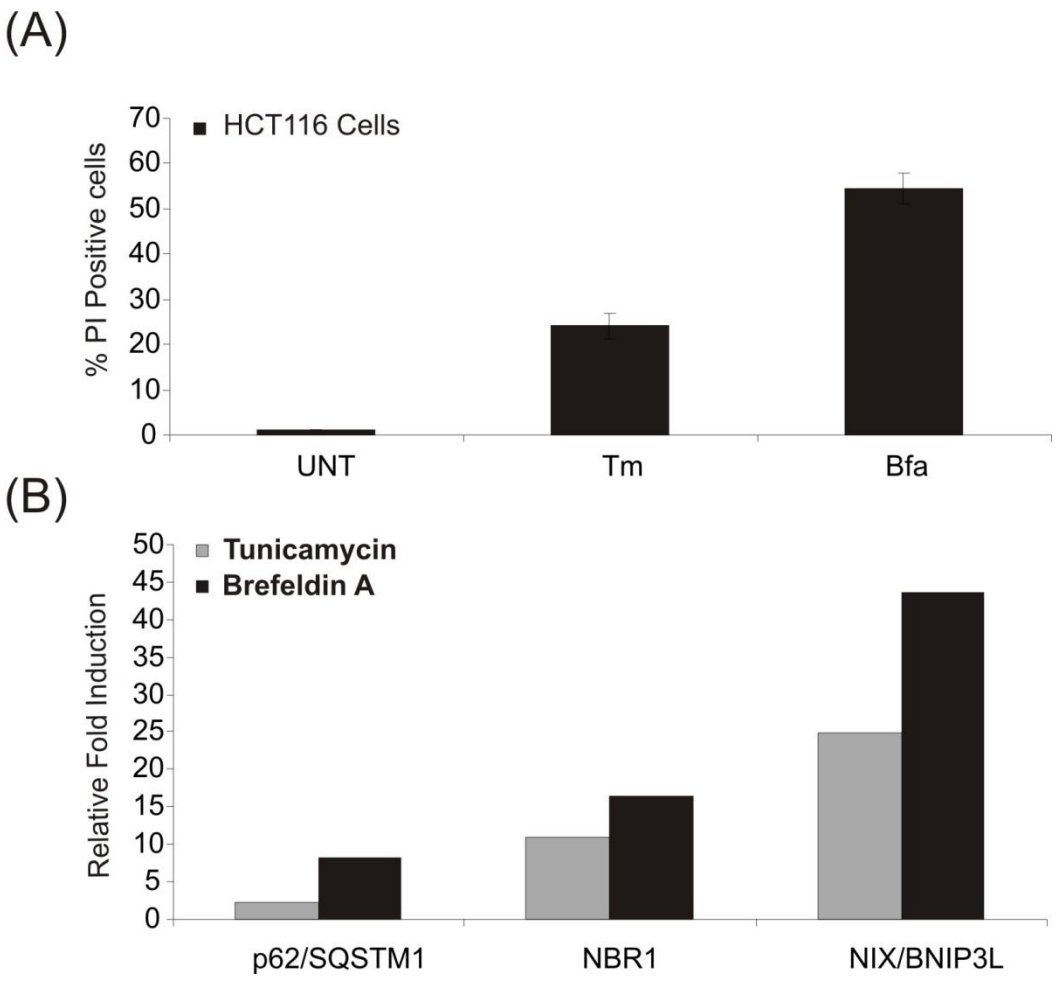

Figure 4.5: Microarray analysis identifies the transcriptional upregulation of the autophagy receptor genes. (A) WT HCT116 cells were treated with 0.5 μg/ml of Bfa or 2 μg/ml of Tm for 24 h. Following treatment, cells were stained with Propidium Iodide (PI) and assessed by FACS analysis for cell viability. **(B)** Microarray data from WT HCT116 cells treated with Tm or Bfa for 24 h shows transcriptional upregulation of p62, NBR1 and NIX transcripts.

To confirm the microarray data, we treated WT HCT116 cells with 0.5 μg/ml of Bfa and carried out a time course of 0, 6, 12, 24, 32 and 36 h (Fig 4.6A). Furthermore we confirmed the induction of the autophagy receptors with additional ER stress inducing agents, tunicamycin (0.5 μg/ml Tm) and thapsigargin (0.5 μM Tg) (Fig 4.6B). To confirm that this was not a cell-type specific effect we treated MDA-MB-468 breast cancer cells with 0.5 μg/ml of Bfa and monitored the transcriptional upregulation of the autophagy receptor genes at the indicated time points (Fig 4.6C). Following treatment, cells were harvested and lysed in TRIzol reagent. RNA was extracted from the lysate and revere transcribed into cDNA. The cDNA was diluted to a 1:5 ratio. Realtime PCR was carried out using probes specific for NIX/BNIP3L, p62 and NBR1cDNA.

Our results confirm the transcriptional upregulation of the autophagy receptor genes, NIX/BNIP3L, p62 and NBR1, in response to ER stress. Furthermore we showed that this was not a cell type specific event, using both HCT116 colon cancer cells and MDA-MB-468 breast cancer cells.

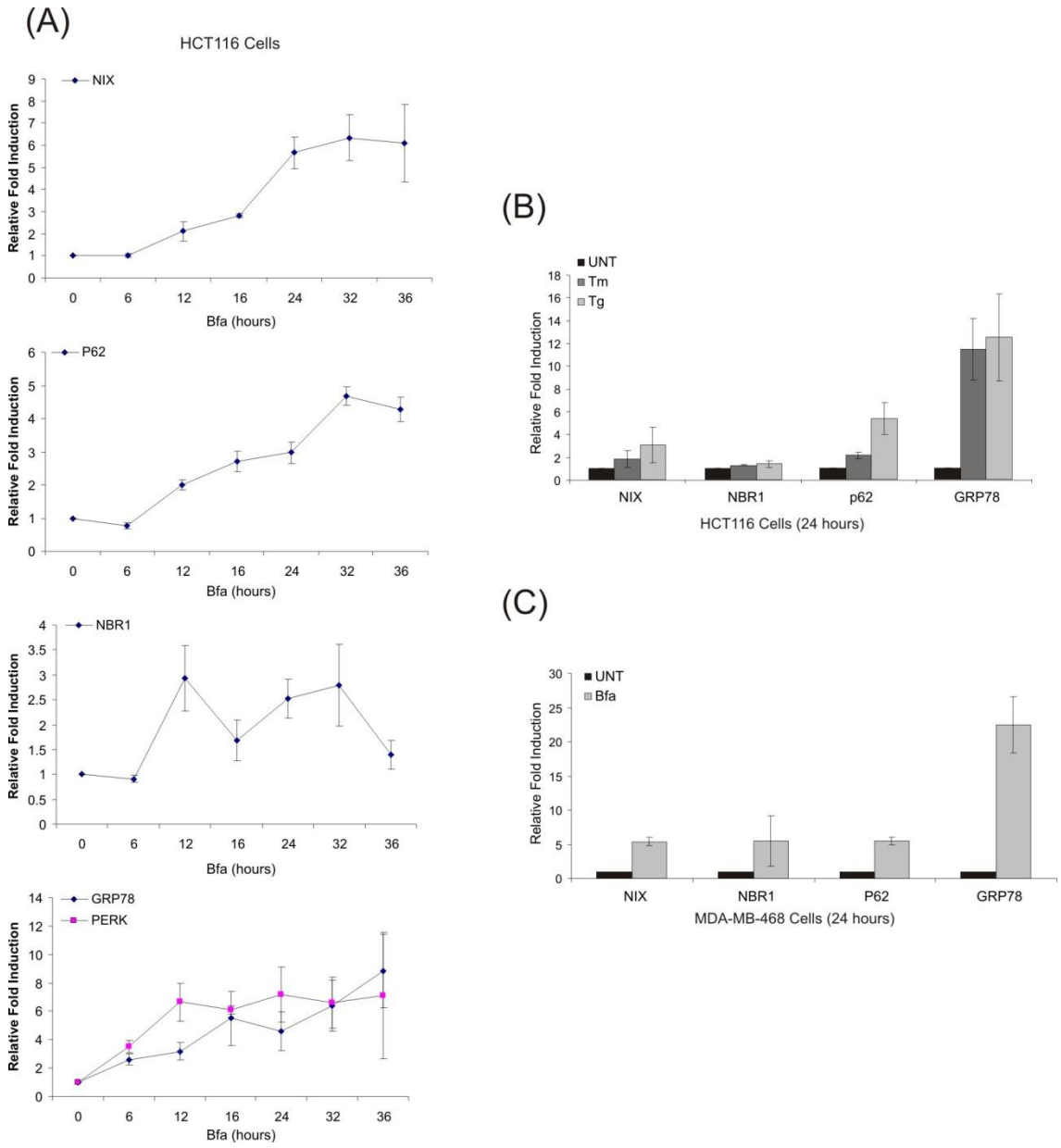

Figure 4.6: Real-Time PCR confirms the transcriptional upregulation of the autophagy receptor genes. Real-Time PCR was carried out on HCT116 cells and MDA-MB-468 cells to monitor autophagy receptor gene expression in response to ER stress. **(A)** WT HCT116 cells were treated with 0.5 μg/ml of Bfa for over an extensive time course to monitor the gene expression kinetics. Cells were harvested at the indicated time points and lysed in TRIzol reagent. RNA was extracted and reverse transcribed into cDNA. cDNA was diluted to a 1:5 ratio and real-time PCR was carried out to monitor the expression of p62, NBR1 and NIX over the time course. **(B)** WT HCT116 cells were treated with 2 μg/ml Tm or 0.5 μM Tg for 24 h. Following treatment cells were harvested and lysed in TRIzol reagent. Real-time PCR was carried out as in (A). **(C)** MDA-MB-468 cells were treated with 0.5 μg/ml Bfa for 24 h. Following treatment cells were harvested and lysed in TRIzol reagent. Real-time PCR was carried out as in (A).

4.2.5 The PERK arm of the UPR is required for the transcriptional upregulation of the autophagy receptor genes

Next we wanted to determine which arm of the UPR was involved in the upregulation of the autophagy receptor genes. Our preliminary data suggests that the transcriptional upregulation of the autophagy receptor genes is dependent on the PERK arm of the UPR. PERK has been previously described as an essential factor for the regulation of the autophagy pathway, involved in ATF4 mediated upregulation of LC3, and Chop mediated upregulation of ATG5. Our data suggests that PERK is also involved in the upregulation of the autophagy receptor genes.

MDA-MB-468 breast cancer cell lines stably expressing PERK shRNA or PLKO ctrl, were treated with 0.5 μg/ml of Bfa for 24 h. Following treatment, cells were harvested and lysed in TRIzol reagent and RNA was extracted from the lysate. The RNA was revere transcribed and the cDNA was diluted to a 1:5 ratio. Realtime PCR was carried out using probes specific for NIX/BNIP3L, p62, NBR1, PERK and GRP78 cDNA (Fig 4.7).

Our results confirm that PERK is indeed knocked down; subsequently, knockdown of PERK resulted in reduced levels of GRP78. Furthermore we also observe reduced induction of the autophagy receptor genes, indicating that a downstream transcription factor of the PERK arm is involved in the regulation of the autophagy receptor genes in response to ER stress. Although these results are convincing they are preliminary and thus most be confirmed with different ER stress inducing drugs and different cell lines.

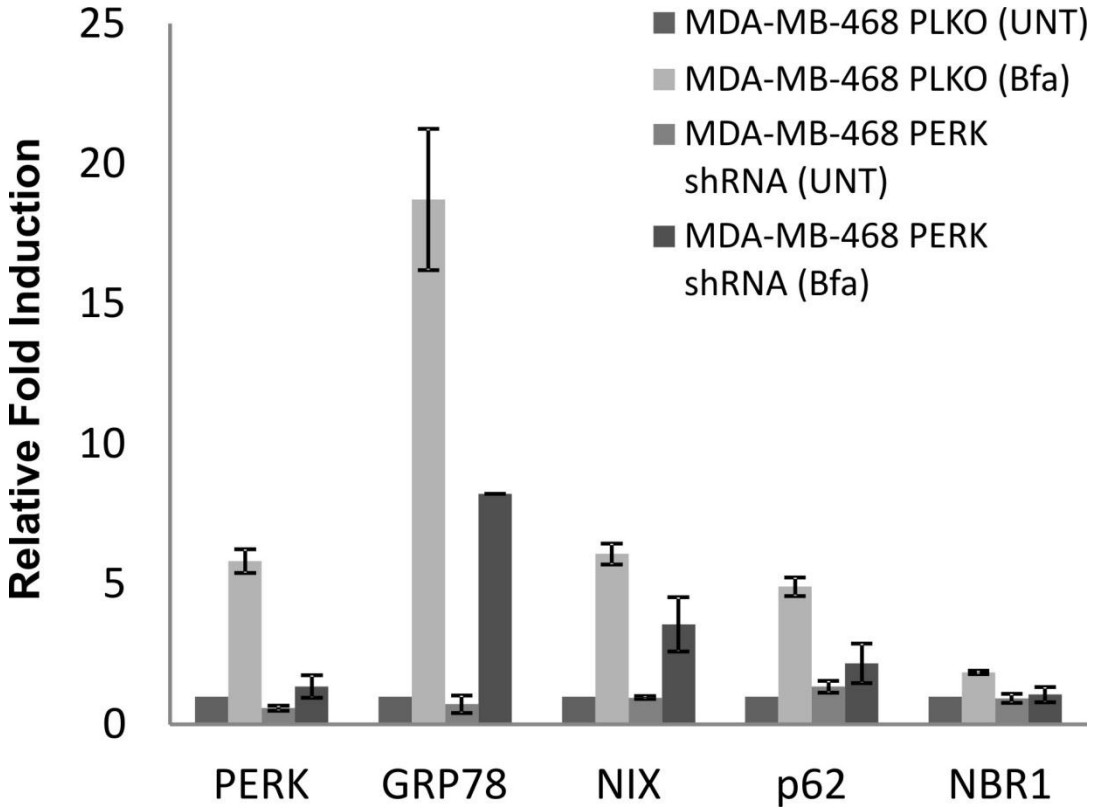

Figure 4.7: Preliminary data suggest that PERK is involved in the regulation of the autophagy receptor genes in response to ER stress. MDA-MB-468 PLKO control and MDA-MB-468PERK shRNA expressing cells were treated with 0.5 μg/ml of Bfa for 24 h. Following treatment, Cells were harvested and lysed in TRIzol reagent. RNA was extracted and reverse transcribed into cDNA. cDNA was diluted to a 1:5 ratio and real-time PCR was carried out to monitor the expression of p62, NBR1, NIX, PERK and GRP78. Graphs represent the mean ± SEM of three independent experiments

4.3 Discussion

The UPR and autophagy are independent processes; however, although the UPR and autophagy can act independently, it is clear that these processes are quite tightly interlinked in response ER stress. As mentioned, there are many indirect and direct connections between the UPR and the autophagy pathway demonstrated throughout the literature, of which our group has recently reviewed[38].

The Microarray analysis performed here, emphasizes this connection with the identification of over 20 genes involved in the regulation of autophagy in response to ER stress, most of which have not yet been connected to the UPR. Of these genes we have identified the upregulation of the autophagy receptor genes NIX/BNIP3L, p62 and NBR1. Experts in the field of ER stress and autophagy agree that ER stress is a potent inducer of autophagy; however, whether autophagy is a selective or non-selective process in response to ER stress becomes a matter of debate. Here we investigated the regulation of the autophagy receptor genes by the UPR to try and shed some light on this controversial topic.

Autophagy has long been considered a non-selective bulk degradation process. In the last few years the identification of the autophagy receptor proteins has re-established the importance of this process in many cellular events for the selective removal of unwanted substrates such as invading pathogens, protein aggregates and old or damaged organelles[47]. There have been many autophagy receptor proteins identified, characterized by the presence of an LC3 interacting region (LIR); however of these proteins the best characterized is p62 and more recently NBR1, a protein shown to behave and function similar to that of p62. Both p62 and NBR1 are involved in the selective degradation of ubiquitinated substrates and aggregates. p62 and NBR1 contain a UBA domain which facilitates binding of ubiquitinated substrates, and a LC3 interacting region (LIR) which targets the ubiquitin substrates to the autophagosome via direct interaction with LC3 family members[229-231] Although it is proposed that p62 and Nbr1 can target soluble single ubiquitinated proteins to the autophagosome it has not yet been clearly demonstrated. However p62 and NBR1 are capable of oligomerizing via an N-terminal Phox and Bem1p (PB1) domain resulting in the formation of

unfolded protein aggregates in the cytosol. These aggregates have been clearly shown to co-localize with autophagosomal structures[232]. The results in this chapter show that both p62 and NBR1 are transcriptionally upregulated in response to multiple ER stress inducing agents in both HCT116 colon cancer cells and MDA-MB-468 breast cancer cells. Inhibition of autophagy degradation with the addition of CQ resulted in the accumulation of ubiquitinated substrates in response to ER stress. This data confirms that ubiquitinated substrates require autophagy for their removal in response to ER stress; however single and co-knockdown studies of p62 and NBR1 will be required to confirm that these proteins are required for autophagy mediated degradation of ubiquitinated substrates.

Mitochondrial degradation or "Mitophagy" is a process that is characterized by autophagy-mediated degradation of mitochondria. NIX/BNIP3L has been identified as an important adaptor for the removal of mitochondria. Nix was first established as an important mediator for the removal of mitochondria in reticulocyte development[233], however further studies demonstrate that damaged or depolarized mitochondria can also be removed by autophagy and this process is dependent on NIX[87]. In this chapter we show co-localization of mitochondria and autophagosomes in response to ER stress both by fluorescent tagging experiments and electron microscopy. Furthermore we show that NIX is transcriptionally upregulated in response to ER stress both in HCT116 cells and MDA-MB-468 cells. Knocking down NIX in this system will be crucial in determining if (a) the mitophagy observed in response to ER stress requires NIX and (b) if mitophagy plays a role in protecting cells against ER stress.

PERK knockdown in MDA-MB-468 cells demonstrated that the transcriptional upregulation of NIX, p62 and NBR1 are dependent on transcription factors downstream of this arm. However, this data is preliminary and thus knockdown of IRE1 and ATF6 would need to be done to demonstrate that it is a PERK dependent effect. Because the UPR is such a complex and dynamic system, knockdown of one arm of the UPR can result in an enhancement or differential regulatory effect on the other UPR arms which may result in obscured results.

This study has provided a lot of information and thus a lot of questions which need to be addressed. Here I specifically concentrate on the hypothesis that the UPR may regulate the autophagy receptors to aid in the removal of damaged organelles and ubiquitinated substrates. In this study I show that ER stress induced autophagy results in the degradation of mitochondria and ubiquitinated substrates. Furthermore I show that the UPR can transcriptional induce the autophagy receptor genes which have been shown, in different contexts, to be play a crucial role in there degradation. Moreover, I show that the transcriptional regulation of the autophagy receptors may be dependent on the PERK arm of the UPR.

Concluding Remarks and Future Prospects

In this thesis we have examined the dynamics of cell death and the close relationship that exists between ER stress, the UPR and autophagy; furthermore, we show the integral crosstalk that occurs between these processes.

In the first results section (chapter 3) we demonstrate the ability of the cell to use alternative mechanisms to induce cell death when the intrinsic apoptotic pathway is compromised. To understand these alternative forms of cell death we use cells that are resistant to mitochondrial-mediated apoptosis and expose them to cellular stress stimuli such as ER stress inducing agents and chemotherapeutic drugs. Although we use quite an artificial system, it is required for primarily elucidating these mechanisms without speculating what level of death is being contributed from the intrinsic pathway and what is being contributed from the death pathway under investigation. Once the intrinsic pathway is initiated and caspase-9 becomes activated a cascade of cleavage events occurs, including cleavage of other apical caspases, further amplifying cell death. If we are to monitor other forms of cell death independent to this process it is essential that our observations aren't obscured by even negligible amounts of apoptosome activation. For this reason we use $C9^{-/-}$ MEFs; however, by using different cell lines and knockout models we confirm that our observations are not an artifact of these cells. To date apoptosis is the king of programmed cell death, there is an immense amount of literature describing how apoptosis is initiated and how it executes cell death in many contexts. It is clear that other forms of cell death also exist; however, because these pathways are not frequently observed under culture conditions they tend to be ignored and consequently are poorly defined. It is important to elucidate how other forms of cell death are activated and how they execute cell death. If these other forms of cell death are characterized as well as apoptosis it could revolutionize therapeutic approaches against diseases such as cancer. Intrinsic apoptosis is clearly a very powerful system for inducing cell death; however for most cancer cells this mechanism of death is abrogated. In this section we show that although the intrinsic pathway is compromised these cells can still undergo cell death, albeit at a slower, less efficient rate. The slow, less efficient characteristic of these pathways is clearly a disadvantage; however if we can understand how these pathways are activated and identify the regulatory

components involved, pharmacological manipulation could expose these pathways to be as efficient if not more efficient than the intrinsic apoptotic pathway.

In this section (chapter 3) we show that cells compromised in the MMA pathway, treated with ER stress inducing agents or chemotherapeutic drugs, undergo cell death with features of caspase activation, necroptosis and a requirement for ATG5. Furthermore, we show this pathway is quite dynamic in determining cell death, depending on the cellular context this pathway can execute cell death through either caspase-8 mediated apoptosis or RIP mediated necroptosis. We show that this death pathway requires RIP1, caspase-8 and ATG5. Furthermore we show that both TRADD and RIP1 kinase activity are required for the optimal functioning of this pathway. Immunoprecipitation of ATG5 suggests that at least RIP1, FADD, ATG5 and caspase-8 are all components of one complex.

In this study we propose the formation of an ATG5-FADD-RIP1-caspase-8 containing complex that is capable of signaling cell death through either caspase-8 mediated activation of executioner caspases and subsequent apoptosis or through RIP1 mediated activation of the Necrosome and subsequent necroptosis. As this complex resembles the dynamics of other RIP1-containing complexes, such as complex II and the ripoptosome, we assume that similar regulators, such as FLIP proteins, are capable of having similar effects on our complex. With this in mind we can assume that depending on the levels of FLIP proteins in the cell this complex will signal through either apoptosis or necroptosis. Knockdown of ATG5 and subsequently autophagy inhibited caspase-3 processing and subsequently reduced the levels of cell death in the $C9^{-/-}$ MEFs. This may implicate the autophagosome acting as a platform for the formation of this complex; alternatively, ATG5 may be an essential component of this caspase-8 activating complex independent of its role in autophagy. Studies have shown a direct interaction between ATG5 and FADD of which were very convincing. Subsequent studies have presumed that this interaction correlates directly with autophagy and hypothesize that the autophagosome acts as a signaling platform for the formation of an iDISC; however, although this seems logical, as of yet, this has not been adequately demonstrated.

Future investigation is required to address if ATG5 is acting independent of autophagy in this complex or if the autophagosome is required as a signaling platform. To address this question, proteins essential for the induction of autophagy need to be targeted for knockdown, such as Beclin1 or ULK1, to demonstrate that the autophagosome and not specifically ATG5 is required for this complex to form. Furthermore upon knockdown of these genes, ATG5 must be monitored within the same experiment to ensure that inhibition upstream of autophagy has no effect on the stability of downstream components in the autophagy pathway. To try and further address this issue, Gold particle labeling of active caspase-8 followed by electron microscopy would be the most convincing, observing the outer membrane of the autophagosomes for gold dotted caspase-8. One possible method would be to add biotin labeled zVAD to the cells during treatment, followed by the addition of a gold labeled anti-biotin antibody. In addition to determining the role of ATG5 and autophagy in this complex, it is important to understand how this complex if regulated. Depicting the role of the different FLIP isoforms and the IAP family proteins in the regulation of this complex will also be essential, this will determine if its regulation is similar to that of complex II and the ripoptosome or if it requires completely different regulatory partners. Finally to confirm that all these components are indeed in complex, reciprocal IPs for some of the other partners would be required followed by mass spectrometry to determine other interacting partners.

In the second result section (chapter 4) we examine the close relationship between the UPR and its regulation of the autophagy pathway. Although these processes are known to be tightly connected not much evidence exists to directly relate these two processes. Treatment of HCT116 cells with ER stress inducing agents followed by microarray analysis revealed an array of autophagy-related genes transcriptionally upregulated. Of these genes we identified the transcriptional upregulation of the autophagy receptors p62, NIX and NBR1.

Autophagy is an exceptionally complex system and plays many essential roles in the cell. The early characterization of this process as being a non-selective process is slowly being shunned with mounting evidence to suggest that the removal of substrates by

autophagy requires selective labeling with an autophagy receptor protein. Here we show that in response to ER stress p62, NIX and NBR1 are transcriptionally upregulated. Furthermore we show that the knockdown of the UPR arm, PERK, abrogated the upregulation of these genes.

Further investigation in to the functional relevance of these proteins in response to ER stress is required. Theoretically if ER stress induced autophagy is a selective process the inhibition of these receptors should show similar functional defects to the knockdown of the autophagy pathway. Moreover, inhibition of the other UPR arms will be required to determine if PERK is the main arm involved in their regulation. Commercially available shRNAs for the knockdown of the UPR arms in human cell lines have, in our experience, been very problematic; however, the recently available PERK inhibitor and IRE1 inhibitors have demonstrated exceptionally high specificity for the inhibition of these proteins and will make addressing questions such as this very easy.

On a broader scale, this thesis demonstrates the close connection between ER stress, autophagy and cell death. We show that the cell is a very dynamic system which is capable of using multiple processes to deliver different outcomes. In the context of the UPR and autophagy, both are induced by ER stress as a survival response; however, if the stress persists the same processes are capable of inducing cell death. Furthermore inhibition of the cells primary mode of cell death in response to severe cellular stresses will result in the activation of a non-canonical cell death pathway to carry out the job. Elucidating the players involved in these processes and understanding how these switches are regulated will further our understanding of the cell and its behavior in response to cellular stress.

References

1 McLaughlin, M. & Vandenbroeck, K. The endoplasmic reticulum protein folding factory and its chaperones: new targets for drug discovery? *British Journal of Pharmacology* **162**, 328-345, doi:10.1111/j.1476-5381.2010.01064.x (2011).
2 Gotoh, T. *et al*. Endoplasmic Reticulum Stress-Related Inflammation and Cardiovascular Diseases. *International Journal of Inflammation* **2011** (2011).
3 Gorman, A. M. *et al*. Stress management at the ER: Regulators of ER stress-induced apoptosis. *Pharmacology & Therapeutics*, doi:10.1016/j.pharmthera.2012.02.003 (2012).
4 Cawley, K.. *et al*Assays for detecting the unfolded protein response. *Methods in Enzymology* Vol. Volume 490 (ed P. Michael Conn) 31-51 (Academic Press, 2011).
5 Szegezdi, E. *et al*. Mediators of endoplasmic reticulum stress-induced apoptosis. *EMBO reports* **7**, 880-885 (2006).
6 Reddy, R. K. *et al.* Endoplasmic Reticulum Chaperone Protein GRP78 Protects Cells from Apoptosis Induced by Topoisomerase Inhibitors. *Journal of Biological Chemistry* **278**, 20915-20924, doi:10.1074/jbc.M212328200 (2003).
7 Goldson, T. M. *et al.* Eukaryotic initiation factor 4E variants alter the morphology, proliferation, and colony-formation properties of MDA-MB-435 cancer cells. *Molecular Carcinogenesis* **46**, 71-84, doi:10.1002/mc.20276 (2007).
8 Saito, A. *et al.* Endoplasmic Reticulum Stress Response Mediated by the PERK-eIF2α-ATF4 Pathway Is Involved in Osteoblast Differentiation Induced by BMP2. *Journal of Biological Chemistry* **286**, 4809-4818, doi:10.1074/jbc.M110.152900 (2011).
9 Harding, H. P. *et al*. Perk Is Essential for Translational Regulation and Cell Survival during the Unfolded Protein Response. *Molecular Cell* **5**, 897-904 (2000).
10 Harding, H. P. *et al.* An Integrated Stress Response Regulates Amino Acid Metabolism and Resistance to Oxidative Stress. *Molecular Cell* **11**, 619-633, doi:10.1016/s1097-2765(03)00105-9 (2003).
11 Woo, C. W. *et al.* Adaptive suppression of the ATF4-CHOP branch of the unfolded protein response by toll-like receptor signalling. *Nature Cell Biology* **11**, 1473-1480, doi:http://www.nature.com/ncb/journal/v11/n12/suppinfo/ncb1996_S1.html (2009).
12 McCullough, K. D. *et al*. Gadd153 sensitizes cells to endoplasmic reticulum stress by down-regulating Bcl2 and perturbing the cellular redox state. *Molecular and Cellular Biology* **21**, 1249-1259 (2001).
13 Cazanave, S. C. *et al.* CHOP and AP-1 cooperatively mediate PUMA expression during lipoapoptosis. *Am J Physiol Gastrointest Liver Physiol* **299**, 29 (2010).
14 Puthalakath, H. *et al.* ER stress triggers apoptosis by activating BH3-only protein Bim. *Cell* **129**, 1337-1349 (2007).
15 Kim, H. *et al.* Stepwise activation of BAX and BAK by tBID, BIM, and PUMA initiates mitochondrial apoptosis. *Molecular Cell* **36**, 487-499 (2009).

16 Oyadomari, S. *et al.* Targeted disruption of the Chop gene delays endoplasmic reticulum stress–mediated diabetes. *The Journal of Clinical Investigation* **109**, 525-532 (2002).
17 Chan, J. Y. & Kwong, M. Impaired expression of glutathione synthetic enzyme genes in mice with targeted deletion of the Nrf2 basic-leucine zipper protein. *Biochimica et Biophysica Acta* **15**, 19-26 (2000).
18 Cullinan, S. B. *et al.* Nrf2 Is a Direct PERK Substrate and Effector of PERK-Dependent Cell Survival. *Molecular and Cellular Biology.* **23**, 7198-7209, doi:10.1128/mcb.23.20.7198-7209.2003 (2003).
19 Ho, H. K. *et al.* Nrf2 Activation Involves an Oxidative-Stress Independent Pathway in Tetrafluoroethylcysteine-Induced Cytotoxicity. *Toxicological Sciences* **86**, 354-364, doi:10.1093/toxsci/kfi205 (2005).
20 Cullinan, S. B. & Diehl, J. A. Coordination of ER and oxidative stress signaling: The PERK/Nrf2 signaling pathway. *The International Journal of Biochemistry & Cell Biology* **38**, 317-332, doi:10.1016/j.biocel.2005.09.018 (2006).
21 Haze, K.. *et al*. Mammalian Transcription Factor ATF6 Is Synthesized as a Transmembrane Protein and Activated by Proteolysis in Response to Endoplasmic Reticulum Stress. *Molecular Biology of the Cell* **10**, 3787-3799 (1999).
22 Shen, J. *et al*. ER Stress Regulation of ATF6 Localization by Dissociation of BiP/GRP78 Binding and Unmasking of Golgi Localization Signals. *Developmental Cell* **3**, 99-111 (2002).
23 Ye, J. *et al.* ER Stress Induces Cleavage of Membrane-Bound ATF6 by the Same Proteases that Process SREBPs. *Molecular Cell* **6**, 1355-1364, doi:10.1016/s1097-2765(00)00133-7 (2000).
24 Li, M. *et al.* ATF6 as a Transcription Activator of the Endoplasmic Reticulum Stress Element: Thapsigargin Stress-Induced Changes and Synergistic Interactions with NF-Y and YY1. *Molecular and Cellular Biology* **20**, 5096-5106, doi:10.1128/mcb.20.14.5096-5106.2000 (2000).
25 Haze, K. *et al*. Mammalian transcription factor ATF6 is synthesized as a transmembrane protein and activated by proteolysis in response to endoplasmic reticulum stress. *Molecular Biology of the Cell* **10**, 3787-3799 (1999).
26 Yamamoto, K.. *et al* . Differential contributions of ATF6 and XBP1 to the activation of endoplasmic reticulum stress-responsive cis-acting elements ERSE, UPRE and ERSE-II. *Journal of Biochemistry* **136**, 343-350 (2004).
27 Yamamoto, K. *et al*. Differential Contributions of ATF6 and XBP1 to the Activation of Endoplasmic Reticulum Stress-Responsive cis-Acting Elements ERSE, UPRE and ERSE-II. *Journal of Biochemistry* **136**, 343-350, doi:10.1093/jb/mvh122 (2004).
28 Belmont, P. J. *et al*. Regulation of microRNA expression in the heart by the ATF6 branch of the ER stress response. *Journal of Molecular and Cellular Cardiology*, doi:10.1016/j.yjmcc.2012.01.017 (2012).
29 Kaufman, R. J. & Cao, S. Inositol-requiring 1/X-box-binding protein 1 is a regulatory hub that links endoplasmic reticulum homeostasis with innate immunity and metabolism. *EMBO Molecular Medicine* **2**, 189-192, doi:10.1002/emmm.201000076 (2010).

30 Hocking, L. J. *et al*. Functional interaction between Sequestosome-1/p62 and Autophagy-Linked FYVE-containing protein WDFY3 in human osteoclasts. *Biochemical and Biophysical Research Communications* **402**, 543-548, doi:10.1016/j.bbrc.2010.10.076 (2010).
31 Korennykh, A. V. *et al.* The unfolded protein response signals through high-order assembly of Ire1. *Nature* **457**, 687-693, doi:http://www.nature.com/nature/journal/v457/n7230/suppinfo/nature07661_S1.html (2009).
32 Lin, J. H. *et al.* IRE1 Signaling Affects Cell Fate During the Unfolded Protein Response. *Science* **318**, 944-949, doi:10.1126/science.1146361 (2007).
33 Trevino, L. R. *et al.* Germline genomic variants associated with childhood acute lymphoblastic leukemia. *Nature Genetics* **41**, 1001-1005, doi:http://www.nature.com/ng/journal/v41/n9/suppinfo/ng.432_S1.html (2009).
34 Drogat, B. *et al.* IRE1 Signaling Is Essential for Ischemia-Induced Vascular Endothelial Growth Factor-A Expression and Contributes to Angiogenesis and Tumor Growth In vivo. *Cancer Research* **67**, 6700-6707, doi:10.1158/0008-5472.can-06-3235 (2007).
35 Wang, F. M. *et al*. Regulation of unfolded protein response modulator XBP1s by acetylation and deacetylation. *Biochemical Journal* **433**, 245-252, doi:10.1042/bj20101293 (2010).
36 Urano, F. *et al.* Coupling of Stress in the ER to Activation of JNK Protein Kinases by Transmembrane Protein Kinase IRE1. *Science* **287**, 664-666, doi:10.1126/science.287.5453.664 (2000).
37 Kaneko, M. *et al*. Activation Signal of Nuclear Factor-κB in Response to Endoplasmic Reticulum Stress is Transduced via IRE1 and Tumor Necrosis Factor Receptor-Associated Factor 2. *Biological & Pharmaceutical Bulletin* **26**, 931-935 (2003).
38 Deegan, S. *et al*. Stress-induced self-cannibalism: on the regulation of autophagy by endoplasmic reticulum stress. *Cellular and molecular life sciences : Cellular and Molecular Life Sciences*, doi:10.1007/s00018-012-1173-4 (2012).
39 De Duve, C. & Wattiaux, R. Functions of lysosomes. *Annual Review of Physiology* **28**, 435-492, doi:10.1146/annurev.ph.28.030166.002251 (1966).
40 Ohsumi, Y. Molecular mechanism of autophagy in yeast, Saccharomyces cerevisiae. *Philosophical transactions of the Royal Society of London. Series B, Biological sciences* **354**, 1577-1580; discussion 1580-1571, doi:10.1098/rstb.1999.0501 (1999).
41 Rubinsztein, D. C. Autophagy: where next? *EMBO reports* **11**, 3-3 (2010).
42 Kondo, Y. *et al*. The role of autophagy in cancer development and response to therapy. *Nature Reviews Cancer* **5**, 726-734, doi:nrc1692 [pii]10.1038/nrc1692 (2005).
43 Moretti, L. *et al*. Switch between apoptosis and autophagy: radiation-induced endoplasmic reticulum stress? *Cell Cycle* **6**, 793-798, doi:4036 [pii] (2007).
44 Levine, B. Cell biology: autophagy and cancer. *Nature* **446**, 745-747, doi:446745a [pii]10.1038/446745a (2007).

45 Kroemer, G. *et al*. Autophagy and the integrated stress response. *Molecular Cell* **40**, 280-293, doi:S1097-2765(10)00751-3 [pii]10.1016/j.molcel.2010.09.023 (2010).
46 Rosenfeldt, M. T. & Ryan, K. M. The role of autophagy in tumour development and cancer therapy. *Expert Reviews in Molecular Medicine* **2** 2009;11:e36. doi: 10.1017/S1462399409001306.
47 Weidberg, H. *et al*. Biogenesis and cargo selectivity of autophagosomes. *Annual Review of Biochemistry* **80**, 125-156, doi:10.1146/annurev-biochem-052709-094552 (2011).
48 Mizushima, N. Autophagy: process and function. *Genes & Development* **21**, 2861-2873, doi:21/22/2861 [pii]10.1101/gad.1599207 (2007).
49 Maiuri, M. C. *et al*. Self-eating and self-killing: crosstalk between autophagy and apoptosis. *Nature Reviews Molecular Cell Biology* **8**, 741-752, doi:nrm2239 [pii]10.1038/nrm2239 (2007).
50 Jung, C. H. *et al.* ULK-Atg13-FIP200 complexes mediate mTOR signaling to the autophagy machinery. *Molecular Biology of the Cell* **20**, 1992-2003, doi:E08-12-1249 [pii]10.1091/mbc.E08-12-1249 (2009).
51 Egan, D. F. *et al.* Phosphorylation of ULK1 (hATG1) by AMP-activated protein kinase connects energy sensing to mitophagy. *Science* **331**, 456-461, doi:10.1126/science.1196371 (2011).
52 Kim, J. *et al*. AMPK and mTOR regulate autophagy through direct phosphorylation of Ulk1. *Nature Cell Biology* **13**, 132-141, doi:10.1038/ncb2152 (2011).
53 Shackelford, D. B. & Shaw, R. J. The LKB1-AMPK pathway: metabolism and growth control in tumour suppression. *Nature Reviews Cancer* **9**, 563-575, doi:nrc2676 [pii]10.1038/nrc2676 (2009).
54 Hosokawa, N. *et al.* Nutrient-dependent mTORC1 association with the ULK1-Atg13-FIP200 complex required for autophagy. *Molecular Biology of the Cell* **20**, 1981-1991, doi:10.1091/mbc.E08-12-1248 (2009).
55 Dunlop, E. A. *et al*. ULK1 inhibits mTORC1 signaling, promotes multisite Raptor phosphorylation and hinders substrate binding. *Autophagy* **7**, 737-747 (2011).
56 Loffler, A. S. *et al.* Ulk1-mediated phosphorylation of AMPK constitutes a negative regulatory feedback loop. *Autophagy* **7**, 696-706 (2011).
57 Chan, E. Y. Regulation and Function of Uncoordinated-51 Like Kinase Proteins. *Antioxidants & Redox Signaling*, doi:10.1089/ars.2011.4396 (2012).
58 Simonsen, A. & Tooze, S. A. Coordination of membrane events during autophagy by multiple class III PI3-kinase complexes. *The Journal of Cell Biology* **186**, 773-782, doi:jcb.200907014 [pii]10.1083/jcb.200907014 (2009).
59 Polson, H. E. *et al.* Mammalian Atg18 (WIPI2) localizes to omegasome-anchored phagophores and positively regulates LC3 lipidation. *Autophagy* **6** (2010).
60 Proikas-Cezanne, T. *et al.* WIPI-1alpha (WIPI49), a member of the novel 7-bladed WIPI protein family, is aberrantly expressed in human cancer and is linked to starvation-induced autophagy. *Oncogene* **23**, 9314-9325, doi:10.1038/sj.onc.1208331 (2004).

61 Axe, E. L. *et al.* Autophagosome formation from membrane compartments enriched in phosphatidylinositol 3-phosphate and dynamically connected to the endoplasmic reticulum. *The Journal of Cell Biology* **182**, 685-701, doi:10.1083/jcb.200803137 (2008).
62 Simonsen, A. *et al.* Alfy, a novel FYVE-domain-containing protein associated with protein granules and autophagic membranes. *Journal of Cell Science* **117**, 4239-4251, doi:10.1242/jcs.01287 (2004).
63 Stromhaug, P. E. *et al*. Purification and characterization of autophagosomes from rat hepatocytes. *Biochemical Journal* **335 (Pt 2)**, 217-224 (1998).
64 Fengsrud, M. *et al.* Ultrastructural and immunocytochemical characterization of autophagic vacuoles in isolated hepatocytes: effects of vinblastine and asparagine on vacuole distributions. *Experimental Cell Research* **221**, 504-519, doi:10.1006/excr.1995.1402 (1995).
65 Hailey, D. W. *et al.* Mitochondria supply membranes for autophagosome biogenesis during starvation. *Cell* **141**, 656-667, doi:10.1016/j.cell.2010.04.009 (2010).
66 Ravikumar, B. *et al*. Plasma membrane contributes to the formation of pre-autophagosomal structures. *Nature Cell Biology* **12**, 747-757, doi:10.1038/ncb2078 (2010).
67 Mizushima, N. *et al.* Mouse Apg16L, a novel WD-repeat protein, targets to the autophagic isolation membrane with the Apg12-Apg5 conjugate. *Journal of Cell Science* **116**, 1679-1688 (2003).
68 Pankiv, S. *et al.* FYCO1 is a Rab7 effector that binds to LC3 and PI3P to mediate microtubule plus end-directed vesicle transport. *The Journal of Cell Biology* **188**, 253-269, doi:10.1083/jcb.200907015 (2010).
69 Knaevelsrud, H. & Simonsen, A. Fighting disease by selective autophagy of aggregate-prone proteins. *FEBS Letters* **584**, 2635-2645, doi:S0014-5793(10)00325-X [pii]10.1016/j.febslet.2010.04.041 (2010).
70 Hirota, Y. *et al*. [Mitophagy: selective degradation of mitochondria by autophagy]. *Seikagaku. The Journal of Japanese Biochemical Society* **83**, 126-130 (2011).
71 Bernales, S. *et al*. ER-phagy: selective autophagy of the endoplasmic reticulum. *Autophagy* **3**, 285-287 (2007).
72 Kraft, C. *et al*. Mature ribosomes are selectively degraded upon starvation by an autophagy pathway requiring the Ubp3p/Bre5p ubiquitin protease. *Nature Cell Biology* **10**, 602-610, doi:10.1038/ncb1723 (2008).
73 Sakai, Y. *et al*. Pexophagy: autophagic degradation of peroxisomes. *Biochimica et Biophysica Acta* **1763**, 1767-1775, doi:10.1016/j.bbamcr.2006.08.023 (2006).
74 Glaumann, H. Crinophagy as a means for degrading excess secretory proteins in rat liver. *Revisiones Sobre Biologia Celular : RBC* **20**, 97-110 (1989).
75 Mousavi, S. A. *et al.* Effects of inhibitors of the vacuolar proton pump on hepatic heterophagy and autophagy. *Biochimica et Biophysica Acta* **1510**, 243-257 (2001).
76 Knodler, L. A. & Celli, J. Eating the strangers within: host control of intracellular bacteria via xenophagy. *Cellular Microbiology* **13**, 1319-1327, doi:10.1111/j.1462-5822.2011.01632.x (2011).

77 Yamamoto, A. & Simonsen, A. The elimination of accumulated and aggregated proteins: a role for aggrephagy in neurodegeneration. *Neurobiology of Disease* **43**, 17-28, doi:10.1016/j.nbd.2010.08.015 (2011).
78 Weidberg, H. *et al*. Lipophagy: selective catabolism designed for lipids. *Developmental Cell* **16**, 628-630, doi:10.1016/j.devcel.2009.05.001 (2009).
79 Kristensen, A. R. *et al.* Ordered organelle degradation during starvation-induced autophagy. *Molecular & Cellular Proteomics : MCP* **7**, 2419-2428, doi:10.1074/mcp.M800184-MCP200 (2008).
80 Sandilands, E. *et al.* Autophagic targeting of Src promotes cancer cell survival following reduced FAK signalling. *Nature Cell Biology* **14**, 51-60, doi:10.1038/ncb2386 (2012).
81 Wild, P. *et al.* Phosphorylation of the autophagy receptor optineurin restricts Salmonella growth. *Science* **333**, 228-233, doi:10.1126/science.1205405 (2011).
82 Kirkin, V. *et al*. A role for ubiquitin in selective autophagy. *Molecular Cell* **34**, 259-269, doi:10.1016/j.molcel.2009.04.026 (2009).
83 Ivanov, S. & Roy, C. R. NDP52: the missing link between ubiquitinated bacteria and autophagy. *Nature Immunology* **10**, 1137-1139, doi:10.1038/ni1109-1137 (2009).
84 Novak, I. *et al.* Nix is a selective autophagy receptor for mitochondrial clearance. *EMBO Reports* **11**, 45-51, doi:embor2009256 [pii]10.1038/embor.2009.256 (2010).
85 Tolkovsky, A. M. Mitophagy. *Biochim Biophys Acta* **1793**, 1508-1515, doi:S0167-4889(09)00060-3 [pii]10.1016/j.bbamcr.2009.03.002 (2009).
86 Narendra, D. P. & Youle, R. J. Targeting mitochondrial dysfunction: role for PINK1 and Parkin in mitochondrial quality control. *Antioxidants & Redox Signaling* **14**, 1929-1938, doi:10.1089/ars.2010.3799 (2011).
87 Ding, W. X. *et al.* Nix is critical to two distinct phases of mitophagy, reactive oxygen species-mediated autophagy induction and Parkin-ubiquitin-p62-mediated mitochondrial priming. *The Journal of Biological Chemistry* **285**, 27879-27890, doi:10.1074/jbc.M110.119537 (2010).
88 Gao, W. *et al*. Induction of macroautophagy by exogenously introduced calcium. *Autophagy* **4**, 754-761 (2008).
89 Høyer-Hansen, M. *et al.* Control of Macroautophagy by Calcium, Calmodulin-Dependent Kinase Kinase-β, and Bcl-2. *Molecular Cell* **25**, 193-205, doi:10.1016/j.molcel.2006.12.009 (2007).
90 Egan, D. F. *et al.* Phosphorylation of ULK1 (hATG1) by AMP-Activated Protein Kinase Connects Energy Sensing to Mitophagy. *Science*, doi:10.1126/science.1196371 (2010).
91 Ferrari, D. *et al.* Endoplasmic reticulum, Bcl-2 and Ca2+ handling in apoptosis. *Cell Calcium* **32**, 413-420, doi:10.1016/s0143416002002014 (2002).
92 Bassik, M. C. *et al*. Phosphorylation of BCL-2 regulates ER Ca2+ homeostasis and apoptosis. *EMBO Journal* **23**, 1207-1216, doi:http://www.nature.com/emboj/journal/v23/n5/suppinfo/7600104a_S1.html (2004).

93 Li, G. *et al.* Role of ERO1-alpha-mediated stimulation of inositol 1,4,5-triphosphate receptor activity in endoplasmic reticulum stress-induced apoptosis. *The Journal of Cell Biology* **186**, 783-792, doi:10.1083/jcb.200904060 (2009).
94 Ramming, T. & Appenzeller-Herzog, C. The Physiological Functions of Mammalian Endoplasmic Oxidoreductin 1 (Ero1): On Disulfides and More. *Antioxidants & Redox Signaling*, doi:10.1089/ars.2011.4475 (2012).
95 Jia, W. *et al*. Autophagy Regulates Endoplasmic Reticulum Homeostasis and Calcium Mobilization in T Lymphocytes. *The Journal of Immunology* **186**, 1564-1574, doi:10.4049/jimmunol.1001822 (2011).
96 Whitney, M. L. *et al*. ATF4 is necessary and sufficient for ER stress-induced upregulation of REDD1 expression. *Biochem Biophys Res Commun* **379**, 451-455 (2009).
97 Jin, H.-O. *et al.* Activating transcription factor 4 and CCAAT/enhancer-binding protein-β negatively regulate the mammalian target of rapamycin via Redd1 expression in response to oxidative and endoplasmic reticulum stress. *Free Radical Biology and Medicine* **46**, 1158-1167, doi:10.1016/j.freeradbiomed.2009.01.015 (2009).
98 Brugarolas, J. *et al.* Regulation of mTOR function in response to hypoxia by REDD1 and the TSC1/TSC2 tumor suppressor complex. *Genes & Development* **18**, 2893-2904, doi:10.1101/gad.1256804 (2004).
99 Zhang, H. *et al.* Loss of Tsc1/Tsc2 activates mTOR and disrupts PI3K-Akt signaling through downregulation of PDGFR. *The Journal of Clinical Investigation* **112**, 1223-1233 (2003).
100 Gingras, A.-C. *et al*. 4E-BP1, a repressor of mRNA translation, is phosphorylated and inactivated by the Akt(PKB) signaling pathway. *Genes & Development* **12**, 502-513 (1998).
101 Manning, B. D. a. C., L.C. United at last: the tuberous sclerosis complex gene products connect the phosphoinositide 3-kinase/Akt pathway to mammalian target of rapamycin (mTOR) signalling. *Biochemical Society Transactions* **31**, 573-578 (2003).
102 Qin, L. *et al*. ER stress negatively regulates AKT/TSC/mTOR pathway to enhance autophagy. *Autophagy* **6**, 239-247 (2010).
103 Salazar, M. *et al.* Cannabinoid action induces autophagy-mediated cell death through stimulation of ER stress in human glioma cells. *The Journal of Clinical Investigation* **119**, 1359-1372 (2009).
104 Yung, H. W. *et al*. Regulation of AKT phosphorylation at Ser473 and Thr308 by endoplasmic reticulum stress modulates substrate specificity in a severity dependent manner. *PLoS One* **6** (2011).
105 Baumeister, P. *et al.* Endoplasmic Reticulum Stress Induction of the Grp78/BiP Promoter: Activating Mechanisms Mediated by YY1 and Its Interactive Chromatin Modifiers. *Molecular and Cellular Biology* **25**, 4529-4540, doi:10.1128/mcb.25.11.4529-4540.2005 (2005).
106 Ohoka, N. *et al*. TRB3, a novel ER stress-inducible gene, is induced via ATF4-CHOP pathway and is involved in cell death. *The EMBO Journal* **24**, 1243-1255, doi:10.1038/sj.emboj.7600596 (2005).

107 Du, K.. *et al*. TRB3: a tribbles homolog that inhibits Akt/PKB activation by insulin in liver. *Science* **300**, 1574-1577, doi:10.1126/science.1079817 (2003).
108 Sinha, S. & Levine, B. The autophagy effector Beclin 1: a novel BH3-only protein. *Oncogene* **27**, S137-S148 (0000).
109 Boya, P. & Kroemer, G. Beclin 1: a BH3-only protein that fails to induce apoptosis. *Oncogene* **28**, 2125-2127 (2009).
110 McCullough, K. D. *et al*. Gadd153 Sensitizes Cells to Endoplasmic Reticulum Stress by Down-Regulating Bcl2 and Perturbing the Cellular Redox State. *Molecular and Cellular Biology* **21**, 1249-1259, doi:10.1128/mcb.21.4.1249-1259.2001 (2001).
111 Szegezdi, E. *et al*. Bcl-2 family on guard at the ER. *American Journal of Physiology - Cell Physiology* **296**, C941-C953, doi:10.1152/ajpcell.00612.2008 (2009).
112 Szegezdi, E. *et al*. Mediators of endoplasmic reticulum stress-induced apoptosis. *EMBO Reports* **7**, 880-885, doi:7400779 [pii]10.1038/sj.embor.7400779 (2006).
113 Yamamoto, K.. *et al*. BCL-2 is phosphorylated and inactivated by an ASK1/Jun N-terminal protein kinase pathway normally activated at G(2)/M. *Molecular and Cellular Biology* **19**, 8469-8478 (1999).
114 Lei, K. & Davis, R. J. JNK phosphorylation of Bim-related members of the Bcl2 family induces Bax-dependent apoptosis. *Proceedings of the National Academy of Sciences of the United States of America* **100**, 2432-2437 (2003).
115 Wei, Y. *et al*. JNK1-mediated phosphorylation of Bcl-2 regulates starvation-induced autophagy. *Molecular Cell* **30**, 678-688, doi:S1097-2765(08)00389-4[pii]10.1016/j.molcel.2008.06.001 (2008).
116 Ogata, M. *et al.* Autophagy is activated for cell survival after endoplasmic reticulum stress. *Molecular and Cellular Biology* **26**, 9220-9231, doi:10.1128/MCB.01453-06 (2006).
117 Ogata, M. *et al.* Autophagy Is Activated for Cell Survival after Endoplasmic Reticulum Stress. *Molecular and Cellular Biology* **26**, 9220-9231, doi:10.1128/mcb.01453-06 (2006).
118 Oh, S.-H. & Lim, S.-C. Endoplasmic Reticulum Stress-Mediated Autophagy/Apoptosis Induced by Capsaicin (8-Methyl-N-vanillyl-6-nonenamide) and Dihydrocapsaicin is Regulated by the Extent of c-Jun NH2-Terminal Kinase/Extracellular Signal-Regulated Kinase Activation in WI38 Lung Epithelial Fibroblast Cells. *Journal of Pharmacology and Experimental Therapeutics* **329**, 112-122, doi:10.1124/jpet.108.144113 (2009).
119 Gozuacik, D. *et al.* DAP-kinase is a mediator of endoplasmic reticulum stress-induced caspase activation and autophagic cell death. *Cell Death and Differentiation* **15**, 1875-1886, doi:10.1038/cdd.2008.121 (2008).
120 Zalckvar, E. *et al.* DAP-kinase-mediated phosphorylation on the BH3 domain of beclin 1 promotes dissociation of beclin 1 from Bcl-XL and induction of autophagy. *EMBO Reports* **10**, 285-292, doi:10.1038/embor.2008.246 (2009).
121 Kouroku, Y. *et al.* ER stress (PERK/eIF2alpha phosphorylation) mediates the polyglutamine-induced LC3 conversion, an essential step for autophagy formation. *Cell Death and Differentiation* **14**, 230-239, doi:10.1038/sj.cdd.4401984 (2007).

122 Rouschop, K. M. *et al.* The unfolded protein response protects human tumor cells during hypoxia through regulation of the autophagy genes MAP1LC3B and ATG5. *The Journal of Clinical Investigation* **120**, 127-141, doi:40027 [pii]10.1172/JCI40027 (2010).
123 Salih, D. A. M. & Brunet, A. FoxO transcription factors in the maintenance of cellular homeostasis during aging. *Current Opinion in Cell Biology* **20**, 126-136, doi:10.1016/j.ceb.2008.02.005 (2008).
124 Medema, R. H. & Jaattela, M. Cytosolic FoxO1: alive and killing. *Nature Cell Biology* **12**, 642-643 (2010).
125 Xu, P. *et al.* JNK regulates FoxO-dependent autophagy in neurons. *Genes & Development* **25**, 310-322, doi:10.1101/gad.1984311 (2011).
126 Zhao, Y. *et al.* Cytosolic FoxO1 is essential for the induction of autophagy and tumour suppressor activity. *Nature Cell Biology* **12**, 665-675, doi:http://www.nature.com/ncb/journal/v12/n7/suppinfo/ncb2069_S1.html (2010).
127 Vidal, R. L. *et al.* Targeting the UPR transcription factor XBP1 protects against Huntington's disease through the regulation of FoxO1 and autophagy. *Human Molecular Genetics*, doi:10.1093/hmg/dds040 (2012).
128 Gupta, S. *et al.* Mechanisms of ER Stress-Mediated Mitochondrial Membrane Permeabilization. *International Journal of Cell Biology* **2010** (2010).
129 Ullman, E. *et al.* Autophagy promotes necrosis in apoptosis-deficient cells in response to ER stress. *Cell Death and Differentiation* **15**, 422-425, doi:10.1038/sj.cdd.4402234 (2008).
130 Young, M. M. *et al.* Autophagosomal membrane serves as platform for intracellular death-inducing signaling complex (iDISC)-mediated caspase-8 activation and apoptosis. *The Journal of Biological Chemistry* **287**, 12455-12468, doi:10.1074/jbc.M111.309104 (2012).
131 Kroemer, G. *et al.* Classification of cell death: recommendations of the Nomenclature Committee on Cell Death 2009. *Cell Death and Differentiation* **16**, 3-11, doi:10.1038/cdd.2008.150 (2009).
132 Kerr, J. F. *et al.* Apoptosis: a basic biological phenomenon with wide-ranging implications in tissue kinetics. *British Journal of Cancer* **26**, 239-257 (1972).
133 Taylor, R. C. *et al.* Apoptosis: controlled demolition at the cellular level. *Nature Reviews Molecular Cell Biology* **9**, 231-241, doi:http://www.nature.com/nrm/journal/v9/n3/suppinfo/nrm2312_S1.html (2008).
134 Timmer, J. C. & Salvesen, G. S. Caspase substrates. *Cell death and differentiation* **14**, 66-72, doi:10.1038/sj.cdd.4402059 (2007).
135 Li, J. & Yuan, J. Caspases in apoptosis and beyond. *Oncogene* **27**, 6194-6206, doi:10.1038/onc.2008.297 (2008).
136 Tenev, T. *et al.* The Ripoptosome, a signaling platform that assembles in response to genotoxic stress and loss of IAPs. *Molecular Cell* **43**, 432-448, doi:10.1016/j.molcel.2011.06.006 (2011).
137 Crook, N. E. *et al.* An apoptosis-inhibiting baculovirus gene with a zinc finger-like motif. *Journal of Virology* **67**, 2168-2174 (1993).

138 Lorick, K. L. *et al.* RING fingers mediate ubiquitin-conjugating enzyme (E2)-dependent ubiquitination. *Proceedings of the National Academy of Sciences of the United States of America* **96**, 11364-11369 (1999).
139 Wei, Y. *et al*. Inhibitor of apoptosis proteins and apoptosis. *Acta Biochimica et Biophysica Sinica* **40**, 278-288 (2008).
140 Eckelman, B. P. *et al*. Human inhibitor of apoptosis proteins: why XIAP is the black sheep of the family. *EMBO Reports* **7**, 988-994, doi:10.1038/sj.embor.7400795 (2006).
141 Varfolomeev, E. *et al.* Cellular inhibitors of apoptosis are global regulators of NF-kappaB and MAPK activation by members of the TNF family of receptors. *Science Signaling* **5**, ra22, doi:10.1126/scisignal.2001878 (2012).
142 Yang, Q. H. & Du, C. Smac/DIABLO selectively reduces the levels of c-IAP1 and c-IAP2 but not that of XIAP and livin in HeLa cells. *The Journal of Biological Chemistry* **279**, 16963-16970, doi:10.1074/jbc.M401253200 (2004).
143 Srinivasula, S. M. *et al.* A conserved XIAP-interaction motif in caspase-9 and Smac/DIABLO regulates caspase activity and apoptosis. *Nature* **410**, 112-116, doi:10.1038/35065125 (2001).
144 Yang, Q. H. *et al*. Omi/HtrA2 catalytic cleavage of inhibitor of apoptosis (IAP) irreversibly inactivates IAPs and facilitates caspase activity in apoptosis. *Genes & Development* **17**, 1487-1496, doi:10.1101/gad.1097903 (2003).
145 Aggarwal, B. B. Signalling pathways of the TNF superfamily: a double-edged sword. *Nature Reviews. Immunology* **3**, 745-756, doi:10.1038/nri1184 (2003).
146 Dickens, L. S. *et al*. The 'complexities' of life and death: death receptor signalling platforms. *Experimental Cell Research* **318**, 1269-1277, doi:10.1016/j.yexcr.2012.04.005 (2012).
147 Peter, M. E. *et al.* The CD95 receptor: apoptosis revisited. *Cell* **129**, 447-450, doi:10.1016/j.cell.2007.04.031 (2007).
148 Lavrik, I. N. *et al.* CD95 stimulation results in the formation of a novel death effector domain protein-containing complex. *The Journal of Biological Chemistry* **283**, 26401-26408, doi:10.1074/jbc.M800823200 (2008).
149 Ponton, A. *et al*. The CD95 (APO-1/Fas) receptor activates NF-kappaB independently of its cytotoxic function. *The Journal of Biological Chemistry* **271**, 8991-8995 (1996).
150 Cao, X. *et al*. The role of TRADD in TRAIL-induced apoptosis and signaling. *FASEB journal : official publication of the Federation of American Societies for Experimental Biology* **25**, 1353-1358, doi:10.1096/fj.10-170480 (2011).
151 Wajant, H., Pfizenmaier, K. & Scheurich, P. Tumor necrosis factor signaling. *Cell Death and Differentiation* **10**, 45-65, doi:10.1038/sj.cdd.4401189 (2003).
152 Vucic, D. *et al*. Ubiquitylation in apoptosis: a post-translational modification at the edge of life and death. *Nature Reviews Molecular Cell Biology* **12**, 439-452, doi:10.1038/nrm3143 (2011).
153 Meylan, F. *et al.* The TNF-family receptor DR3 is essential for diverse T cell-mediated inflammatory diseases. *Immunity* **29**, 79-89, doi:10.1016/j.immuni.2008.04.021 (2008).
154 Kumar, A. *et al*. The ectodermal dysplasia receptor activates the nuclear factor-kappaB, JNK, and cell death pathways and binds to ectodysplasin A. *The*

Journal of Biological Chemistry **276**, 2668-2677, doi:10.1074/jbc.M008356200 (2001).
155 Zeng, L. *et al.* Death Receptor 6 Induces Apoptosis Not through Type I or Type II Pathways, but via a Unique Mitochondria-dependent Pathway by Interacting with Bax Protein. *The Journal of Biological Chemistry* **287**, 29125-29133, doi:10.1074/jbc.M112.362038 (2012).
156 Tait, S. W. & Green, D. R. Mitochondria and cell death: outer membrane permeabilization and beyond. *Nature Reviews Molecular Cell Biology* **11**, 621-632, doi:10.1038/nrm2952 (2010).
157 Reed, J. C. *et al*. Structure-function analysis of Bcl-2 family proteins. Regulators of programmed cell death. *Advances in Experimental Medicine and Biology* **406**, 99-112 (1996).
158 Youle, R. J. & Strasser, A. The BCL-2 protein family: opposing activities that mediate cell death. *Nature Reviews Molecular Cell Biology* **9**, 47-59, doi:10.1038/nrm2308 (2008).
159 Chipuk, J. E. *et al*. The BCL-2 family reunion. *Molecular Cell* **37**, 299-310, doi:10.1016/j.molcel.2010.01.025 (2010).
160 Martinez-Caballero, S. *et al.* Assembly of the mitochondrial apoptosis-induced channel, MAC. *The Journal of Biological Chemistry* **284**, 12235-12245, doi:10.1074/jbc.M806610200 (2009).
161 Li, P. *et al.* Cytochrome c and dATP-dependent formation of Apaf-1/caspase-9 complex initiates an apoptotic protease cascade. *Cell* **91**, 479-489 (1997).
162 Shiozaki, E. N. & Shi, Y. Caspases, IAPs and Smac/DIABLO: mechanisms from structural biology. *Trends in Biochemical Sciences* **29**, 486-494, doi:10.1016/j.tibs.2004.07.003 (2004).
163 Acehan, D. *et al.* Three-dimensional structure of the apoptosome: implications for assembly, procaspase-9 binding, and activation. *Molecular Cell* **9**, 423-432 (2002).
164 Shi, Y. Apoptosome assembly. *Methods in Enzymology* **442**, 141-156, doi:10.1016/S0076-6879(08)01407-9 (2008).
165 Reubold, T. F. *et al*. Crystal structure of full-length Apaf-1: how the death signal is relayed in the mitochondrial pathway of apoptosis. *Structure* **19**, 1074-1083, doi:10.1016/j.str.2011.05.013 (2011).
166 Lin, Y. *et al*. Pidd, a new death-domain-containing protein, is induced by p53 and promotes apoptosis. *Nature Genetics* **26**, 122-127, doi:10.1038/79102 (2000).
167 Tinel, A. & Tschopp, J. The PIDDosome, a protein complex implicated in activation of caspase-2 in response to genotoxic stress. *Science* **304**, 843-846, doi:10.1126/science.1095432 (2004).
168 Gu, H. *et al*. Caspase-2 functions upstream of mitochondria in endoplasmic reticulum stress-induced apoptosis by bortezomib in human myeloma cells. *Molecular Cancer Therapeutics* **7**, 2298-2307, doi:10.1158/1535-7163.MCT-08-0186 (2008).
169 Tu, S. *et al.* In situ trapping of activated initiator caspases reveals a role for caspase-2 in heat shock-induced apoptosis. *Nature Cell Biology* **8**, 72-77, doi:10.1038/ncb1340 (2006).

170 Tinel, A. *et al.* Regulation of PIDD auto-proteolysis and activity by the molecular chaperone Hsp90. *Cell Death and Differentiation* **18**, 506-515, doi:10.1038/cdd.2010.124 (2011).
171 Janssens, S. *et al.* PIDD mediates NF-kappaB activation in response to DNA damage. *Cell* **123**, 1079-1092, doi:10.1016/j.cell.2005.09.036 (2005).
172 Bouchier-Hayes, L. *et al.* Characterization of cytoplasmic caspase-2 activation by induced proximity. *Molecular Cell* **35**, 830-840, doi:10.1016/j.molcel.2009.07.023 (2009).
173 Wang, R. *et al.* Autoinhibition of UNC5b revealed by the cytoplasmic domain structure of the receptor. *Molecular Cell* **33**, 692-703, doi:10.1016/j.molcel.2009.02.016 (2009).
174 Tinel, A. *et al.* Autoproteolysis of PIDD marks the bifurcation between pro-death caspase-2 and pro-survival NF-kappaB pathway. *The EMBO Journal* **26**, 197-208, doi:10.1038/sj.emboj.7601473 (2007).
175 Ando, K. *et al.* PIDD Death-Domain Phosphorylation by ATM Controls Prodeath versus Prosurvival PIDDosome Signaling. *Molecular Cell* **47**, 681-693, doi:10.1016/j.molcel.2012.06.024 (2012).
176 Bonzon, C. *et al.* Caspase-2-induced apoptosis requires bid cleavage: a physiological role for bid in heat shock-induced death. *Molecular Biology of the Cell* **17**, 2150-2157, doi:10.1091/mbc.E05-12-1107 (2006).
177 Korsmeyer, S. J. *et al.* Pro-apoptotic cascade activates BID, which oligomerizes BAK or BAX into pores that result in the release of cytochrome c. *Cell Death and Differentiation* **7**, 1166-1173, doi:10.1038/sj.cdd.4400783 (2000).
178 O'Reilly, L. A. *et al.* Caspase-2 is not required for thymocyte or neuronal apoptosis even though cleavage of caspase-2 is dependent on both Apaf-1 and caspase-9. *Cell Death and Differentiation* **9**, 832-841, doi:10.1038/sj.cdd.4401033 (2002).
179 Oliver, T. G. *et al.* Caspase-2-mediated cleavage of Mdm2 creates a p53-induced positive feedback loop. *Molecular Cell* **43**, 57-71, doi:10.1016/j.molcel.2011.06.012 (2011).
180 Kitevska, T. *et al.* Caspase-2: controversial killer or checkpoint controller? *Apoptosis : an international journal on programmed cell death* **14**, 829-848, doi:10.1007/s10495-009-0365-3 (2009).
181 Feoktistova, M. *et al.* cIAPs block Ripoptosome formation, a RIP1/caspase-8 containing intracellular cell death complex differentially regulated by cFLIP isoforms. *Molecular Cell* **43**, 449-463, doi:10.1016/j.molcel.2011.06.011 (2011).
182 Laster, S. M. *et al.* Tumor necrosis factor can induce both apoptic and necrotic forms of cell lysis. *Journal of Immunology* **141**, 2629-2634 (1988).
183 Vanlangenakker, N. *et al.* Many stimuli pull the necrotic trigger, an overview. *Cell Death and Differentiation* **19**, 75-86, doi:10.1038/cdd.2011.164 (2012).
184 Pyo, J. O. *et al.* Essential roles of Atg5 and FADD in autophagic cell death: dissection of autophagic cell death into vacuole formation and cell death. *The Journal of Biological Chemistry* **280**, 20722-20729, doi:10.1074/jbc.M413934200 (2005).

185 Newton, K.. *et al*. A dominant interfering mutant of FADD/MORT1 enhances deletion of autoreactive thymocytes and inhibits proliferation of mature T lymphocytes. *The EMBO Journal* **17**, 706-718, doi:10.1093/emboj/17.3.706 (1998).
186 Salmena, L. *et al.* Essential role for caspase 8 in T-cell homeostasis and T-cell-mediated immunity. *Genes & Development* **17**, 883-895, doi:10.1101/gad.1063703 (2003).
187 Chau, H. *et al.* Cellular FLICE-inhibitory protein is required for T cell survival and cycling. *The Journal of Experimental Medicine* **202**, 405-413, doi:10.1084/jem.20050118 (2005).
188 Li, C. *et al.* Autophagy is induced in CD4+ T cells and important for the growth factor-withdrawal cell death. *Journal of Immunology* **177**, 5163-5168 (2006).
189 Pua, H. H. *et al*. A critical role for the autophagy gene Atg5 in T cell survival and proliferation. *The Journal of Experimental Medicine* **204**, 25-31, doi:10.1084/jem.20061303 (2007).
190 Laussmann, M. A. *et al.* Proteasome inhibition can induce an autophagy-dependent apical activation of caspase-8. *Cell Death and Differentiation* **18**, 1584-1597, doi:10.1038/cdd.2011.27 (2011).
191 Shao, Y. *et al*. Apoptotic and autophagic cell death induced by histone deacetylase inhibitors. *Proceedings of the National Academy of Sciences of the United States of America* **101**, 18030-18035, doi:10.1073/pnas.0408345102 (2004).
192 Ding, W. X. *et al.* Differential effects of endoplasmic reticulum stress-induced autophagy on cell survival. *The Journal of Biological Chemistry* **282**, 4702-4710, doi:10.1074/jbc.M609267200 (2007).
193 Ohmuraya, M. *et al.* Autophagic cell death of pancreatic acinar cells in serine protease inhibitor Kazal type 3-deficient mice. *Gastroenterology* **129**, 696-705, doi:10.1016/j.gastro.2005.05.057 (2005).
194 Bonapace, L. *et al.* Induction of autophagy-dependent necroptosis is required for childhood acute lymphoblastic leukemia cells to overcome glucocorticoid resistance. *The Journal of Clinical Investigation* **120**, 1310-1323, doi:10.1172/JCI39987 (2010).
195 Lytton, J. *et al*. Thapsigargin inhibits the sarcoplasmic or endoplasmic reticulum Ca-ATPase family of calcium pumps. *The Journal of Biological Chemistry* **266**, 17067-17071 (1991).
196 Bassik, M. C. & Kampmann, M. Knocking out the door to tunicamycin entry. *Proceedings of the National Academy of Sciences of the United States of America* **108**, 11731-11732, doi:10.1073/pnas.1109035108 (2011).
197 Lin, J. H. *et al*. Endoplasmic reticulum stress in disease pathogenesis. *Annual Review Pathology* **3**, 399-425, doi:10.1146/annurev.pathmechdis.3.121806.151434 (2008).
198 Schroder, M. & Kaufman, R. J. The mammalian unfolded protein response. *Annual Review of Biochemistry* **74**, 739-789, doi:10.1146/annurev.biochem.73.011303.074134 (2005).

199 Ron, D. & Walter, P. Signal integration in the endoplasmic reticulum unfolded protein response. *Nature Review Molecular Cell Biology* **8**, 519-529, doi:nrm2199 [pii]10.1038/nrm2199 (2007).
200 Ding, W. X. *et al.* Linking of autophagy to ubiquitin-proteasome system is important for the regulation of endoplasmic reticulum stress and cell viability. *American Journal Pathology* **171**, 513-524, doi:ajpath.2007.070188 [pii]10.2353/ajpath.2007.070188 (2007).
201 Giam, M. *et al*. BH3-only proteins and their roles in programmed cell death. *Oncogene* **27**, S128-S136 (0000).
202 Szegezdi, E. *et al*. Bcl-2 family on guard at the ER. *Am erican Journal Physiology Cell Physiology*, doi:00612.2008 [pii]10.1152/ajpcell.00612.2008 (2009).
203 Fuchs, Y. & Steller, H. Programmed cell death in animal development and disease. *Cell* **147**, 742-758, doi:10.1016/j.cell.2011.10.033 (2011).
204 Vanlangenakker, N. *et al*. TNF-induced necroptosis in L929 cells is tightly regulated by multiple TNFR1 complex I and II members. *Cell Death & Disease* **2**, e230, doi:10.1038/cddis.2011.111 (2011).
205 Zhang, D. W. *et al.* RIP3, an energy metabolism regulator that switches TNF-induced cell death from apoptosis to necrosis. *Science* **325**, 332-336, doi:10.1126/science.1172308 (2009).
206 Di Sano, F. *et al.* Endoplasmic reticulum stress induces apoptosis by an apoptosome-dependent but caspase 12-independent mechanism. *Journal of Biological Chemistry* **281**, 2693-2700, doi:M509110200 [pii]10.1074/jbc.M509110200 (2006).
207 Boyce, M. *et al.* A selective inhibitor of eIF2alpha dephosphorylation protects cells from ER stress. *Science* **307**, 935-939, doi:307/5711/935 [pii]10.1126/science.1101902 (2005).
208 Gupta, S. *et al*. The mitochondrial death pathway: A promising therapeutic target in Diseases. *Journal of Cellular and Molecular Medicine*, doi:JCMM697 [pii]10.1111/j.1582-4934.2009.00697.x (2009).
209 Yang, Q. *et al.* Tumour necrosis factor receptor 1 mediates endoplasmic reticulum stress-induced activation of the MAP kinase JNK. *EMBO Reports* **7**, 622-627, doi:10.1038/sj.embor.7400687 (2006).
210 Bell, B. D. *et al.* FADD and caspase-8 control the outcome of autophagic signaling in proliferating T cells. *Proceedings of the National Academy of Sciences of the United States of America* **105**, 16677-16682, doi:10.1073/pnas.0808597105 (2008).
211 Mace, P. D. & Riedl, S. J. Molecular cell death platforms and assemblies. *Current Opinion in Cell Biology* **22**, 828-836, doi:10.1016/j.ceb.2010.08.004 (2010).
212 Bodmer, J. L. *et al.* TRAIL receptor-2 signals apoptosis through FADD and caspase-8. *Nature Cell Biology* **2**, 241-243, doi:10.1038/35008667 (2000).
213 Kischkel, F. C. *et al.* Apo2L/TRAIL-dependent recruitment of endogenous FADD and caspase-8 to death receptors 4 and 5. *Immunity* **12**, 611-620 (2000).
214 Peter, M. E. & Krammer, P. H. Mechanisms of CD95 (APO-1/Fas)-mediated apoptosis. *Current Opinion in Immunology* **10**, 545-551 (1998).

215 Micheau, O. & Tschopp, J. Induction of TNF receptor I-mediated apoptosis via two sequential signaling complexes. *Cell* **114**, 181-190 (2003).
216 Feoktistova, M. *et al*. Pick your poison: the Ripoptosome, a cell death platform regulating apoptosis and necroptosis. *Cell Cycle* **11**, 460-467, doi:10.4161/cc.11.3.19060 (2012).
217 Hu, P. *et al*. Autocrine tumor necrosis factor alpha links endoplasmic reticulum stress to the membrane death receptor pathway through IRE1alpha-mediated NF-kappaB activation and down-regulation of TRAF2 expression. *Molecular and Cellular Biology* **26**, 3071-3084, doi:10.1128/MCB.26.8.3071-3084.2006 (2006).
218 Dickens, L. S. *et al.* A death effector domain chain DISC model reveals a crucial role for caspase-8 chain assembly in mediating apoptotic cell death. *Molecular Cell* **47**, 291-305, doi:10.1016/j.molcel.2012.05.004 (2012).
219 Schleich, K. *et al.* Stoichiometry of the CD95 death-inducing signaling complex: experimental and modeling evidence for a death effector domain chain model. *Molecular Cell* **47**, 306-319, doi:10.1016/j.molcel.2012.05.006 (2012).
220 Bernales, S. *et al*. Autophagy counterbalances endoplasmic reticulum expansion during the unfolded protein response. *PLoS Biology* **4**, e423, doi:10.1371/journal.pbio.0040423 (2006).
221 Yorimitsu, T. *et al*. Endoplasmic reticulum stress triggers autophagy. *The Journal of Biological Chemistry* **281**, 30299-30304, doi:10.1074/jbc.M607007200 (2006).
222 Drake, K. R. *et al*. Nucleocytoplasmic distribution and dynamics of the autophagosome marker EGFP-LC3. *PloS One* **5**, e9806, doi:10.1371/journal.pone.0009806 (2010).
223 Lin, W. C. *et al.* Endoplasmic reticulum stress stimulates p53 expression through NF-kappaB activation. *PloS One* **7**, e39120, doi:10.1371/journal.pone.0039120 (2012).
224 Maiuri, M. C. *et al.* Stimulation of autophagy by the p53 target gene Sestrin2. *Cell Cycle* **8**, 1571-1576 (2009).
225 Ellisen, L. W. *et al.* REDD1, a developmentally regulated transcriptional target of p63 and p53, links p63 to regulation of reactive oxygen species. *Molecular Cell* **10**, 995-1005 (2002).
226 Crighton, D. *et al.* DRAM, a p53-induced modulator of autophagy, is critical for apoptosis. *Cell* **126**, 121-134, doi:10.1016/j.cell.2006.05.034 (2006).
227 Fei, P. *et al.* Bnip3L is induced by p53 under hypoxia, and its knockdown promotes tumor growth. *Cancer Cell* **6**, 597-609, doi:10.1016/j.ccr.2004.10.012 (2004).
228 Belmont, P. J. *et al*. Regulation of microRNA expression in the heart by the ATF6 branch of the ER stress response. *Journal of Molecular and Cellular Cardiology* **52**, 1176-1182, doi:10.1016/j.yjmcc.2012.01.017 (2012).
229 Vadlamudi, R. K. *et al*. p62, a phosphotyrosine-independent ligand of the SH2 domain of p56lck, belongs to a new class of ubiquitin-binding proteins. *The Journal of Biological Chemistry* **271**, 20235-20237 (1996).

230 Waters, S. *et al*. Interactions with LC3 and polyubiquitin chains link nbr1 to autophagic protein turnover. *FEBS Letters* **583**, 1846-1852, doi:10.1016/j.febslet.2009.04.049 (2009).
231 Pankiv, S. *et al.* p62/SQSTM1 binds directly to Atg8/LC3 to facilitate degradation of ubiquitinated protein aggregates by autophagy. *The Journal of Biological Chemistry* **282**, 24131-24145, doi:10.1074/jbc.M702824200 (2007).
232 Bjorkoy, G. *et al.* p62/SQSTM1 forms protein aggregates degraded by autophagy and has a protective effect on huntingtin-induced cell death. *The Journal of Cell Biology* **171**, 603-614, doi:10.1083/jcb.200507002 (2005).
233 Schweers, R. L. *et al.* NIX is required for programmed mitochondrial clearance during reticulocyte maturation. *Proceedings of the National Academy of Sciences of the United States of America* **104**, 19500-19505, doi:10.1073/pnas.0708818104 (2007).